



**UNIVERSITY of the
WESTERN CAPE**

**POLYMER COATING OF AN OPTIMIZED NANO LIPID CARRIER SYSTEM OF
HARPAGOPHYTUM PROCUMBENS EXTRACT FOR ORAL DELIVERY**

Somaya Saleh Almajdoub

3515576

A thesis submitted in partial fulfilment of the requirements for the degree

M.Pharm (Pharmaceutics)

In

School of Pharmacy at the University of the Western Cape

Cape Town

**UNIVERSITY of the
WESTERN CAPE**

Supervisor: Dr. A. Dube.

Co-supervisor: Dr. N. Ebrahim.

2017



ABSTRACT

Harpagophytum procumbens is a traditional medicinal plant widely used in South African traditional healthcare to treat a range of ailments like degenerative rheumatoid arthritis, osteoarthritis, tendonitis, kidney inflammation, heart disease, dyspepsia and loss of appetite. Analgesic and anti-inflammatory effects of *Harpagophytum procumbens* has been reported to decrease due to stomach acidity. In addition, dried plant extract is water soluble and has poor lipid solubility severely limiting its ability to pass across lipid-rich biological membranes. To overcome this, plant extract was incorporated into a nano lipid alginate coated bead.

Harpagophytum procumbens freeze dried aqueous extract was prepared and the active principle harpagoside was identified by mass spectrometry (MS). A simple, linear, accurate and precise UHPLC method was developed for quantitative determination of the bioactive harpagoside. *Harpagophytum procumbens* was encapsulated in lipid vesicles (liposomes and phytosomes) by using a dry film hydration technique and characterized for particle size, polydispersity index and encapsulation efficiency.

Statistical response surface methodology (RSM) experimental design was used for lipid vesicles formulation optimization. The effects of formulation parameters (input factors) phosphatidylcholine ratio, cholesterol ratio and type of the lipid vesicle on output factors particle size, polydispersity index and percentage entrapment efficiency was investigated. Experimental design was statistically validated by ANOVA and suitable model for each output factor was selected based on non-significant lack of fit p-value and R^2 values. The design matrix showed that particle size of lipid vesicles enhanced as phosphatidylcholine and cholesterol content increases. The particle size of lipid vesicles was in a range of 382.6 to 608.7 nm for liposomes for phytosome was in a range of 207.8 to 596.4 nm. The design matrix also showed that polydispersity index decreases as phosphatidylcholine and cholesterol concentration increases which reflects complete complexation. Phosphatidylcholine had a more positive effect on encapsulation efficacy than cholesterol. High cholesterol content generally decreased percentage encapsulation.

Once the desirability function was included for formulation optimization, the optimized formulation was phosphatidylcholine 80 %, cholesterol 5 % and type of lipid vesicle was

phytosomes. The predicted values of these vesicles was, particle size 531.29 nm, poly disparity index 0.23 and percentage encapsulation efficiency 31 % and a desirability of 0.77. The optimized formulation was verified in 4 replicates and the results were similar to the predicted results.

The zeta potential of the optimized formulation was outside the recommended range. Hence, stearic acid was added to the optimized *H. procumbens* phytosomes formulation as a surface charge inducer. The zeta potential was significantly ($p < 0.05$) improved when stearic acid was added to the optimized formulation from -8.3 ± 0.72 to -30.6 ± 0.80 mV.

Scanning electron microscopy confirmed the formation of the phospholipid vesicles upon hydration of thin lipid film. FTIR analysis indicated the interaction of plant extract to the polar end of the phosphatidylcholine through formation of strong hydrogen bonding between the hydroxyl group of phospholipid and extract phytoconstituents.

The phytosomes showed instability in simulated gastric SGF (pH 1.2), demonstrated by increase in the particle size, polydispersity index and a reduction in zeta potential after 4 hours of incubation.

H. procumbens phytosomes was encapsulated in alginate beads in order to protect phytosomes integrity. This was performed to overcome degradation of the plant extract in an acidic environment. Alginate coated *H. procumbens* phytosomes were successfully prepared by inotropic gelation technique by using sodium alginate and calcium chloride as a cross-linking agent. Alginate coated *H. procumbens* phytosomes formulations at 2 % sodium alginate and 4% calcium chloride was found to be the best parameter values.

The alginate-coated *H. procumbens* phytosomes exhibited high swelling rate in simulated intestinal fluid (SIF) pH 7.4 (92 %), while the swelling rate was lower in gastric simulated fluid (SGF) pH 1.2 (19 %), this is a desirable result. The alginate-coated *H. procumbens* phytosomes in acidic media (SGF) showed no release over the 4 hours and no signs of bead disruption.

The in vitro release study showed that phytosomes and alginate-coated *H. procumbens* phytosomes entered a slow-release phase and delayed the harpagoside release, compared to conventional freeze dried plant extract. *H. procumbens* phytosomes demonstrated Fickian diffusion release mechanism of harpagoside and its release from alginate-coated *H.*

procumbens phytosomes was predominantly by both diffusion drug release and anomalous transport (swelling controlled drug release).

At lower temperature conditions, i.e. 4-8 °C, the phytosomes showed fairly high retention of active in the vesicles over 30 days with only 8.82 % leak. As for alginate coated *H. procumbens* phytosomes, alginate beads exhibited satisfactory stability under all exposed temperatures; however, they showed negligible leaking at the end of 30 days at 37 °C.

Overall, water soluble phytoconstituents of freeze dried *H. procumbens* extract can be converted to alginate coated phytosomes complexes. This can be considered a promising vehicle for control delivery of *H. procumbens* extract as it minimizes release in simulated gastric environment and breakdown in simulated intestinal environment which could lead to increased availability of phytosomes for small intestine absorption.



KEY WORDS

Harpagophytum procumbens, harpagoside, anti-inflammatory, lipid-based drug delivery systems (LBDDS), liposomes, phytosomes, response surface methodology (RSM), alginate beads, simulated gastric fluid (SGF) and simulated intestinal fluid (SIF).



DECLARATION

I declare that “Polymer coating of an optimized nano lipid carrier system of *Harpagophytum procumbens* extract for oral delivery” is my own work, that has not been submitted before for any degree or examination at this or any other University, and that all sources I have used or quoted have been indicated and acknowledged by means of complete references.

Somaya

October 2017.

Signed:

UWC, Bellville.



TABLE OF CONTENTS

ABSTRACT.....	I
KEYWORDS.....	IV
DECLARATION.....	V
TABLE OF CONTENTS.....	VI
LIST OF FIGURES.....	XIV
LIST OF TABLES.....	XIX
LIST OF ABBREVIATIONS.....	XXII
DEDICATION.....	XX IV
ACKNOWLEDGEMNTS.....	XXV
CHAPTER 1 INTRODUCTION.....	1
1.1 Background and Problem Definition	1
1.2 Aim and objectives of the study.....	4
CHAPTER 2 LITERATURE REVIEW.....	5
2.1 Background.....	5
2.2 <i>Harpagophytum procumbens</i>	5
2.2.1 Description	5
2.2.2 Geographical distribution and habitat:	7
2.2.3 Phytochemistry: Main and active constituents	7
2.2.4 Clinical usefulness.....	8
2.2.5 Pharmacological effect as anti-inflammatory	8
2.2.6 Dosage forms.....	9
2.3 Intestinal absorption.....	10

2.3.1	Simulated Gastric Fluid (SGF).....	11
2.3.2	Simulated Intestinal Fluid (SIF).....	11
2.4	Nanotechnology	12
2.5	Lipid-based drug delivery systems:	12
2.5.1	Types of lipid based systems.....	13
2.5.2	Liposomes.....	13
2.5.2.1	Preparation of liposomes.....	14
2.5.2.1.1	Thin-film hydration method.....	14
2.5.2.2	Types of liposomes.....	15
2.5.3	Phytosomes	20
2.5.3.1	Difference between liposome and phytosome.....	16
2.5.3.2	Preparation of phytosomes.....	17
2.5.4	Structural components of lipid based drug delivery systems.....	17
2.5.4.1	Phospholipids.....	17
2.5.4.1.1	Phosphatidylcholine (PC).....	19
2.5.4.1.2	Lecithin.....	19
2.5.4.2	Cholesterol.....	20
2.5.4.3	Stearic acid.....	20
2.5.5	Characterization of liposomes and phytosomes:	21
2.6	Alginate coating.....	27
2.6.1	Alginate hydrogel beads preparation	30

2.6.1.1	Ionic cross-linking.....	26
2.6.1.2	Covalent cross-linking.....	26
2.6.1.3	Thermal gelation.....	26
2.6.2	Physicochemical characterization of alginate hydrogels beads.....	31
2.6.3	Biomedical applications of Alginate beads	29
2.7	Response surface methodology	34
2.7.1	Definition of terms in RSM.....	35
2.7.2	Process for RSM application.....	36
CHAPTER 3	METHODOLOGY	33
3.1	Preparation of freeze dried <i>H.procumbens</i> plant extract.....	33
3.2	Identification of Harpagoside biomarker in plant extract	33
3.2.1	LC/MS.....	33
3.2.1.1	Instrumentation.....	33
3.2.1.2	Method.....	34
3.2.2	UHPLC.....	34
3.2.2.1	Development and validation of an UHPLC method for harpagoside assay.....	34
3.2.2.2	Instrumentation.....	34
3.2.2.3	Chromatographic conditions.....	34
3.2.2.4	Preparation of pure standard harpagoside stock solution.....	35
3.2.2.5	Preparation of mobile phase.....	35
3.2.2.6	Key parameters of the analytical method validation.....	35
3.3	Quantitative determination of harpagoside constituent in <i>H.procumbens</i> plant extract.....	38
3.4	Lipid vesicles (liposomes and phytosomes) preparation.....	38

3.4.1	Preparation of 0.1 M potassium phosphate buffer pH 7.4 at 25°C.....	38
3.4.2	Liposome preparation.....	38
3.4.3	Phytosomes preparation	39
3.5	Physicochemical characterization of <i>H.procumbens</i> liposomes and phytosomes.....	40
3.5.1	Visualization of lipid vesicles by optical microscopy	40
3.5.2	Mean particle size and polydispersity index (PDI) determination	40
3.5.3	Zeta potential determination.....	41
3.5.4	Percentage encapsulation efficiency.....	41
3.6	Preliminary study for determination of nano lipid vesicles formulation parameters.....	43
3.6.1	Investigating the effect of lipid type on percentage encapsulation efficiency.....	43
3.6.2	Investigating the optimal sonication time for vesicle disruption.....	43
3.6.3	Investigation of the influence of lipid vesicle size reduction process on the percentage encapsulation efficiency.....	44
3.6.4	Finding the appropriate plant extract ratio for appropriate percentage encapsulation efficiency.....	44
3.7	RSM optimization process of nano lipid vesicles formulation by design of experiments	44
3.7.1	Generating experimental matrix.....	45
3.7.2	Lipid vesicle characterization of RSM generated experiments	46
3.7.3	RSM Data analysis and evaluation of the fitted response surface models	46
3.7.4	Formulation optimization using desirability function	47
3.7.5	Validation of optimized condition.....	48
3.8	Characterization of selected optimized RSM formulation.....	48
3.8.1	Particle size and polydispersity index	48

3.8.2	Zeta Potential Analysis.....	48
3.8.3	Surface Morphology	48
3.8.4	Apparent solubility study	48
3.8.5	FTIR spectroscopy	49
3.8.6	Stability in simulated gastric fluid (SGF) pH 1.2	49
3.8.6.1	Preparation of simulated GI media.....	49
3.8.6.2	Method.....	50
3.9	Phytosome - alginate system.....	50
3.9.1	Preparation of the alginate coated <i>H.procumbens</i> phytosomes	50
3.9.2	Process variables and optimization.....	52
3.9.3	Characterization of alginate coated <i>H.procumbens</i> phytosomes	53
3.9.3.1	Particle size measurements	53
3.9.3.2	Percentage encapsulation efficiency determination.....	53
3.9.3.3	Alginate coated <i>H. procumbens</i> phytosomes erosion study.....	54
3.9.3.4	Moephology and surface assessment of selected alginate coated <i>H. procumbens</i> phytosomes.....	54
3.9.3.5	Phytosomes- polymer compatibility study	54
3.9.3.6	Swelling index	55
3.9.3.7	Invitro drug release in GIT fluids.....	55
3.9.3.8	Release profile determination.....	56
3.9.3.9	Mechanism of release.....	56

3.9.3.10 Effect of storage temperature on <i>H. procumbens</i> phytosomes and alginate coated phytosomes.....	57
3.10 Statistical analysis of data.....	58
CHAPTER 4 RESULTS AND DISCUSSION.....	59
4.1 <i>H. procumbens</i> plant extract preparation	59
4.2 Identification of harpagoside biomarker in <i>H. procumbens</i> plant extract.....	59
4.2.1 LC/MS.....	59
4.2.2 UHPLC.....	61
4.2.2.1 Development and validation of an UHPLC method for harpagoside assay.....	63
4.2.2.2 Validation UHPLC method of harpagoside.....	65
4.3 Quantitative determination of harpagoside constituent in plant extract.....	72
4.4 Lipid vesicles (liposomes/ phytosomes) preparation and characterization.....	72
4.5 Preliminary study for determination of nano lipid vesicles formulation parameters.....	72
4.5.1 Investigating the effect of lipid type on percentage encapsulation efficiency.....	73
4.5.2 Investigating the optimal sonication time for vesicle disruption.....	74
4.5.3 Investigating the influence of the lipid vesicle size reduction method on percentage encapsulation efficiency.....	74
4.5.4 Finding the appropriate plant extract ratio for appropriate percentage encapsulation efficiency.....	76
4.6 Response Surface Methodology (RSM) optimization process of nano lipid vesicles formulation.....	77
4.6.1 Design of experiments.....	77
4.6.2 Generating experimental matrix.....	77

4.6.3	Lipid vesicle characterization of RSM generated experiments.....	78
4.6.4	Analysis of RSM data and evaluation of the fitted output factor surface models.....	79
4.6.5	Effect of input factor on output factor Y1 _{PS} (particle size).....	84
4.6.6	Effect of input factors on output factor Y2 _{PDI} (polydispersity index).....	87
4.6.7	Effect of input factors on percentage encapsulation efficiency Y3 _{%EE} (percentage encapsulation efficiency).....	89
4.6.8	Formulation optimization using desirability function.....	91
4.6.9	Verification of optimized condition.....	91
4.7	Characterization of selected optimized RSM formulation.....	92
4.7.1	Particle size and polydispersity index.....	92
4.7.2	Zeta Potential Analysis.....	93
4.7.3	Scanning Electron Microscopy (SEM).....	96
4.7.4	Solubility.....	97
4.7.5	FTIR study.....	98
4.7.6	Stability in simulated gastric fluid (SGF) pH 1.2.....	101
4.8	Phytosome - alginate system.....	104
4.8.1	Preparation of the alginate coated <i>H.procumbens</i> phytosomes.....	104
4.8.2	Process variables and process optimization.....	105
4.9	Characterization of alginate coated <i>H.procumbens</i> phytosomes	105
4.9.1	Particle size measurement.....	105

4.9.2	Percentage encapsulation efficiency of alginate coated <i>H. procumbens</i> phytosomes.....	106
4.9.3	Alginate coated <i>H. procumbens</i> phytosomes erosion study.....	108
4.9.4	Shape and surface assessment of selected alginate coated <i>H. procumbens</i> phytosomes	110
4.9.5	Phytosomes- polymer compatibility study.....	110
4.9.6	Swelling index	113
4.9.7	Ivitro release study in GIT fluids.....	114
4.9.8	Release profile determination.....	115
4.9.9	Mechanism of release.....	116
4.9.10	Storage stability study	119
CHAPTER 5 CONCLUSION AND RECOMMENDATIONS.....		124
REFERENCES		127



LIST OF FIGURES

Figure 2-1:	<i>H. procumbens</i> with flower, fruit (seed capsule) and bluish green leaves.....	6
Figure 2-2:	<i>H. procumbens</i> with secondary tubers.....	6
Figure 2-3:	Geographical distribution of <i>H. procumbens</i> (region 1).....	7
Figure 2-4 :	Varying pH in the gastrointestinal tract	10
Figure 2-5:	Classification of lipid based drug delivery system.....	13
Figure 2-6:	Liposomes manufacturing steps with some modification.....	15
Figure 2-7:	Classification of liposomes based on the lamellarity and size.....	15
Figure 2-8:	Difference between phytosome and liposome.	16
Figure 2-9:	A diagram showing a phospholipid molecule with two fatty acids and a modified phosphate group attached to a glycerol backbone.....	18
Figure 2-10:	Illustration of the basic elements of a lipid, with the arrangement into the lipid bilayer structure.....	18
Figure 2-11:	General structure of cholesterol.....	20
Figure 2-12:	Mechanism of drug release	23
Figure 2-13:	Chemical structure of repeated units of alginate: D-mannuronic acid (M) and L-guluronic acid (G).....	24
Figure 2-14:	Schematic crosslink between alginate and the calcium cations resulting in "egg box model" calcium cross-linked junctions.....	25
Figure 2-15:	Schematic representation of alginate beads fabrication process.....	27
Figure 2-16:	Schematic representation of two mechanisms for drug release from a particle embedded in a hydrogel bead.....	29
Figure 3-1:	General lipid vesicles preparation steps.....	40

Figure 3-2:	Preparation of alginate coated <i>H.procumbens</i> phytosomes beads by ionotropic gelation method.....	52
Figure 4-1:	Full scan MS spectrum of pure standard harpagoside in positive ion mode showing $[M+Na]^+$ Ion of harpagoside at m/z 517.....	60
Figure 4-2:	Full scan MS spectrum of plant extract in positive ion mode showing $[M+Na]^+$ Ion of harpagoside at m/z 517.....	60
Figure 4-3:	Full scan MS spectrum of pure standard harpagoside in negative ion mode showing $[M+HCOO]^-$ Ion of harpagoside at m/z 539.23.....	61
Figure 4-4:	Full scan MS spectrum of plant extract in negative ion mode showing $[M+HCOO]^-$ Ion of harpagoside at m/z 539.23.....	61
Figure 4-5-1:	Harpagoside chromatogram in plant extract before spiking.....	62
Figure 4-5-2:	Harpagoside chromatogram in plant extract after spiking.....	62
Figure 4-6:	Spectra for pure standard harpagoside peak at 278nm indicating harpagoside identity and no co elution with harpagoside from other plant extract components.....	63
Figure 4-7:	UHPLC chromatogram of pure harpagoside. Mobile phase (methanol: water; (60:40v/v)).....	63
Figure 4-8:	UHPLC chromatogram of harpagoside in <i>H.procumbens</i> plant extract.....	64
Figure 4-9:	Identical spectra (bottom) acquired across the harpagoside peak in plant extract (top) indicate a pure peak of harpagoside	64
Figure 4-10-1:	Mobile phase component (methanol) chromatogram.....	65
Figure 4-10-2:	Mobile phase component (deionized water) chromatogram.....	65
Figure 4-11-1:	UHPLC chromatogram of pure standard non-degraded harpagoside.....	66
Figure 4-11-2:	UHPLC chromatogram of the forced degradation harpagoside sample in NaOH.....	66
Figure 4-12-1:	Linearity plot of harpagoside dissolved in methanol.....	67
Figure 4-12-2:	Linearity plot of harpagoside dissolved in phosphate buffer solution, pH 7.4	68

Figure 4-13:	Microscopic images of lipid vesicles.....	72
Figure 4-14:	Histogram illustrating lipid type on percentage encapsulation efficiency.....	73
Figure 4-15:	Sonication time for disrupt of lipid vesicles to release maximum amount of loaded drug.....	74
Figure 4-16:	Effect of variation in plant extract content on the percentage encapsulation efficiency of lipid vesicle formulations prepared with constant lipid phase content	76
Figure 4-17:	Illustration of particle size of two randomly selected formulations of according to RSM.....	79
Figure 4-18-1:	Normal plot of residuals (a), normal probability plot of actual and predicted values (b) of particle size.....	83
Figure 4-18-2:	Normal plot of residuals (a), normal probability plot of actual and predicted values (b) of polydispersity index.....	83
Figure 4-18-3:	Normal plot of residuals (a), normal probability plot of actual and predicted values (b) of percentage encapsulation efficiency.....	84
Figure 4-19-1:	Three-dimensional (3D) surface plot showing the effect of phosphatidylcholine and cholesterol content on particle size.....	86
Figure 4-19-2:	Three-dimensional (3D) surface plot showing the effect of phosphatidylcholine and cholesterol content on polydispersity index (PDI)...	88
Figure 4-19-3:	Three-dimensional (3D) surface plot showing the effect of phosphatidylcholine and cholesterol content on percentage encapsulation efficiency.....	90
Figure 4-20:	Desirability ramp for the optimization process optimization.....	91
Figure 4-21:	Observed values of optimized formula (particle size, polydispersity index and percentage encapsulation efficiency) in comparison with proposed optimized formulation of RSM.....	92
Figure 4-22:	Particle size for final optimized phytosomes formulation.....	93
Figure 4-23:	Incorporation of stearic acid as charge inducer significantly.....	95

Figure 4-24:	Zeta potential of empty phytosomes (blue peak), loaded <i>H. procumbens</i> phytosomes (red peak), loaded <i>H. procumbens</i> phytosomes including stearic acid (green peak).....	96
Figure 4-25:	Representative SEM micrograph of optimized <i>H.procumbens</i> phytosomes at two different magnifications.....	97
Figure 4-26:	Represents the apparent solubility of <i>H.procumbens</i> extract and phytosomes in water and n- octanol.....	98
Figure 4-27:	FTIR spectra of (A) empty phytosomes, (B) <i>H.procumbens</i> plant extract and (C) <i>H.procumbens</i> loaded phytosomes.....	100
Figure 4-28-1:	Particle size of empty and loaded <i>H.procumbens</i> phytosomes against simulated gastric fluid (SGF) (mean±sd, n=2).....	101
Figure 4-28-2:	Polydispersity index of empty and loaded <i>H.procumbens</i> phytosomes against simulated gastric fluid (SGF) (mean±sd, n=2).....	102
Figure 4-28-3:	Zeta potential of empty and loaded <i>H.procumbens</i> phytosomes against simulated gastric fluid	103
Figure 4-28-4:	Harpagoside release from <i>H. procumbens</i> phytosomes in simulated gastric fluid (SGF).....	104
Figure 4-29:	Dry and freshly prepared alginate coated <i>H.procumbens</i> phytosomes.....	105
Figure 4-30:	Alginate coated <i>H.procumbens</i> phytosomes particle size as a function of different alginate and calcium chloride concentrations.....	106
Figure 4-31:	Alginate coated <i>H.procumbens</i> phytosomes percentage encapsulation efficiency at different alginate and calcium chloride concentrations	107
Figure 4-32:	Erosion and release from alginate coated <i>H.procumbens</i> phytosomes at different sodium concentrations; (A) 2% calcium chloride (B) 4% calcium chloride as cross linking solution	108
Figure 4-33:	Erosion of alginate coated <i>H.procumbens</i> phytosomes in PBS 7.4 at different sodium alginate concentrations formulation and 4% CaCl ₂	109

Figure 4-34-1:	Spherical shape of dry and freshly prepared alginate coated <i>H.procumbens</i> phytosomes.....	110
Figure 4-34-2:	SEM micrograph of surface microstructure of the dried alginate coated <i>H.procumbens</i> phytosomes.....	110
Figure 4-35:	FTIR spectra of sodium alginate, empty alginate coated phytosomes, <i>H.procumbens</i> phytosomes and alginate coated <i>H.procumbens</i> phytosomes.....	111
Figure 4-36:	Swelling index of alginate coated <i>H.procumbens</i> phytosomes in simulated gastric fluid (SGF) and simulated intestinal fluid (SIF).....	113
Figure 4-37:	Release profile of <i>H.procumbens</i> phytosomes in simulated gastric fluid (SGF) and simulated intestinal fluid (SIF).....	114
Figure 4-38:	Intact alginate coated <i>H.procumbens</i> phytosomes in SGF and eroded alginate coated <i>H.procumbens</i> phytosomes in SIF.....	115
Figure 4-39:	In vitro release profile of coated and un coated <i>H.procumbens</i> phytosomes and freeze dried plant extract in phosphate buffer solution (pH 7.4).....	116
Figure 4-40-1:	Release kinetics of phytosomes.....	118
Figure 4-40-2:	Release kinetics of alginate beads.....	119
Figure 4-41:	Physical stability of optimized <i>H.procumbens</i> phytosomes formulation at 3 different temperatures.....	120
Figure 4-42:	Instability of <i>H.procumbens</i> phytosomes at 37 °C.....	122
Figure 4-43:	Particle size stability of optimized alginate coated <i>H.procumbens</i> phytosomes formulation at 3 different temperatures.....	123

LIST OF TABLES

Table 2-1:	Standard zeta potential values and their related stability behaviour.....	23
Table 3.1:	Lipid vesicles formulations with diversity in lipid type.....	44
Table 3.2:	Lipid vesicle formulations prepared with constant lipid phase content and variation in plant extract content	45
Table 3.3:	The upper and lower levels of input factors set for optimization process.....	46
Table 3.4:	Generated experimental matrix by RSM optimal design.....	47
Table 3.5:	Desirability specifications of numerical optimization for <i>H.procumbens</i> nano formulation.....	48
Table 3.6:	Composition of alginate coated <i>H.procumbens</i> phytosomes formulations.....	54
Table 4.1:	Intra-day precision (repeatability)	68
Table 4.2:	Intermediate precision	69
Table 4.3:	Percentage recovery of the harpagoside	70
Table 4.4:	Method robustness	71
Table 4.5:	System suitability	71
Table 4.6:	Influence vesicles sizing down method on the percentage encapsulation efficiency.....	75
Table 4.7:	Experimental matrix of RSM optimal design.....	78
Table 4.8:	Estimation of regression model, fit summary of the output factors Y_{1PS} , Y_{2PDI} and $Y_{3\%EE}$, respectively.....	80
Table 4.9:	Statistical parameters obtained from the ANOVA for the selected regression model of Y_{1PS} generated from RSM software.....	81

Table 4.10:	Statistical parameters obtained from the ANOVA for the selected regression model for Y2PDI generated from RSM.....	81
Table 4.11:	Statistical parameters obtained from the ANOVA for the selected regression model for Y3 _{%EE} generated from RSM software.....	82
Table 4.12:	Particle size of liposomes and phytosomes formulation (extracted from table 4.7).....	85
Table 4.13:	Polydispersity index of liposomes and phytosomes formulation (extracted from table 4.7).....	87
Table 4.14:	Percentage encapsulation efficiency of liposomes and phytosomes formulations (extracted from table 4.7).....	89
Table 4.15:	Zeta potential results of proposed formulation by RSM	94
Table 4.16:	Regression coefficient (R^2) and release exponent (n) values of different <i>H.procumbens</i> formulations.....	117
Table 4.17:	Exponent <i>n</i> of the power law and drug release mechanism from phytosome delivery systems.....	118



LIST OF ABBREVIATIONS

abbervation	Full name
<i>H. procumbens</i>	<i>Harpagophytum procumben.</i>
PC	Phosphotydylcholine.
Lec	Lecithin.
Chol	Cholesterol.
PBS	Phosphate buffer solution.
UHPLC	Ultra high performance liquid chromatography.
LC-MS	Liquid chromatography-mass spectrometry.
PS	Particle size.
ZP	Zeta potential.
PDI	Polydispersity index.
% EE	Percentage encapsulation efficiency.
SEM	Scanning electron microscope.
SGF	Simulated gastrointestinal fluid.
SIF	Simulated intestinal fluid.
RSM	Response surface methodology.
ANOVA	Analysis of variance.
Mg/ml	Milligram/ mililiter.
Nm	Nanometer.
mV	Millivolts .

μm	Micrometer.
Cm^{-1}	Centimeter ⁻¹ (reciprocal centimeters).
(R^2)	Correlation coefficient.
M/Z	Mass-to-charge ratio.
% RSD	Percentage relative standard deviation.
min	Minutes



DEDICATION

For my parents (get well soon daddy).

For my family.



UNIVERSITY *of the*
WESTERN CAPE

ACKNOWLEDGEMENTS

First and foremost, praise and thanks must be given to God (ALLAH), the creator and the guardian, for giving me the opportunity to undertake such a momentous task for giving me the courage, patience, strength and the knowledge to get through to the end.

Especially thank for the following people:

My supervisor, Dr. Dube, my Co-supervisor Dr. Ebrahim, for their help, support and guidance in completing this research project. This would not be possible without you.

Profe M. Mayer, I sincerely thank you for welcoming me into the biotechnology department. Your welcoming attitude will forever be appreciated. Dr. M. Drah, I wish to express my sincere appreciation for his support and the valuable advice given throughout the study. I truly value and appreciate your contribution to this thesis.

Mr. R. Baboo for his editing service. Mr. M. Y. Kippe for his help with LC/MS and UHPLC analysis throughout this research, Thank you for all the help in the analytical laboratory and always being there for me your wisdom and understanding will always be remembered.

Mr. S. Dyantyi and Mrs. E. Kuhn; Many thanks for all your assistance. My writing coach S. Omoruyi and My statistician M. Mulubwa your help, advice are truly appreciated.

My dearest friends Hanan, Reem, Souad, Jean, Tendai, Myolisi and pharmaceuticals colleagues, for your kindness and always listening and, support. Your friendship has given me strength and added so much positive energy to my life. Thank you for your wise, inspirational advice and unfaltering encouragement. To school of pharmacy staff members, for their encouragement.

Special thanks to my parents, whose never-ending love, encouragement, wisdom, motivation, support and confidence in me have enabled me to acquire this achievement. I wish to thank my sister and my brothers for their love, support and encouragement.

And finally but most importantly thanks to my dear husband and my little boy and girl for all the motivation, continuing support and the understanding during the time that I was busy with this research. This meant a lot to me. Your love, wisdom, encouragement, kindness and calm

temperament has given me the strength to complete this thesis even when times were tough. Your wisdom and understanding will always be remembered.

Thank you for all the help with completing this research project. This research would be impossible to complete without all of you.



Chapter 1

Introduction

1.1 Background and Problem Definition

Medicinal plants are commonly used in South African traditional healthcare to treat a range of ailments (Clarkson *et al.*, 2004). According to recent estimates by the World Health Organisation (WHO), more than 3.5 billion people in the developing world rely on plants as components of their primary health care (Xego *et al.*, 2016).

South Africa is a country with a strong history of traditional healing which hosts around 30,000 plant species of which 3000 species are used therapeutically. Around 80% of the South African population use traditional medicines for their primary health care needs (Street, 2012). The reliance on traditional medicine of such a large portion of the population can be attributed to a number of factors; relatively good accessibility to the plants, affordability and extensive local knowledge and expertise amongst the communities (Street *et al.*, 2008).

One of the phytopharmaceuticals that exert anti-inflammatory effects is *Harpagophytum procumbens* (Pedaliaceae). Extracts of this herbal drug have become the focus of research as a potential therapeutic agent in the treatment of arthritis and pain due to its favourable side effects profile compared to synthetic alternatives. Moreover, non-steroidal anti-inflammatory drugs (NSAIDs) are often associated with serious adverse effects in long-term use, such as gastric ulceration, hepatic toxicity, and haemorrhage (Tan *et al.*, 2016).

Harpagophytum procumbens, also known as Devil's Claw, is an herbaceous plant species that has high medicinal value in southern Africa (Lim *et al.*, 2014). This plant grows mainly in Namibia, Botswana, Zimbabwe and South Africa. The secondary tubers of *H. procumbens* are effective in the treatment of degenerative rheumatoid arthritis, osteoarthritis, tendonitis, kidney inflammation (Mncwangi *et al.*, 2012). Therefore, *H. procumbens* has been increasingly considered an alternative to non-steroidal anti-inflammatory drugs (Ludwig-Müller *et al.*, 2008.). Harpagoside is believed to be a main bioactive compound of *H. procumbens* related to the anti-inflammatory efficacy of this plant (Kim *et al.*, 2015).

H. procumbens has been claimed to possess inhibition potential of inducible nitric oxide (NO), inflammatory cytokines (IL-6, IL-1 β) and tumour necrosis factor-alpha (TNF- α), and prostaglandine-2 (PGE₂), direct inhibition of cyclooxygenase-2 (COX-2) enzyme as well as prevention of arachidonic acid metabolism and eicosanoid biosynthesis, leading to COX-2 inhibition and reducing inflammation (Gyurkovska *et al.*, 2011; Akhtar *et al.*, 2012; Ebrahim *et al.*, 2011; Sheu *et al.*, 2015).

H. procumbens was mainly administered as one of the following: an infusion, decoction, tincture, powder, and extract. While infusions and decoctions are the most central traditional methods of preparation, the main active principles in the plant are prone to hydrolysis (Street *et al.*, 2012). It has been proposed that stomach digestion influences the pharmacological activity of *H. procumbens* (Hostanska *et al.*, 2014; Soulimani *et al.*, 1994) resulting in reduced activity when administered orally (Catelan *et al.*, 2006). This may be due to acid hydrolysis or denaturing of the active principles as they pass through the stomach (Soulimani *et al.*, 1994; Mncwangi *et al.*, 2012).

Encapsulation of plant extract in lipid based drug delivery systems might be a good solution for protecting the plant material and obtaining the required properties. The bioavailability and absorption of water soluble phytoconstituents is erratic due either to their large molecular size which cannot be absorbed by passive diffusion, or to their poor lipid solubility in the gastrointestinal tract. This severely limits their ability to cross the lipid-rich biological membranes, resulting in poor bioavailability (Bhattacharya *et al.*, 2009; Udapurkar *et al.*, 2016). This could be overcome by a novel drug delivery system (NDDS); that converts the water-soluble plant extract molecules into a lipid-compatible molecular complex.

Nanotechnology may be applied to NDDS that enables a weight reduction of drug particles accompanied by an increase in stability and improved functionality. Various approaches such as liposomes, niosomes, and phytosomes, are used for the enhancement of bioavailability (Abhinav *et al.*, 2016). These systems have various advantages over the traditional formulations such as improved solubility & bioavailability, controlled drug delivery, protection of plant actives from degradation (Sharma *et al.*, 2016).

Liposomes and phytosomes are microscopic vesicles consisting of phospholipid bilayers and are utilized for hydrophilic and lipophilic drugs (Udapurkar *et al.*, 2016). The basic difference between liposomes and phytosomes is that, in the former, the active biomaterial is dissolved

in the internal pocket or it floats in the layer membrane, whereas in phytosomes the active is anchored through chemical bonds to the polar phospholipids heads and becomes an integral part of the membrane, while no bonds are formed in liposomes (Rawat *et al.*, 2012). Phytosomal technology has been effectively used to enhance the bioavailability, solubility, prolong the duration of action, reduce side effects and increase therapeutic effect of many popular plant extracts. Some of the phytoconstituents incorporated in phytosomes include extracts of *Ginkgo biloba*, grape seed, milk thistle (Sharma, 2014, Saraf, 2010) and in liposomes include colchicine, silymarin, and rosemary essential oil (Mathur, 2013, Kiaee *et al.*, 2016).

Following oral administration, the lipid component of the lipid based drug delivery system (liposomes and phytosomes) may be subjected to hydrolysis in the presence of acidic pH and eliminate the encapsulated plant materials and lose their function as a carrier. Hence, to overcome this, a possible solution is to coat the lipid vesicles with pH sensitive polymer matrices. This serves to protect the lipid vesicles from the influence of acidic environment and promote their breakdown in the intestinal medium for increased absorption of the intact liposome or phytosomes.

Alginate is a polysaccharide found in brown algae, composed mainly by linear polymers of β -(1-4)-D-mannuronic (M) and α -L-gluronic (G) acids, which are different in terms of their proportions and linear arrangements (Xu *et al.*, 2017). Alginate, a pH sensitive polymer stable at acidic pH but unstable in alkaline medium (intestinal environment) (Abbas *et al.*, 2017), have been proven to protect compounds from hostile environments, such as low pH and enzymes in the stomach. It enhances the stability of drug delivery in the stomach and achieves controlled release in the intestine (Liu *et al.*, 2017). Sodium alginate is a suitable carrier matrix because it is biodegradable, biocompatible and nontoxic orally (Devi *et al.*, 2010) and has been used as a gastro-resistant carrier in simulated gastric fluid (Smith *et al.*, 2010; Cerciello *et al.*, 2016).

Inspired by this knowledge we aimed to design a novel delivery system based on alginate hydrogel micro beads containing *Harpagophytum procumbens* extract loaded lipid vesicles (liposomes) to enhance the stability in the acidic region of the gastro-intestinal tract for improved intact delivery and release of liposomes in the small intestinal environment.

1.2 Aim and objectives of the study

The aim of the study is to develop an optimized lipo/phytosomal carrier system consisting of *Harpagophytum procumbens* coated with alginate for protection from gastric digestion. To achieve the aim the following objectives were set:

- Development and validation of a rapid, simple and reliable UHPLC method for identification and quantification of harpagoside in *Harpagophytum procumbens* crude plant extract.
- Preparation of liposomes and phytosomes formulations containing *Harpagophytum procumbens* plant extract.
- Optimization studies of liposomes and phytosomes formulation parameters using response surface methodology (RSM).
- Physio-chemical characterization of prepared liposomes and phytosomes.
- Formulation and development of an alginate coating method for phytosomal formulation encapsulation.
- To perform *in vitro* stability of the optimized nano lipid vesicles and alginate coated beads in simulated gastric and intestinal medium.
- Determine the mechanism of release of harpagoside from phytosomes and alginate coated phytosomes.
- Determine the stability of harpagoside in phytosomes and alginate coated phytosomes at various temperatures over time.

Chapter 2

Literature review

2.1 Background

For a very long time, herbal medicine has a topic of global importance, making an impact on both world health and international trade. Medicinal plants continue to play a central role in the healthcare system of large proportions of the world's population (Akerele, 1988). This is particularly true in developing countries, where herbal medicine has a long and uninterrupted history of use. Recognition and development of the medicinal and economic benefits of these plants are on the increase in both developing and industrialized nations (WHO, 1998).

The WHO estimates that up to 80 percent of people still rely on herbal remedies for their health care (Mahomoodally, 2013). Several factors are responsible for this, namely, the high cost of drugs, drug resistance which often lead to treatment failure and expensive treatment of some chronic diseases which the general populace cannot afford (Afolayan *et al.*, 2004). In Africa, traditional healers and remedies made from plants play an important role in the health of millions of people. There are an estimated 200 000 indigenous traditional healers in South Africa and up to 80 % of South Africans consult these healers, usually in addition to using modern biomedical services (Xego *et al.*, 2016). It is estimated that over 3000 species of South African plants are used regularly in traditional medicine and around 38 species are being exploited commercially which include *Harpagophytum procumbens* (Kuate, 2013).

2.2 *Harpagophytum procumbens*

2.2.1 Description

Harpagophytum procumbens (*H. procumbens*) is a perennial herb belonging to the *pedaliaceae* family commonly known as Devil's Claw. Other common names include grapple plant, wood spider, and harpago. The vernacular name, Devil's Claw is derived from the fact that the fruits of the plant are covered in small claw-like protrusions. Similarly, its herbal name *Harpagophytum* translates from the Greek 'harpago', which means 'a grappling hook'

(Grant *et al.*, 2007). A photograph of *H. procumbens* leaves; flower and fruit can be seen in figure 2.1.



Figure 2-1: *H. procumbens* with flower, fruit (seed capsule) and bluish green leaves. (Source: Muzila, 2016).

The part used medicinally is the water-storing secondary tuberous roots as can be seen in figure 2.2 which are formed in order to survive the dry seasons encountered in the sub-Saharan regions. The roots are harvested and subsequently sliced into sections and dried before being used therapeutically (Grant *et al.*, 2007).



Figure 2-2: *H. procumbens* with secondary tubers. (Source: Georgiev *et al.*, 2013.).

H. procumbens plant tubers have been used by the native population of southern Africa for treating a number of ailments, including fever, diabetes, diarrhoea and blood diseases (Van Wyk *et al.*, 2011). More recently, extracts of the secondary roots of the species have been found to be effective in the treatment of degenerative rheumatoid arthritis, osteoarthritis, tendonitis, kidney inflammation and heart disease (Georgiev *et al.*, 2010). Therefore *H. procumbens* has been increasingly considered an alternative to non-steroidal anti-inflammatory drugs (Georgiev *et al.*, 2010).

2.2.2 Geographical distribution and habitat

H. procumbens occurs in Namibia, Botswana, South Africa, Angola and to a lesser extent Zambia, Zimbabwe and Mozambique, the geographical distribution of *H. procumbens* is depicted in figure 2.3. It typically grows in areas with low annual rainfall such as the red sandy soils of the Kalahari desert. Both the abundance and visibility of the plant strongly depends on rainfall. It is most abundant in open, overgrazed areas as it does not compete well with grasses and has a clumped distribution (Stewart *et al.*, 2005). To enable survival during long severe dry periods, the plant forms water-storing secondary tubers which branches off horizontally from the primary tubers.

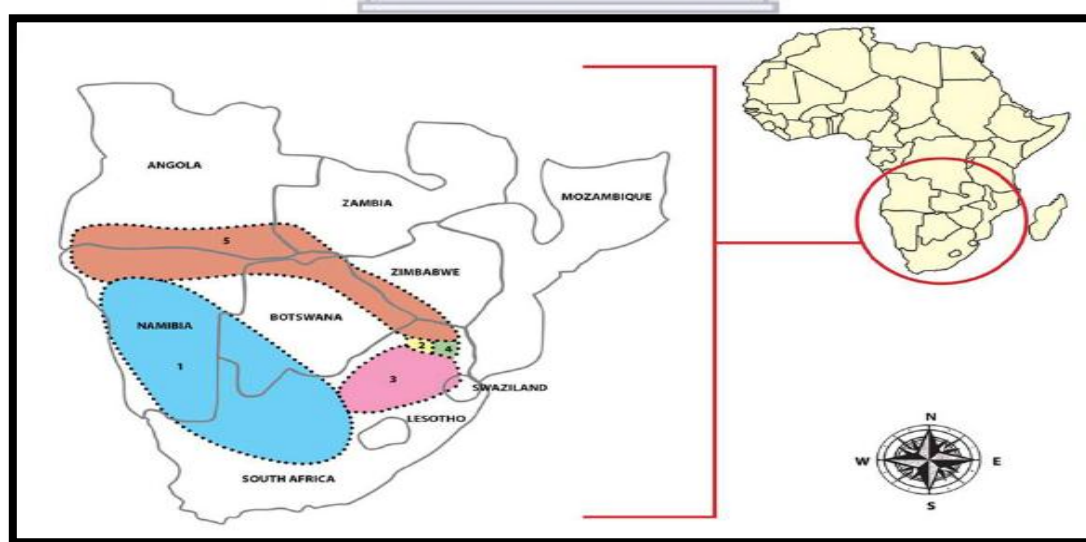


Figure 2-3: Geographical distribution of *H. procumbens* (region 1). (Sorec: Mncwangi *et al.*, 2014).

2.2.3 Phytochemistry: Main and active constituents

H. procumbens has been known as a medicinal plant with the San of the Kalahari having

used it first, many generations ago. The major chemical constituents of *Harpagophytum* are iridoid glycosides (primarily harpagoside, harpagide, and procumbide), sugars (mainly the tetrasaccharide, stachyose), triterpenoids (oleanolic and ursolic acid), phytosterols (primarily beta-sitosterol), aromatic acids (caffeic, cinnamic, and chlorogenic acids), and flavonoids such as luteolin and kaempferol (Akhtar *et al.*, 2012). However, the main pharmacological activity of *H. procumbens* extracts is attributed to harpagoside, and its content is used to standardize commercial *H. procumbens* products, which should contain at least 1.2 % of the compound. Iridoid glycosides are believed to act synergistically or antagonistically in modulating the enzymes responsible for inflammation. However, most official monograph specifications are based on harpagoside content alone (Viljoen *et al.*, 2012).

2.2.4 Clinical usefulness

The European Scientific Cooperative on Phytotherapy (ESCOP) monograph ESCOP recommends the use of Devil's claw for symptomatic treatment of painful osteoarthritis, relief of low back pain, loss of appetite, and dyspepsia (Babili *et al.*, 2012). It has also been used as a folk remedy for the relief of arthritis, lumbago, and muscular pain and has anti-rheumatic and anti-inflammatory properties (Naidoo *et al.*, 2014). It has been shown to exhibit a variety of biological activities and used as pharmaceutical products for the treatment of inflammatory ailments, rheumatoid arthritis, and osteoarthritis (Chrubasik *et al.*, 2007). Several clinical and animal studies have demonstrated the efficacy of *H. procumbens* in rheumatic diseases, in addition to its analgesic properties (Andersen *et al.*, 2004). Several investigations have also found that extracts have good anti-inflammatory and analgesic activities in carrageenan-induced acute inflammation (Dimitrova *et al.*, 2013).

A standardized extract of *H. procumbens* has been shown to alleviate rheumatic pain (Chrubasik *et al.*, 2000). Preparations are also used in the treatment of osteoarthritis (OA) (Saanders *et al.*, 2011; Chrubasik *et al.*, 2007). A recent study by Gyourkovska, *et al.* (2011) reported anti-inflammatory action by several fractions as well as pure compounds of this extract.

2.2.5 Pharmacological effect as anti-inflammatory

H. procumbens has anti-inflammatory effects (Viljoen *et al.*, 2012) through a variety of mechanisms for inflammation. The main mechanism is by inhibiting the release of different pro-inflammatory mediators. A review of clinical trials utilizing its preparations for the

treatment of inflammatory disorders shows that extracts from tubers of *H. procumbens* also inhibit different pro-inflammatory mediators; suppressed the release of TNF- α (tumor necrosis factor gene), IL-6 and IL-8 (interleukins genes expression), in LPS-stimulated monocytic THP-1 cells at non-cytotoxic concentrations, thereby inhibiting inflammation (50-250 $\mu\text{g/ml}$) (Hostanska *et al.*, 2014). Extracts tested on isolated murine macrophages, has shown strong anti-inflammatory properties related to nitric oxide (NO) and cytokine (TNF- α and IL-6) release as well as COX-1 and COX-2 inhibition expression by macrophages (Gyurkovska *et al.*, 2011). Ebrahim and Eubel, (2011) demonstrated direct inhibition of COX-2 enzyme by *H. procumbens* extract and its active components namely, harpagoside and harpagide.

2.2.6 Dosage forms

H. procumbens was first administered as an infusion but currently it is almost exclusively supplied as an ethanol tincture or as a dry extract in tablet or capsule form (Grant *et al.*, 2007). However, the dried extract is generally more acceptable than the solution form, but it may also have further disadvantages. For instance, the dried extract powder may not have uniform particle size, adequate flow characteristics and might be hygroscopic. Further, it has been proposed that stomach digestion influences the pharmacological activity of *H. procumbens*. Some studies have indicated that the analgesic and anti-inflammatory effects of *H. procumbens* are decreased by the acidity of stomach due to acid hydrolysis or denaturing of the active principles (Bone *et al.*, 2013; Soulimani *et al.*, 1994). Catelan *et al.* reported that the intraperitoneal administration of *H. procumbens* extracts administered to rats 30 min prior to carrageenan injection exerted inhibitory effects on the acute inflammatory response. More importantly, they observed it was ineffective to reduce the intensity of inflammatory response when administered orally (Catelan *et al.*, 2006).

The delivery of plant/herbal therapeutic molecules is problematic due to poor solubility, poor permeability, low bioavailability, instability in biological milieu and extensive first pass metabolism. These limitations of herbal drugs can be overcome by attaching or encapsulating them with suitable nanomaterials. The nanomaterials can significantly enhance the pharmacokinetics and therapeutic index of plant drugs. Targeted delivery and combination therapy can drastically improve the performance of herbal drugs (Kumari *et al.*, 2012).

2.3 Intestinal absorption

The most desirable route of administration for therapeutic agents is oral; as it avoids pain and risk of infection associated with parenteral administration and thereby increases patient compliance. However most of the orally administered drugs display low systemic availability and diminished efficacy (Gavhane *et al.*, 2012). As for the drug absorption after oral administration, the gastrointestinal (GI) transit of a drug is an important factor to determine the drug absorption (Kimura *et al.*, 2002). The luminal environment is complex, and drug absorption may be affected by several physiological factors, including volume and viscosity of the gastrointestinal fluids, the pH and buffer capacity of these fluids. These can vary greatly in different regions of the gastrointestinal (GI) tract (Fadda *et al.*, 2010). One requirement for successfully delivering drugs orally is by protecting drugs from degradation in the acidic environment (low pH) of stomach. Figure 2.4 shows the pH range in the GI tract.

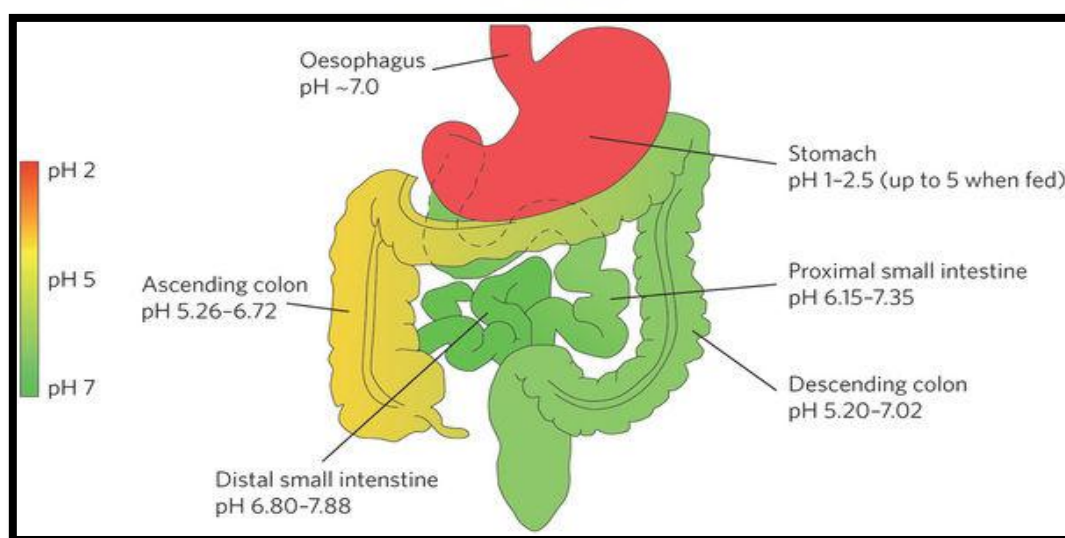


Figure 2-4: Varying pH in the gastrointestinal tract (source, Khutoryanskiy *et al.*, 2015).

The stomach is typically the first section of the GI tract, in which disintegration and dissolution take place. The intestines are the main absorption site for nutrients and drugs. Moreover, literature suggests a subsequent increase of the pH value from pH 6 in the duodenum to pH 7–8 in the terminal ileum. The transit time through the small bowel in healthy humans typically amounts to 3 to 6 hours (Koziolek *et al.*, 2015).

The investigation of drug dissolution in media mimicking gastric and intestinal conditions is required to understand drug formulations and their delivery processes. Dissolution testing is frequently used to determine the rate and extent at which a drug released from a dosage form

and it plays many important roles throughout drug product development (Fang *et al.*, 2010). Drug dissolution in the physiological environment of the GI tract is the primary step in the oral absorption process from a pharmaceutical dosage form.

During drug dosage form development it is essential to investigate factors which influence absorption especially after oral administration (Dressman *et al.*, 2000). Simulation of gastrointestinal conditions is essential to adequately predict the *in vivo* performance of drug formulations. *In vitro* dissolution tests should mimic a drug performance in a human proximal gastrointestinal tract (GIT). To establish reliable *in vitro* testing it is important that artificial environments simulate physiological conditions as closely as possible. The level of the simulation is dependent on many factors related to equipment and simulated medium (Gruberova *et al.*, 2017).

2.3.1 Simulated Gastric Fluid (SGF)

SGF is a traditional medium to simulate gastric conditions. This synthetic fluid will mimic the effect of the gastric juice in the stomach on a particular drug. This medium contains hydrochloric acid and sodium chloride and water, and has a pH of 1.2. Drugs made for dissolution and disintegration in the small intestine must not disintegrate or dissolve in the in the Simulated Gastric Fluid (SGF). On the other hand, drugs designed to act in the stomach will dissolve in this synthetic solution of Simulated Gastric Fluid (SGF) (Klein, 2010).

2.3.2 Simulated Intestinal Fluid (SIF)

SIF is an artificial dissolution medium form of intestinal solution for the simulation of small intestinal (SI) conditions. It is used to predict the *in vivo* behaviour of drug formulations when administered orally (Klein, 2010). The extent to which the analysed pharmaceutical dissolves and releases its actives in the simulated intestinal is a good indicator of how the pharmaceutical will be available for absorption into the system from the villi in the intestine.

Simulated gastric fluid (SGF) and simulated intestinal fluid (SIF) are widely used media in dissolution tests in the pharmaceutical industry to mimic the natural environment in which the dosage forms will be administered and to evaluate the predictive capability of a dissolution test. More commonly SGF and SIF media are prepared and utilized in dissolution tests without enzymes (Medina *et al.*, 2017).

2.4 Nanotechnology

Nanotechnology is defined as the intentional design, characterization, production and application of materials, structures, devices, and systems by controlling their size and shape in the nanoscale range (Solano-Umaña *et al.*, 2015). Nanotechnology plays a central role in the recent technological advances in the areas of disease diagnosis, drug design and drug delivery and could overcome challenges such as drug toxicity, sustaining the release of drugs in the body and improving bioavailability. Drugs, which are water insoluble and unstable in the biological environment, may be delivered properly with nanotechnology. Nanostructures can protect drugs from hydrolytic and enzymatic degradation (Caban *et al.*, 2014). They also prevent drugs from first-pass metabolism and increase the blood residence time. They can penetrate tissues efficiently due to their reduced size. In addition, drugs which are produced at nanoscale may pass biological barriers (Caban *et al.*, 2014). Nanostructures exhibit unique physicochemical and biological properties (e.g., an enhanced reactive area as well as an ability to cross cell and tissue barriers) due to their small sizes, which make them a favourable material for biomedical applications (Abhinav *et al.*, 2016). Various approaches such as liposomes, niosomes, nanoemulsions, phytosome etc., are used for the enhancement of bioavailability (Abhinav *et al.*, 2016).

2.5 Lipid-based drug delivery systems

Lipid based drug delivery systems (LDDS) consists of a diverse group of formulations, each consisting of varying functional and structural properties that are amenable to modifications achieved by varying the composition of lipid excipients and other additives. Generally, most lipid drug delivery systems used as drug carriers have high stability, high carrier capacity, feasible for incorporating into both hydrophilic and hydrophobic substances and variable routes of administration, including oral, topical, parenteral and pulmonary routes (Chime *et al.*, 2013).

Lipids have gained much interest as carriers for the delivery of drugs with poor water solubility (Pouton, 2006). The availability of novel lipid excipients with acceptable regulatory and safety profiles coupled with their ability to enhance oral bioavailability has helped in the development of lipid based formulations as a means for drug delivery

Lipid-based formulations, in many cases may reduce or eliminate the influence of food on the absorption of these drugs (Shrestha *et al.*, 2014). Despite this, marketed oral drug products

employing lipid-based formulations are currently outnumbered 25 to 1 by conventional formulations (Shrestha *et al.*, 2014).

Lipid-based formulations can be applied to influence the absorption of active ingredients through different mechanisms, such as modifying the release of active ingredients, improving their bioavailability and stability, changing the composition and character of the intestinal environment, stimulating the lymphatic transport of active ingredients, and interact with enterocyte-based transport processes and reducing unwanted drug side effects (Fricker *et al.*, 2010).

2.5.1 Types of lipid based systems

A wide variety of lipid based systems have been explored and it is broadly classified into three types, namely, emulsion based system, vesicular system and lipid particulate system. These systems have the potential to solubilize the drug in a controlled manner with a unique mechanism for each classification of lipid based drug delivery systems are given in figure 2.5.

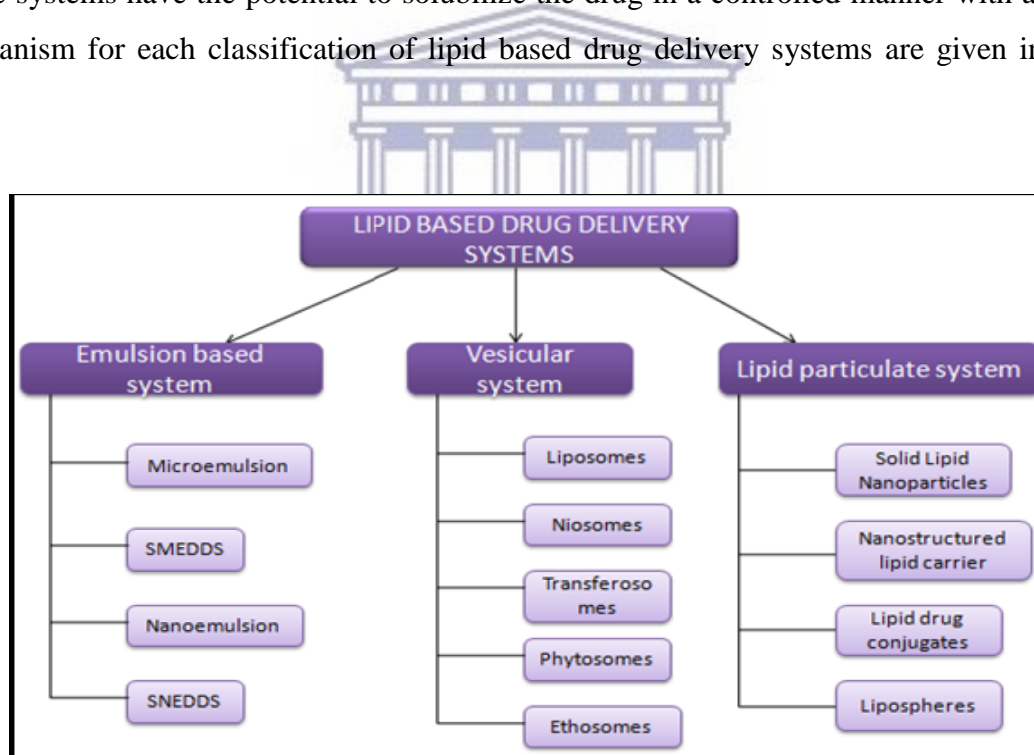


Figure 2-5: Classification of lipid based drug delivery system. (Source: Singh, 2015).

2.5.2 Liposomes

The word “liposome” is derived from two Greek words viz. lipo- meaning fat and soma- meaning body. They were called “Bangasomes” honouring Dr. Bangham, and finally liposomes (Kim, 2016). A liposome is colloidal, spherical vesicle with a membrane

composed of a phospholipid bilayer used to deliver drug or genetic material into a cell. Liposomes were first produced in England in 1961 by Alec D. Bangham, who found that phospholipids combined with water immediately and formed a sphere because one end of each molecule is hydrophilic, while the opposite end is hydrophobic. Water soluble medications added to the water were trapped inside the aggregation of hydrophobic ends while fat-soluble medications were incorporated into the phospholipid layer (Shailesh *et al.*, 2009).

Liposomes are the most common and well-investigated nanocarriers for targeted drug delivery. They have improved therapies for a range of biomedical applications by stabilizing therapeutic compounds, overcoming obstacles to cellular and tissue uptake, and improving biodistribution of compounds to target sites in vivo (Ding *et al.*, 2006; Hua *et al.*, 2013).

As a drug delivery system, liposomes offer several advantages including biocompatibility, biodegradability, low toxicity, capacity for self-assembly, ability to trap both hydrophilic and lipophilic drugs, and a wide range of physicochemical and biophysical properties that can be modified to control their biological characteristics (Akbarzadeh *et al.*, 2013).

2.5.2.1 Preparation of liposomes

There are several methods for the preparation of liposomes: thin film hydration method, ether injection method, reverse phase evaporation method, lyophilization method. The type of preparation method influences the properties of liposomes, including their shape, size, stability and drug loading efficiency (Akhtar, 2014).

2.5.2.1.1 Thin-film hydration method

One of the most widely used techniques for liposome manufacturing is the thin-film hydration or Bangham method. Briefly, as represented in figure 2.6, this method involves dissolving the lipids in an organic solvent, evaporation of the solvent under reduced pressure to produce a thin film of lipids, and the hydration of the obtained lipid film in aqueous media. The drug to be entrapped can be included in the aqueous media (for hydrophilic drugs) or in the lipid film (for lipophilic drugs). However, this method produces large and nonhomogeneous multi lamellar vesicles (MLVs) that require sonication or extrusion processes to produce homogeneous small unilamellar vesicles (ULVs) (Bozzuto *et al.*, 2015).

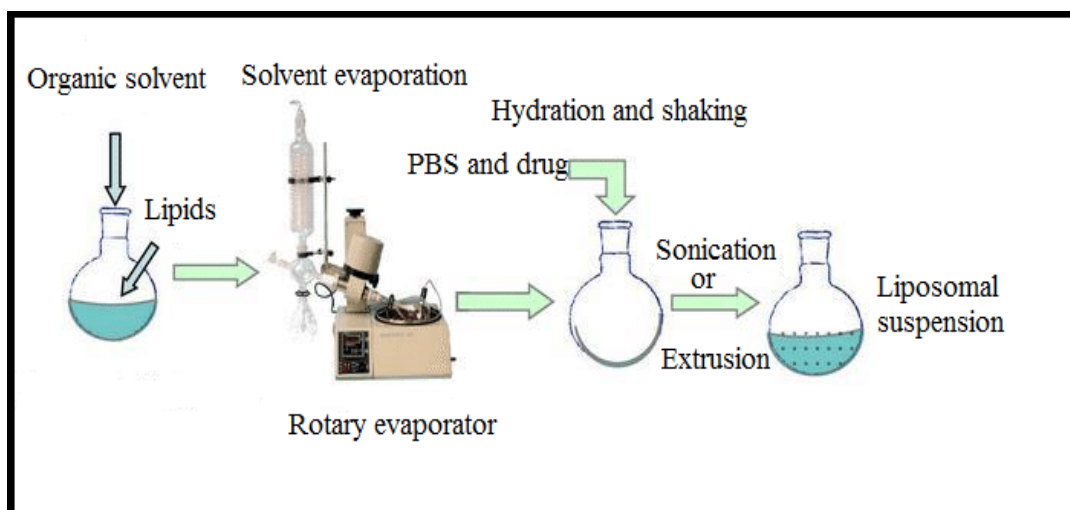


Figure 2-6: Liposomes manufacturing steps. (Source: Ghanbarzadeh *et al.*, 2013) with some modification.

2.5.2.2 Types of liposomes

Liposome size can vary from very small to large vesicles and may have one or bilayer membranes as depicted in figure 2.7. On the basis of their size and number of bilayers, liposomes can also be classified into one of two categories: (1) multilamellar vesicles (MLV): these vesicles have many bilayers and big in size and may be up to 5 μm and (2) unilamellar vesicles: these vesicle has a single phospholipid bilayer sphere enclosing the aqueous solution. Unilamellar vesicles can also be classified into three categories: (1) large unilamellar vesicles (LUV) with a size range from 100 to 1000 nm and (2) small unilamellar vesicles (SUV) with sizes range of 20 to 100 nm (3) oligolamellar vesicles, these are made up of bilayers of lipids surrounding a large internal volume (Shashi *et al.*, 2012).

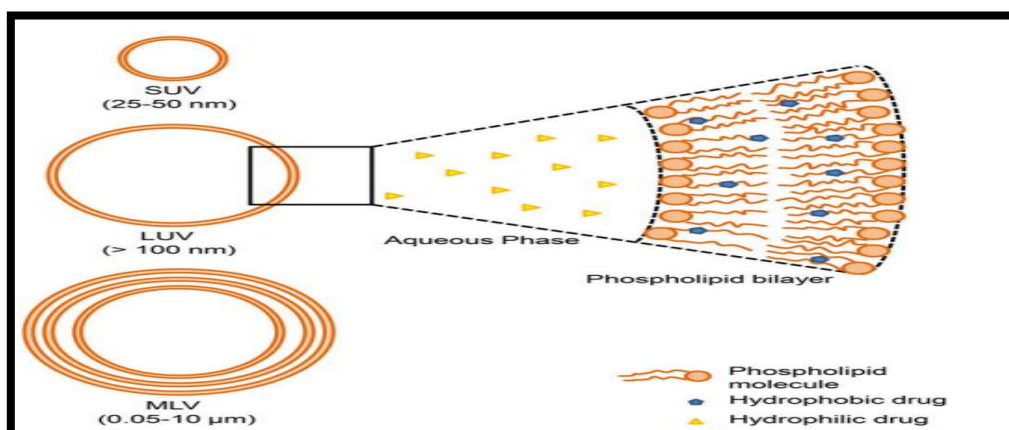


Figure 2-7: Classification of liposomes based on the lamellarity and size. (Source: Yingchoncharoen *et al.*, 2016).

2.5.3 Phytosomes

The term *phyto* means plant while *some* means cell-like (Sharma *et al.*, 2016). Phytosome structures contain the active ingredients of the herb surrounded by the phospholipids. Phytosomes are advanced forms of herbal products that are better absorbed, utilized, and as a result produce better results than conventional herbal extracts (Shelke, 2012). Phytosomes protect valuable component of herbal extracts from destruction by digestive secretion, demonstrates better absorption which produces better bioavailability and improved pharmacological parameters than conventional herbal extracts (Pawar *et al.*, 2015). In phytosomes, the complex of phospholipids and water soluble active plant components involve chemical bond formation and therefore becomes more stable (Nayyer *et al.*, 2015).

2.5.3.1 Difference between liposome and phytosome

In principle, both liposome and phytosome systems are vesicular structures prepared by phospholipids and the fundamental difference between them is the way of drug incorporation in their structure. Phytosomes are not liposomes - structurally, the two are distinctly different as shown in figure 2.8. The phytosome is a unit of a few molecules bonded together, while the liposome is an aggregate of many phospholipid molecules that can enclose other phytoactive molecules but without specifically bonding to them (Rawat *et al.*, 2012).

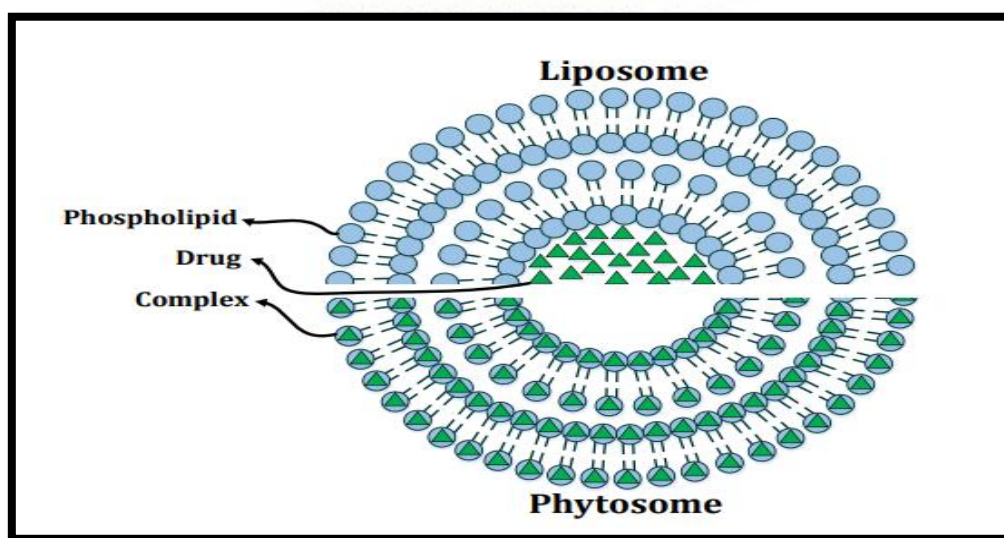


Figure 2-8: Difference between phytosome and liposome. The molecular organization of phytosomes (lower segment) and liposomes (upper segment). (Source: Karimi *et al.*, 2015).

In liposomes the active ingredient is dissolved in the medium contained in the cavity or in the layers of the membrane, no chemical bond is formed; the phosphatidylcholine molecules

collectively surround the water-soluble substance (Rawat *et al.*, 2012). There may be hundreds or even thousands of phosphatidylcholine molecules surrounding the water-soluble compound. In contrast, with the phytosome it is an integral part of the membrane, being the molecules anchored through chemical bonds to the polar head of the phospholipid. The phosphatidylcholine and the individual plant components actually a 1:1 or a 2:1 complex depending on the substance. Unlike liposome, chemical bonds are formed between phosphatidylcholine molecule and phytoconstituent, so the phytosomes show better stability profile (Rani *et al.*, 2007).

2.5.3.2 Preparation of phytosomes

Phytosomes are formulated by the processes in which the standardized extract of active ingredient are bound to phospholipid like phosphatidylcholine (PC), phosphatidylethanolamin or phosphatidylserine through a polar end (Amit *et al.*, 2013). Phytosomes are prepared by one of the following methods: anti-solvent precipitation technique, rotary evaporation technique, solvent evaporation technique, ether injection technique (Udapurkar *et al.* 2016).

In recent years, a variety of phospholipid-related formulations (phytosomes and liposomes) have been reported to increase the bioavailability of poor lipid soluble extracts by increasing the absorption in gastrointestinal tract. Phytosome has been effectively used to enhance the bioavailability of many popular herbal extracts or active molecules as Silybin, Ginseng, Grape seed, Curcumin and olive oil (Prasad *et al.*, 2016; Dewan *et al.*, 2016). Liposome has been effectively used to enhance the bioavailability of many popular herbal extracts or active molecules as Artemisia, Catechin, Quercetin and Myrtus communis (Thapa *et al.*, 2013; Sharma, 2014).

2.5.4 Structural components of lipid based drug delivery systems

There are a number of the structural and non-structural components of lipid based formulations. The major structural components of lipid based drug delivery system are:

2.5.4.1 Phospholipids

Phospholipids are amphiphilic molecules, consisting of hydrophobic tails and a hydrophilic head. The hydrophilic head contains the negatively charged phosphate group, and may contain other polar groups. The hydrophobic tail usually consists of long fatty acid

hydrocarbon chains (Suriyakala *et al.*, 2014). When placed in water, they form various structures depending on their specific properties. Mostly, they form micelles or are organized as lipid bilayers with the hydrophobic tails lined up against one another and the hydrophilic head-group facing the water on both sides. Phospholipid molecule and its arrangement into the lipid bilayer structure are depicted in figure 2.9 and 2.10, respectively.

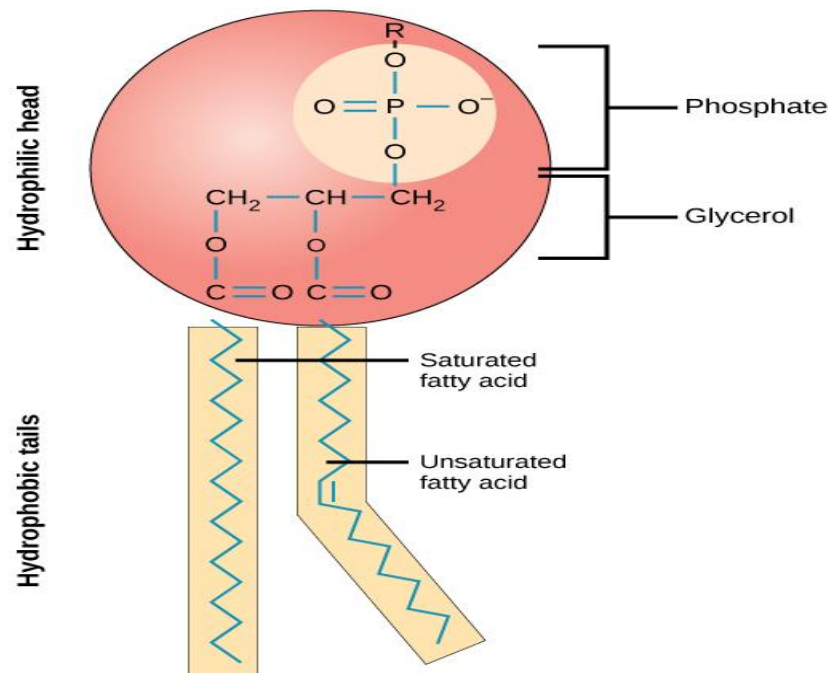


Figure 2-9: A diagram showing a phospholipid molecule with two fatty acids and a modified phosphate group attached to a glycerol backbone. (Source: Boundless, 2017).

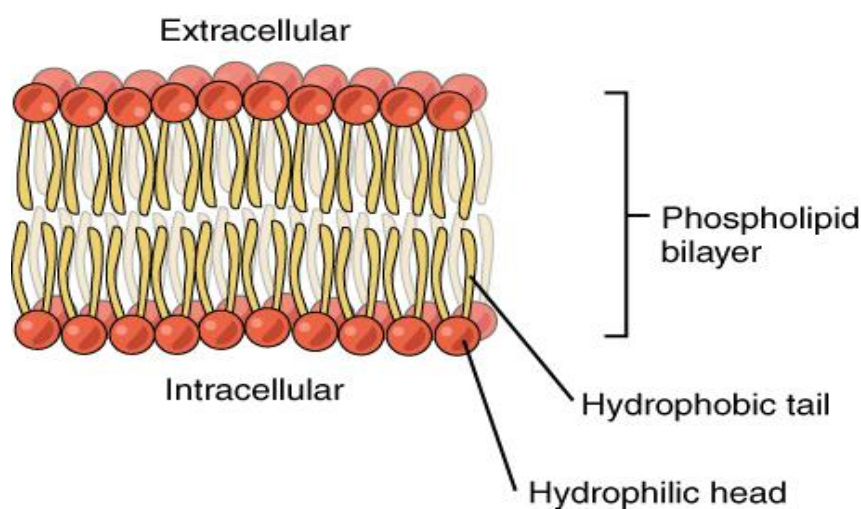


Figure 2-10: Illustration of the basic elements of a lipid, with the arrangement into the lipid bilayer structure. (Source: Boundless, 2017).

Glycerol containing phospholipids are most commonly used component of liposome formulation and represent more than 50 % of weight of lipid in biological membranes. These are derived from phosphatidic acid. The back bone of the molecule is the phosphoric ester of glycerol (Anwekar *et al.*, 2011). One of the OH groups of phosphoric acid may be further esterified to a wide range of organic alcohols including glycerol, choline, ethanolamine, serine and inositol. Examples of phospholipids are phosphatidylcholine (PC), phosphatidyl ethanolamine (PE), phosphatidyl serine (PS), phosphatidyl inositol (PI), and phosphatidyl glycerol (PG) for stable liposomes, saturated fatty acids are used. Unsaturated fatty acids are not used generally (Anwekar *et al.*, 2011).

2.5.4.1.1 Phosphatidylcholine (PC)

The commonly used lipid phase substances for producing liposomes and phytosomes are phospholipids from soy, and mainly phosphatidylcholine (PC) (Choubey, 2011). Soybean phosphatidylcholine (SPC) has been clinically available for several decades due to its biocompatibility, biodegradability, metabolic activity, and low toxicity compared to its synthetic alternatives. These abundant characteristics make SPC an attractive candidate for production of pharmaceutical dosage forms (Hou *et al.*, 2012).

Phosphatidylcholine is miscible in both water and lipid environment and well absorbed when taken orally. It has two polar and non-polar portions where, the polar head of PC, choline, interacts with phytoconstituents by creation of an H-band between phosphatidylcholine's phosphate group and hydroxyl group of phytoconstituents. Due to the chemical bond between the H-band of PC and phytoconstituents, phytosomes show better physical stability which enhances absorption of hydrophilic polar phytoconstituents resulted in enhanced bioavailability and greater therapeutic benefits (Bhattacharya, 2009).

2.5.4.1.2 Lecithin

Lecithin (phosphatidylcholine) is a generic term which is used to designate a yellow brownish fatty substance present in animal or plant tissue composed of phospholipids, phosphoric acid, triglyceride, glycolipids, etc. Lecithin is extracted from sources such as soya beans, eggs, milk, marine sources, rapeseed, cottonseed and sunflower chemically by using hexane, ethanol, etc. Lecithin has emulsification and lubricant properties (Tiwari, 2013).

2.5.4.2 Cholesterol

The presence of cholesterol in the lipid bilayer enhances the stability and can be incorporated into phospholipid membranes in very high concentration up to 1:1 or even 2:1 molar ratio of cholesterol to phosphatidylcholine. The chemical structure of cholesterol is demonstrated in figure 2.11. Cholesterol inserts into the membrane with its hydroxyl group oriented towards the aqueous surface and aliphatic chain aligned parallel to the acyl chains in the centre of the bilayer. The high solubility of cholesterol in phospholipid liposome has been attributed to both hydrophobic and specific head group interaction (Anwekar *et al.*, 2011). Cholesterol serves many biological functions. Cholesterol and its derivatives are included in the lipid bilayer membrane generally to reduce the fluidity or microviscosity of the outer membrane. Cholesterol alters the packing of phospholipid molecule in the structure, it enhances vesicle resistance capacity to form aggregates, decrease the permeability of the bilayer membrane to water soluble (hydrophilic) molecules and helps in the formation of a stable membrane in the presence of biological fluids such as plasma (Andhale *et al.*, 2016). Liposomes without cholesterol are known to interact rapidly with plasma protein such as albumin, transferrin, and macroglobulin. These proteins tend to extract bulk phospholipids from liposomes, thereby depleting the outer monolayer of the vesicles leading to physical instability. Cholesterol appears to substantially reduce this type of interaction. Cholesterol has been called the mortar of bilayers, because by virtue of its molecular shape and solubility properties, it fills in empty spaces among the Phospholipids molecules, anchoring them more strongly into the structure (Patidar *et al.*, 2015).

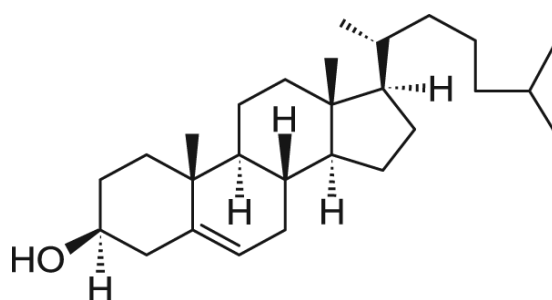


Figure 2-11: General structure of cholesterol (Source: www.avantilipids.com).

2.5.4.3 Stearic acid

Stearic acid a charge inducer used to stabilize the bilayer membrane is often incorporated in lipid based formulation because they increase the surface charge density and prevent vesicle aggregation, flocculation and fusion. The net surface charge of liposome can be modified by

the incorporation of charge inducers such as stearic acid and other compounds such as stearylamine, cetylpyridinium chloride, sodium deoxycholate, phosphatidic acid and dicethylphosphate (Nimmathota, 2016; Junyaprasert *et al.*, 2008; Khan *et al.*, 2017; Thulasiramaraju *et al.*, 2012).

An appropriate selection of lipid vehicles, formulation strategies and rational delivery system design can lead to the success of lipid based drug delivery systems (Kalepu *et al.*, 2013).

2.5.5 Characterization of liposomes and phytosomes

The behaviour of phytosomes in both physical and biological systems is governed by factors such as size, membrane permeability, percentage entrapped, chemical composition as well as the quantity and purity of the starting materials. Therefore, the phytosomes are characterized for physical attributes i.e. shape, size, its distribution, percentage drug capture, percentage drug release and chemical composition (Jain *et al.*, 2010). In order to assess the liposome and phytosomes to obtain quantitative measures that allow comparison between different lipid vesicles formulations, various parameters can be examined.

1) Morphology: The shape of lipid vesicles can be seen using Transmission and Scanning Electron Microscopy (TEM) and techniques (Ravi *et al.*, 2015; Dewan *et al.*, 2016).

2) Particle size and size distribution: The improved drug bioavailability of nanoparticles is attributed to the fact that particles in the nano-size range are efficient in crossing permeability barriers (Pandey *et al.*, 2005). The size of the vesicle governs the *in vivo* fate of lipid vesicles, because it determines the fraction cleared by the reticulo-endothelial system (RES) (Sharma *et al.*, 2016). Several techniques are available for assessing submicrometer size and polydispersity index which include microscopy techniques, size exclusion chromatography (SEC), field-flow fractionation and static or dynamic light scattering (Laouini *et al.*, 2012).

3) Zeta Potential: The zeta potential (ZP) indicates the overall charge a particle acquired in a specific medium. Stability of nanodispersion during storage can be predicted from the zeta potential value. The zeta potential indicates the degree of repulsion between close and similarly charged particles in the dispersion. High zeta potential indicates highly charged particles. Generally, high zeta potential (negative or positive) prevents aggregation

of the particles due to electric repulsion and electrically stabilizes the nanoparticle dispersion. On the other hand, in the case of low zeta potential, attraction exceeds repulsion and the dispersion coagulates or flocculates (Das *et al.*, 2011).

It is reported that microspheres with a zeta potential above (+/-) 30 mV demonstrates stabilization in suspensions (Kumar *et al.*, 2010; Al-Shdefat *et al.*, 2012). Zeta potential values and their related stability behaviour are illustrated in table 2.1 (Mayuri *et al.*, 2016).

Table 2.1: Standard zeta potential values and their related stability behaviour.

Zeta potential (mV)	Stability behaviour
0 to ± 5	Swift flocculation
± 10 to ± 30	Initial instability
± 30 to ± 40	Modest stability
± 40 to ± 60	Fine stability
More than ± 61	Tremendous stability

4) Encapsulation efficiency: The amount of drug encapsulated/entrapped in a lipid vesicle is given by the percent drug encapsulation. The first step for the determination of the encapsulation efficiency is the separation between the encapsulated drug (within the carrier) and the free drug (Laouini *et al.*, 2012). Several separation techniques have been reported which include, column chromatography, dialysis membranes and ultracentrifugation. The ultracentrifugation technique is the most common as it is a simple and fast method for the separation of drug-loaded liposomes from their medium.

5) Fourier transform infrared spectroscopy (FTIR): FTIR spectroscopy is a useful tool to determine the stability of phytosomes when dispersed in water. Complex formation can be confirmed by IR spectroscopy by comparing the spectrum of the lipid complex with the spectrum of the individual components and their mechanical mixtures. From a practical point of view, the stability can be confirmed by comparing the spectrum of the complex in solid form (phytosomes) with the spectrum of its dispersion in water after lyophilization, at different times (Sravanthi *et al.*, 2013).

6) Release study: In vitro release studies are usually based on a dialysis method (Achim *et al.*, 2009). No drug adsorption may occur and the membrane should be freely permeable to the active ingredient (the cut off molecular weight shouldn't be a limiting step in the diffusion process). The drug release from nanoparticles as represented in figure 2.12. This is either through bulk erosion in the matrix or by surface erosion in the polymer depending on the nature of drug and method of preparation adopted (Singh, 2015).

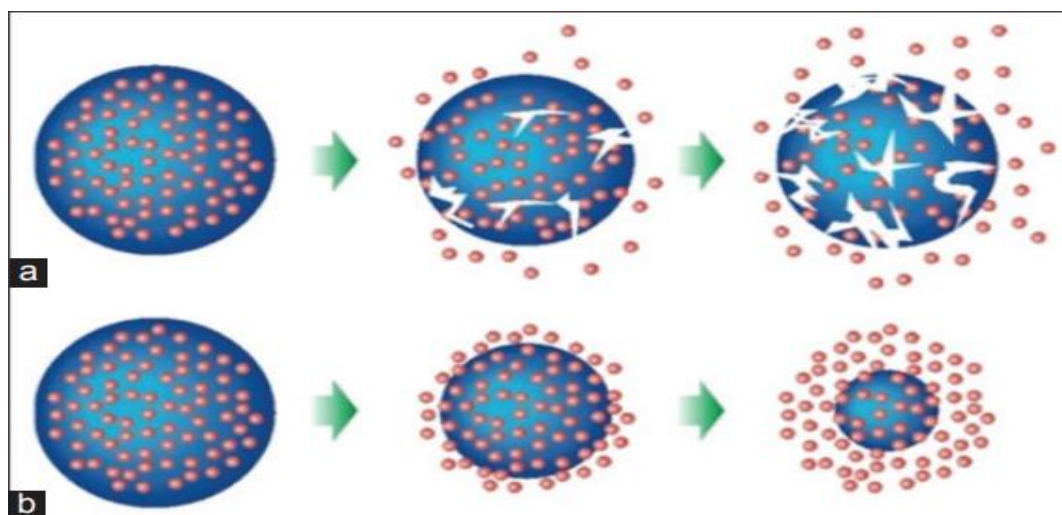


Figure 2-12: Mechanism of drug release (a) Bulk erosion (b) Surface erosion (Source: Singh, 2015).

7) Stability study: During the development of liposomal/phytosomal drug products, the stability of the developed formulation is of major consideration. The therapeutic activity of the drug is governed by the stability of the lipid vesicles from the manufacturing steps to storage and delivery (Kalepu *et al.*, 2013). A stable dosage form maintains the physical stability and chemical integrity of the active molecule during its developmental procedure and storage (Kalepu *et al.*, 2013).

2.6 Alginate coating

Alginate is a naturally occurring hydrophilic biopolymer that is extracted from brown seaweed. It is polysaccharide which contains repeating monomeric units of 1, 4-linked α -L-guluronic acid (G) and D-mannuronic acid (M) in blocks which are arranged in homopolymeric M blocks (MM) or homo-polymeric G (GG) blocks interspersed with heteropolymeric (MG) blocks as depicted in figure 2.13 (Mandal *et al.*, 2010).

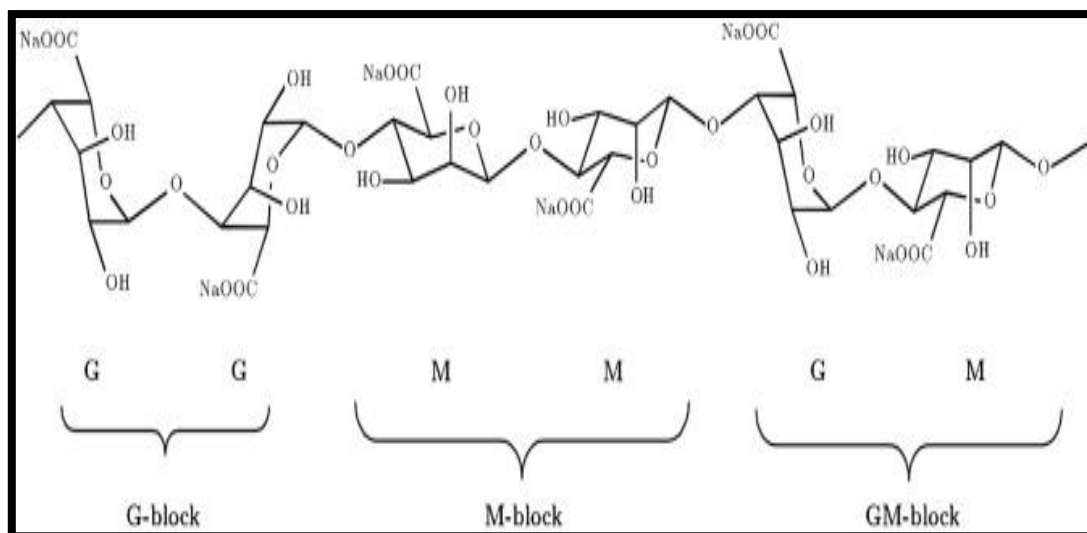


Figure 2-13: Chemical structure of repeated units of alginate: D-mannuronic acid (M) and L-guluronic acid (G). (Source: Daemi *et al.*, 2012).

Alginate is a versatile biopolymer, which has been extensively investigated and used for many biomedical applications, due to biocompatibility and biodegradability (Lee *et al.*, 2012; Sun *et al.*, 2013). In the presence of divalent cations such as calcium, binding to the negative charges of the G-blocks occurs, resulting in sodium alginate spontaneously crosslinking and forming a spherical hydrogel matrix with regular shape and size known as an alginate beads. The gelation and crosslinking of the polymer are mainly formed by chemical reaction. The calcium displaces the sodium from the alginate and holds the long alginate molecules together to form the characteristic egg-box structure shown in figure 2.14. Each alginate chain can dimerize to form junctions with many other chains and as a result gel networks are formed rather than insoluble precipitates (Jaiswal *et al.*, 2009). Alginates have different affinity for divalent cations in an increasing manner as shown: $\text{Ca}^{2+} < \text{Sr}^{2+} < \text{Ba}^{2+}$. Calcium is the most frequently used cation to ionically cross-link alginate because it is considered clinically safe, easily accessible and economical (Reis *et al.*, 2006).

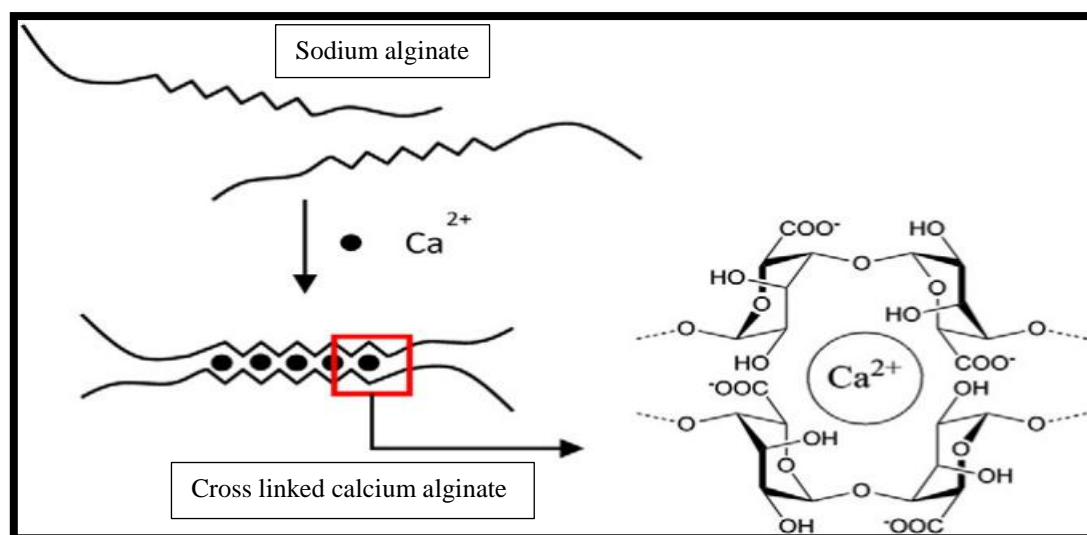


Figure 2-14: Schematic crosslink between alginate and the calcium cations resulting in “egg box model” calcium cross-linked junctions. (Source: Paques *et al.*, 2014).

Alginate bead coating is a microencapsulation technique used to improve the stability and bioavailability of products and control the rate of active agent release (Aizpurua-Olaizola *et al.*, 2016). In the presence of divalent cations such as calcium, which bind to the alginate negative charges resulting in sodium alginate spontaneously crosslinking and forming a spherical hydrogel matrix with regular shape and size, to form what is known as an alginate bead. The main strengths of alginate devices are that it withstands the degradation by gastric acid and rapid erosion at neutral pH (d’Ayala *et al.*, 2008).

Liposomes encapsulated within an alginate hydrogel have been formulated to overcome the problems of liposomes instability designed for oral consumption (Grijalvo *et al.*, 2016). Alginate hydrogels have been used as oral delivery systems in the presence of acid environment of the gastrointestinal tract. Liposomal formulation entrapping manganese porphyrin (Mn-por), was protected from the gastrointestinal tract acid environment, and embedded in alginate hydrogel beads. Both alginate hydrogels and liposomes were able to maintain their physical properties under acidic pH, allowing the delivery of Mn-por to the intestine (Aikawa *et al.*, 2015).

Alginate beads are pH sensitive rendering it suitable for the intestinal delivery systems. When cross linked alginate matrix systems are exposed to low pH, it shrinks and the encapsulated drugs are not released, forming an insoluble alginic acid in the gastric environment. Once passed into higher pH of the intestinal tract, the alginic acid is converted to a soluble viscous

layer which results in faster degradation and release of molecules. This pH dependent behaviour of alginate can be exploited to customize release profiles (Wang *et al.*, 2013; Mittal *et al.*, 2016).

2.6.1 Alginate hydrogel beads preparation

Alginate hydrogels beads can be prepared by various cross-linking approaches, including:

2.6.1.1 Ionic cross-linking

The most common methods used to fabricate alginate gel beads employ external soluble ionic cross-linking agents, such as divalent cations (i.e. Ca^{2+}). When a droplet of aqueous sodium alginate dripping from a needle tip and enters a CaCl_2 bath, Ca^{2+} ions diffuse into the alginate rich droplet faster than the rate of diffusion of alginate molecules. This results in conversion of the alginate droplets to gel beads, kinetically entrapping the originally dispersed material in the alginate solution. The gelation and crosslinking of the polymers are mainly achieved by exchange of sodium ions from the guluronic acids with divalent cations, and the stacking of these guluronic groups to form the characteristic egg-box structure as represented in figure 2.15 (Lee *et al.*, 2012; Sun *et al.*, 2013).

2.6.1.2 Covalent cross-linking

Covalently cross-linked hydrogels can be prepared from chemically modified alginates; a covalently cross-linked hydrogel is chemically stable and can provide different modes of stress relaxation. However, covalent cross-linking reagents may be toxic, and the unreacted chemicals may need to be removed from the gels. By covalently conjugating methacrylate groups onto the alginate backbone, covalently cross-linked hydrogels can be prepared in the presence of a photo initiator and UV light (Lee *et al.*, 2012; Sun *et al.*, 2013).

2.6.1.3 Thermal gelation

Thermo-sensitive hydrogels have been widely investigated in many drug delivery applications, due to their adjustable swelling properties in response to temperature changes, leading to on demand modulation of drug release from the gels (Lee *et al.*, 2012; Sun *et al.*, 2013).

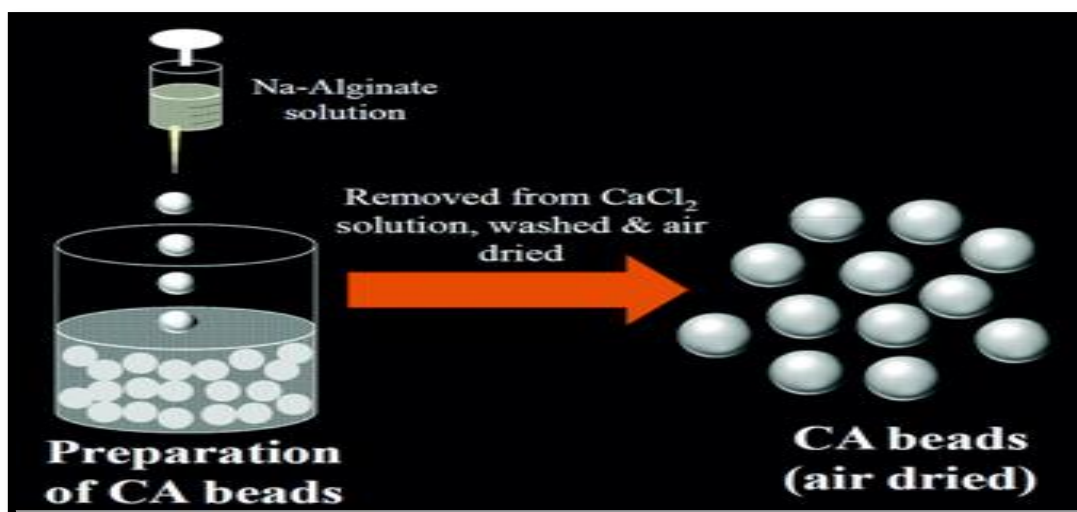


Figure 2-15: Schematic representation of alginate beads fabrication process: step 1: bead production using a syringe; step 2 sieving of the beads out of the CaCl₂ solution for washing and air drying (Source: Juárez *et al.*, 2014).

2.6.2 Physicochemical characterization of alginate hydrogels beads.

The properties of beads prepared by ionotropic gelation are influenced by formulation and processing parameters (Smrdel *et al.*, 2008). Various techniques have been employed for characterization of alginate hydrogel beads, which can be characterised for:

1) Morphology

External surface features like shape, smoothness and porosity are examined to see possible correlation with release behaviour and stability. This can be performed by scanning electron microscopy (SEM) after gold coating under vacuum (Ahmed *et al.*, 2013).

2) Particle size

The common technique for analysis of alginate bead particle sizes is to use optical microscopy with a calibrated stage micrometer (Indira *et al.*, 2012). The size of wet beads depends on the size of a droplet of polymer dispersion, which is influenced by diameter of the nozzle and viscosity of polymer dispersion. However, drying may influence the size and shape of dry beads (Smrdel *et al.*, 2008). The size of alginate beads may also be affected by the concentration of alginate and calcium (Kaza *et al.*, 2011).

3) Percentage encapsulation

The encapsulation efficiency is dependent on many factors which includes the type of drug,

polymer, concentration, additives, drug-polymer weight ratio as well as process variables such as hardening time, type and concentration of cross-linking agent (Smrdel *et al.*, 2008). Low alginate concentration leads to a decrease in drug encapsulation efficiency due to less binding sites for Ca^{2+} ions resulting in the formulation of a less compact gel membrane which increases influx of Ca^{2+} ions (Kundu *et al.*, 2012). Encapsulation also increases with an increase in calcium chloride as demonstrated by Rajesh *et al.*, (2011) when increasing the concentration from 1 % to 2 %.

4) Compatibility study

The existence of a possible interaction between drug and the calcium alginate can be investigated by Fourier transform infra-red (FTIR) analysis (Mandal *et al.*, 2010).

5) Swelling index

The degree of swelling in simulated gastric fluid (SGF) and simulated intestinal fluid (SIF) can be indicative of the stability. Chan *et al.* (2007) reported alginate matrices demonstrate a pH-dependent hydration, swelling and erosion behaviour (Chan *et al.*, 2007). Patel *et al.* reported that the sodium alginate beads exhibited pH-dependent swelling with lowest swelling ratio in pH 1.2 and showed disintegration in pH 7 to 7.5 within 45 to 50 min. This can be explained by the presence of ion exchange between Ca^{2+} ion in the hydrogel and Na^{+} ions in phosphate buffer (Patel *et al.*, 2006).

6) *In vitro* release and mechanism of release studies

Release from alginate network depends on various parameters, including particle size, hydrogel mesh size, and hydrophilicity of the incorporated drug, as well as the composition of the particle and hydrogel (Buwalda *et al.*, 2017).

Mechanisms for drug release from a particle embedded in hydrogel beads are depicted in figure 2.16. It can be either via release of the drug from the entrapped particles and subsequent drug diffusion through the polymer matrix of the hydrogel (figure 2.16, top), .This can also be via the slow release of drug loaded particles from the hydrogel and subsequent release of the drug from nano particles (figure 2.16, bottom) or via a combination of these mechanisms (Mokale *et al.*, 2014).

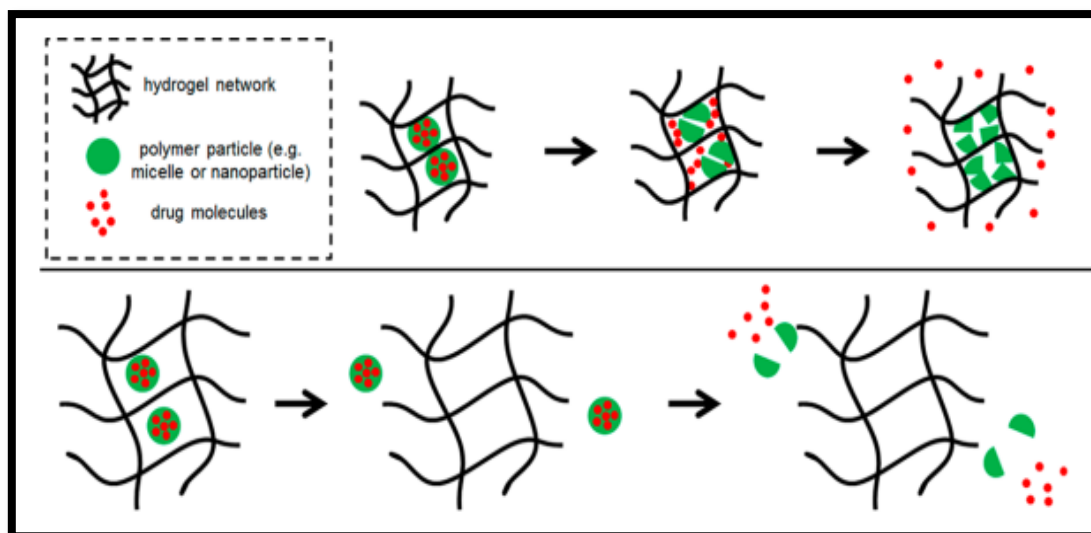


Figure 2-16: Schematic representation of two mechanisms for drug release from a particle embedded in a bead: (top) release of the drug from the entrapped particles and subsequent drug diffusion through the polymer matrix of the hydrogel; (bottom) release of drug entrapped particles from the beads and subsequent release of the drug from the nano particles. (Source, Mokale *et al.*, 2014).

The release of active compounds from matrix beads is pH dependant as reported by Sizery *et al.* (Suzery *et al.*, 2017) Their study demonstrated that alginate beads prevented phycocyanin release in simulated gastric fluid medium (acidic environment). Hence, after 2 hours of incubation, there was no release of phycocyanin in the simulated gastric fluid medium but it released rapidly in the simulated intestinal fluid medium. It has been reported that the release of drug from alginate gel beads is due to diffusion through the swollen matrix and relaxation of the polymer at pH 1.2 to 4.5 and due to the diffusion and erosion mechanism at pH 7–7.5 (Takka *et al.*, 1998).

2.6.3 Biomedical applications of Alginate beads

Calcium alginate gel beads have been developed as a unique vehicle for drug delivery and successfully used as a matrix for the entrapment and/or delivery of biological agents. Various categories of drugs and biomolecular chemicals have been encapsulated. These include nonsteroidal anti-inflammatory drugs, enzymes, peptides/proteins, and acid labile drugs (Nimase *et al.*, 2010; Babu *et al.*, 2007). Alginate has been widely used in a variety of biomedical applications, including cell encapsulation, cell transplantation tissue engineering and drug delivery (Baniasadi *et al.*, 2015). Alginate beads have been used to encapsulate other delivery systems including microspheres and liposomes (Gombotz *et al.*, 2012). It has

also been used for stability improvement of various compounds and oral bioavailability issues (Sankalia *et al.*, 2005; Bhushan *et al.*, 2015; Lin *et al.*, 2016; Davidov-Pardo *et al.*, 2014). In addition, alginate has been used as gastro resistant carrier (El-Sherbiny *et al.*, 2011; Cerciello *et al.*, 2016; Smith *et al.*, 2010; Aikawa *et al.*, 2015).

Alginate-liposome systems have been used for release profile modification (Dhoot *et al.*, 2003; Nagpal *et al.*, 2012). Combinations of liposomes and alginate have been investigated in order to modify the release of drugs from such phospholipid vehicles and to stabilize the products (Tønnesen *et al.*, 2002). The release of nicardipine HCl was extended by employing calcium alginate gel beads (Takka *et al.*, 1998) and liposome-loaded calcium alginate microspheres have also rendered controlled release properties to resveratrol (Balanč *et al.*, 2016).

2.7 Response surface methodology

The design of experiments is a structured, organized method used to determine the relationship between the factors affecting a process and the output of that process (Shaji *et al.*, 2016). In the development of any pharmaceutical product an important issue is to design a formulation with optimized quality in a short time period and minimum number of trials. Among diversity of DOE techniques, Response Surface Methodology (RSM) is the most frequently used optimization technique for designing and optimization of different pharmaceutical formulations, which requires minimum experimentation. Thus, it is less time-consuming and cost-effective compared to conventional methods of formulating dosage forms (Mishra *et al.*, 2016).

The response surface methodology (RSM) is a collection of mathematical and statistical techniques useful for modelling and analysis of problems, in which an output variables of interest is influenced by several input variables and the objective is to simultaneously optimize the levels of these output variables to attain the best system performance. The design based on fit of a polynomial equation to the experimental data for empirical model building. An experiment is a series of tests, called runs, in which changes are made in the input variables in order to identify the reasons for changes in the output response (Ashengroph *et al.*, 2013). It is a useful tool for studying the influence of experimental parameters by varying them simultaneously and for determining experimental factor settings and assesses the relationship between experimental and observed results to find the

optimum conditions for a reaction using a limited number of experiment runs to obtain statistically acceptable results (Khajeh, 2012).

RSM has several advantages compared to the classical experimental or optimization methods in which one variable at a time technique is used. Firstly, RSM trims down the number of experimental runs that are necessary to establish a mathematical trend in the experimental design region allow to determining the optimum level of experimental factors required for a given response, RSM offers a large amount of information from a small number of experiments. Secondly, in RSM it is possible to observe the interaction effect of the independent parameters on the response. The model equation easily clarifies these effects for binary combination of the independent parameters. In addition, the empirical model that related the response to the independent variables is used to obtain information about the process. With respect to these, it can be said that RSM is a useful tool for the optimization of chemical and biochemical process (Singh *et al.*, 2014; Ghanbarzadeh *et al.*, 2014).

Recently, RSM has been extensively applied for the optimization of multiple variables in many bioprocesses and showed satisfactory results; it has been used for optimization of lipid vesicles formulation (Soema *et al.*, 2015; Wang *et al.*, 2014).

2.7.1 Definition of terms in RSM

There are some important terms which describes the response surface methodology to a greater extent, which include the following: (1) Experimental domain is the experimental field that must be investigated. It is the minimum and maximum limits of the experimental variables studied. (2) Experimental design is a specific set of experiments defined by a matrix composed by the different level combinations of the variables studied. (3) Input variables are experimental variables that can be changed independently of each other. Typical independent variables comprise the pH, temperature, reagent concentration etc. (4) Levels of a variable are different values of a variable at which the experiments must be carried out. (5) Responses or output variables are the measured values of the results from experiments. Typical responses are the analytical signal (absorbance, intensity, etc.). (6) Residual is the difference between the calculated and experimental result for a determinate set of conditions. A good mathematical model fitted to experimental data must present low residuals values (Bhan, 2017).

2.7.2 Process for RSM application

Steps involved in the application of the response surface methodology as an optimization technique include: Selection of input and output factors of major effects on the system; choice of the experimental design and performing the experiments according to the selected matrix; measurement of output variables and mathematic–statistical treatment of the obtained experimental data through a polynomial function fit; Evaluation of the model fit; Verification of the necessity and possibility of performing a displacement in direction to the optimal region; and Obtaining the optimum values for each studied variable (Bezerra *et al.*, 2008; Shivakumar *et al.*, 2007).



Chapter 3

Methodology

3.1 Preparation of freeze dried *H. procumbens* plant extract

H. procumbens coarse powder was purchased from (Warren Chem, South Africa). Five hundred grams of plant powder was macerated in 2000 ml distilled water in a 2500 ml glass container and tightly closed to prevent water evaporation. The container was agitated in a shaker (Labcon, USA) at 40 °C for 6 hours, followed by separation of the macerate using a porcelain funnel. This was filtered using Whatman no. 1 filter paper and centrifuged with a (Beckman Coulter, USA) centrifuge for 30 min at 10, 000 rpm. The resultant supernatant was carefully removed and collected. The supernatant was transferred into aliquots of 500 ml round bottom flasks and sealed. The flasks were carefully filled with liquid nitrogen until completely frozen. The containers were connected to a freeze dryer (Virtis[®], UK) and dried under low pressure. The macerate was freeze dried for 2 days and 18 hours. The final powdered product was carefully collected and stored in air tight containers, in a freezer (Mahomed *et al.*, 2006).

3.2 Identification of harpagoside biomarker in plant extract

3.2.1 LC/MS

Liquid chromatography/mass spectrometry (LC/MS) analysis method was used as it offers a good combination of sensitivity and selectivity (Lei *et al.*, 2011). Prepared freeze dried plant extract contains many active ingredients and harpagoside was used as marker compound (Mncwangi *et al.*, 2014; Karioti *et al.*, 2011). LC/MS was used to identify the marker compounds (harpagoside) in the plant extract via exact mass of the compound.

3.2.1.1 Instrumentation

For identification purposes, spectrometric analysis was carried out on reconstituted freeze dried plant extract in distilled water solution recorded mass spectrum was compared to reference standard compounds of harpagoside in methanol using single quadrupole mass spectrometry (Perkin Elmer SQ 300 MS. USA) equipped with electrospray ionisation (ESI) source with operated mode at a voltage of 50,000 V.

3.2.1.2 Method

Direct Infusion Electrospray Ionization (DI-ESI- (+) method was used. Reference standard of harpagoside and plant extract sample solutions were filtered through 0.2 syringe filter (solution A). Solution A was added to 50 % aqueous methanol (MS grade, Merck, South Africa) as diluent containing 0.1 % formic acid, which enhances sample ionization, (solution B). Fifteen microliters of solution B were directly infused into the ESI chamber of the SQ 300 mass spectrometer using the on-board syringe pump at the rate of 15 µl/min and the ions were detected in positive and negative modes, i.e. ESI-MS (+/-), scan spectra from 100 to 2000 m/z was used. The mass spectra were collected and analysed using the Chromera[®] manager V 3.4.4.5945 software. The harpagoside qualitative peak in the plant extract was therefore correlated to the MS spectrum of the reference standard compound.

3.2.2 UHPLC

The biomarker compound was further identified by the spiking method using UHPLC. Pre-analysed plant extract samples were spiked with definite concentration of standard harpagoside and injected into the UHPLC. The subsequent peaks height was measured and compared i.e. before after spiking.

3.2.2.1 Development and validation of an UHPLC method for harpagoside

An isocratic HPLC method adapted from (Babili *et al.*, 2012) with slight modification was utilized.

3.2.2.2 Instrumentation

Ultra-high performance liquid chromatography (Perkin Elmer, USA) was equipped with a programmable Flexar FX-15 auto sampler, a UHPLC pump model FX-15, and a Flexar PDA plus detector model FX-15 and Flexar solvent manager 3-CH degasser was used. The data were recorded using Chromera[®] Manager software version 3.4.4.5945.

3.2.2.3 Chromatographic Conditions

The following chromatographic conditions were used with a Kinetex150 x 4.6 mm, 5 µm C-18 column: Flow rate: 1 ml /min, injection volume: 10 µl, wavelength: 278 nm, column temperature: 25 °C, auto sampler tray temperature: 4 °C, run time: 5 min, diluent: mobile phase 60:40% v/v methanol HPLC-grade methanol (Sigma Aldrich, South Africa) and deionized water (18 MΩ·cm) was obtained by water filtration system (O purity, SA),

acidified with 0.1 % formic acid formic acid (Merck, South Africa),. Elution mode: isocratic, detector: UV/ PDA plus.

3.2.2.4 Preparation of pure standard harpagoside stock solution

One milligram of pure standard harpagoside purchased from (Sigma Aldrich, South Africa) was accurately weighed using semi micron electronic balance (Shimadzu, Japan) and transferred to a 1ml volumetric flask. This was dissolved in 1 ml of methanol, vortexed for 30 seconds using vortex mixer (Benchmark, Taiwan) and the solution filtered through 0.25 µm syringe filter (KimLab, India) prior to performing HPLC analysis.

3.2.2.5 Preparation of mobile phase

Filtered and degassed mobile phase consisting of solvent A: deionized water acidified with 0.1 % formic acid and solvent B: methanol at the selected ratios was utilized. All solvents were filtered through filter apparatus (Millipore[®], USA) using 0.25 µm membrane filter (Millipore, Ireland).

3.2.2.6 Key parameters of the analytical method validation

The UHPLC method was validated to assure the method appropriateness for the quantitative analysis of harpagoside marker compound in plant extract. The validation method met the International Conference on Harmonization guidelines (ICH, 2005). The following analytical parameters were used: a) Specificity b) Linearity. c) Accuracy. d) Precision (repeatability, intermediate precision). e) Sensitivity. g) Robustness. h) System suitability.

a) Specificity

It is the ability to detect the analyte uniquely in the presence of other components (ICH, 2005). Specificity was evaluated by means of analysis of the mobile phase, (Methanol: Water) by injection to determine if there was any interference with harpagoside elution. Specificity was confirmed by the base hydrolysis test by force degrading the test sample in an alkaline medium. One millilitre of sodium hydroxide solution (0.1 M) (B & M Scientific, SA) was added to 9 ml of harpagoside solution, vortexed to disperse the sodium hydroxide solution uniformly in the test sample and allowed to stand for 24 hours, then analysed (Bhimavarapu *et al.*, 2011).

b) Linearity

Linearity of an analytical procedure is its ability (within a given range) to obtain test results which are directly proportional to the concentration of analyte in the sample (ICH, 2005). Linearity was evaluated by linear regression analysis method using a calibration graph. The calibration curve was obtained by plotting the peak area versus injected analyte concentration from six different duplicate concentrations ranging from 0.125(100 %), 0.0625(50 %) 0.03125(25 %), 0.01562(12.5 %), 0.00781(6.25 %), 0.003905(1.56 %) and 0.00195(3.125 %) mg/ml. These were prepared from a standard harpagoside stock solution. The correlation coefficient, y-intercept and slope of the regression line were calculated.

c) Precision

The precision of an analytical procedure expresses the closeness of agreement between results obtained from multiple samplings of the same homogeneous samples under prescribed conditions (ICH, 2005). Precision of the developed method was studied under the headings of repeatability (intra-day precision) and intermediate precision (inter-day precision). The repeatability was assured by six replicates of 0.125 mg/ml of harpagoside standard solution. The intermediate precision was evaluated by analysing three replicates of harpagoside standard solution at three concentration levels (0.125, 0.0625, 0.03125 mg/ml), on three different days. The average, standard deviation and relative standard deviation (coefficient of variation) of the replicates were calculated for each type of precision from the peak area of harpagoside.

d) Accuracy

The accuracy of an analytical procedure expresses the closeness of the test results obtained by the method and the value found (ICH, 2005). The accuracy was assessed by determining the percentage recovery of the known amount of standard harpagoside at six replicates of the level 0.01562 mg/ml and then the individual and mean percentage recovery were calculated using the following formula:

$$\text{Recovery (\%)} = (m_{\text{measured}} / m_{\text{calculated}}) \times 100. \quad \text{Eq 1.}$$

Where m_{measured} is the harpagoside amount measured and $m_{\text{calculated}}$ is the calculated amount of harpagoside obtained from the calibration curve (Babili *et al.*, 2012).

e) Sensitivity

Limit of Quantitation is the lowest amount of analyte in a sample which can be quantitatively determined with suitable precision and accuracy. Limit of detection is the lowest amount of analyte in a sample which can be detected but not necessarily quantitated as an exact value (ICH, 2005).

Limit of Detection (LOD) and Limit of Quantitation (LOQ) were determined using the calibration curve method. The LOD and LOQ of the assay method were evaluated based on the standard deviation of the response and the slope by using linearity data of serial dilutions of harpagoside stock solutions. The values of the slope and the standard deviation of the y-intercepts of the regression line were used to calculate the LOD and LOD of the proposed method and were calculated using the following equations:

$$\text{LOQ} = 10 \times \frac{\sigma}{S} \quad \text{Eq 2.}$$

$$\text{LOD} = 3.3 \times \frac{\sigma}{S} \quad \text{Eq 3.}$$

Where σ = the standard deviation of the response.

S = the slope of the calibration curve.

The slope S was estimated from the harpagoside calibration curve. The standard deviation of y-intercepts of regression line was used as the standard deviation.

f) Robustness

Robustness of an analytical procedure is a measure of its capacity to remain unaffected by small, but deliberate variations in method parameters (ICH, 2005). It was evaluated by applying the developed method while introducing variations, wavelength was altered to (± 2), column temperature was changed to (± 2 °C) units from set value, and the effect of these variations was recorded.

g) System suitability

The purpose of the system suitability test is to ensure that the complete testing system is adequate for the intended analysis. For system suitability, six replicates of (0.125 mg/ml) pure standard harpagoside were injected into UHPLC and column performance factors namely; theoretical plate count, tailing factors, resolution, and retention time were determined.

3.3 Quantitative determination of harpagoside constituent in *H. procumbens* plant extract

The concentration of harpagoside in the freeze dried plant crude extract was determined by applying the validated UHPLC method on a reconstituted solution of freeze dried plant extract in distilled water. The obtained peak area was interpolated to concentration utilizing the generated calibration curve. The experiment was repeated three times and results presented as microgram per milligrams of dry weight \pm standard deviation.

3.4 Lipid vesicles (liposomes and phytosomes) preparation

3.4.1 Preparation of 0.1 M potassium phosphate buffer pH 7.4 at 25 °C

- 1M K_2HPO_4 at $174.18 \text{ g mol}^{-1} = 87.09 \text{ g per 1 L}$.
- 1M KH_2PO_4 at $136.09 \text{ g mol}^{-1} = 68.045 \text{ g per 1 L}$.

Added 80.2 ml of K_2HPO_4 to 19.8 ml of KH_2PO_4 , dilute the combined 1M solutions to 1 litre distilled water (Cold spring harbor protocols).

3.4.2 Liposome preparation

Conventional lipid thin film hydration technique as described by Sha *et al.*, (2012) with slight modifications was used. The liposomes synthesis method consisted of three steps:

Step-1: Drying the lipid phase

The lipid phase components, i.e., L- α Soy phosphatidylcholine (PC) (> 95 % purity) (Avanti[®] polar lipids, Inc. USA) and cholesterol (≥ 99 %) (Sigma Aldrich, USA) were weighed using an analytical balance (Mettler, USA) and dissolved in 2 ml chloroform (Merck, SA); Once the lipids were thoroughly mixed in the organic solvent, the mixture was transferred to a round-bottom flask and attached to a rotary evaporator (Buchi-R11 Rotavapor, Switzerland) attached to a vacuum pump (Buchi V-700, Switzerland). The round-bottom flask was immersed in a

thermostatic water bath, evacuated and rotated at 150 rpm, at 45 °C; the chloroform was evaporated under vacuum to yield a lipid film. The process was allowed to continue 1 hour to affirm the dryness of the lipid film deposited on the walls of the flask. The flask was sealed with parafilm to prevent humidity entrance to the flask and stored for at least 24 hours at – 20 °C.

Step-2: Hydration of dry lipid film.

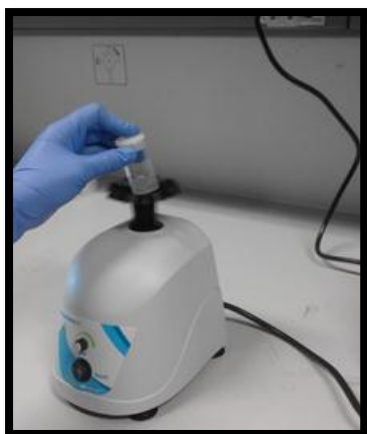
The residual lipid film was hydrated with the aqueous phase which consisted of crude plant extract dissolved in 5 ml phosphate buffered solution (PBS) pH 7.4. The mixture was shaken in a mechanical shaker (Labcon, USA) for 1 hour at 300 rpm and temperature above the transition temperature (T_m) of L- α Soy phosphatidylcholine which is ≈ 39 °C (Süleymanoglu, 2009). The suspension was subjected to five freeze-thaw cycles to produce multi-lamellar vesicles (MLV). The round bottom flask containing the liposomal suspension was placed in ice bath for 5 min and directly transferred to a hot water bath for another 5 min. The freeze-thaw procedure reduces the lamellarity of the vesicles and is an important step to enhance the percentage of encapsulation efficiency values.

Step-3: Homogeneity and Size reduction

Large unilamellar vesicles (LUV) were obtained by extruding the MLV using a manual mini extruder (Avanti Polar Lipids, Inc., USA). The extruder was placed on a hot plate to raise its temperature above the phase transition temperature of PC. The liposomal suspension was passed through polycarbonate membranes five times with 1 ml Hamilton® glass syringes to generate a homogeneous LUV population (Ong *et al.*, 2016).

3.4.3 Phytosomes preparation

Phytosomes were prepared by thin lipid film hydration technique previously reported by Saha *et al.*, (2013). The same steps to prepare liposomes were followed. The only difference was that freeze dried plant extract was added to the lipid phase components in step one. General steps of liposomes and phytosomes preparation by thin film hydration method are shown in figure 3.1.



a-Lipid mixture homogenization



b-Transfer into round bottom flask



c- Solvent evaporation



d- Hydration and mechanical shaking



e- Extrusion

UNIVERSITY of the
WESTERN CAPE

Figure 3-1: General lipid vesicles preparation.

3.5 Physicochemical characterization of *H. procumbens* liposomes and phytosomes

3.5.1 Visualization of lipid vesicles by optical microscopy

Preliminary lipid vesicle formation upon hydration was confirmed by optical microscopy. This involved placing a drop of lipid vesicles suspension on a glass slide without a cover slip, and observing the lipid vesicles through a vertical optical microscope (Zeiss, Germany) at 40X magnification using a differential interference contrast (DIC) objective (Bibi *et al.*, 2011).

3.5.2 Mean particle size and polydispersity index (PDI) determination

Knowledge of liposomes and phytosomes size and polydispersity is important for quantitative

interpretation of results. Particle size is determined by dynamic light scattering based on the principle of the random Brownian motion of particles in a liquid is faster for small particles than for large particles.

The mean particle size (z-average diameter) of the liposomes and phytosomes was determined. To measure the level of homogeneity of particle sizes of the liposomes and phytosomes, the mean particle size (z-average diameter) and polydispersity index (PDI) was measured using photon correlation spectroscopy (PCS) using a Nano ZS 90 Zetasizer (Malvern Instruments Ltd., U.K.) with the 4 mW He–Ne laser operating at a wavelength of 633 nm, temperature of 25 °C and a 90 ° scattering angle. One millilitre of phytosomal or liposomal suspension was loaded into a zeta-potential measurement capillary cell (DTS 1070), the capillary cells were thoroughly rinsed with deionized water before filling to avoid any contamination. Three independent measurements for ten cycles were performed for each sample. The z-average diameter and the polydispersity index of the liposomes were automatically generated by the instrument using cumulant analysis with software loaded the instrument.

3.5.3 Zeta potential determination

The zeta potential is a function of the surface charge of the suspension or dispersion (Demir et al., 2014). The charge present on the surface of colloid particles was measured using the Smoluchowski's equation from the electrophoretic mobility of liposomes and phytosomes. The same instrument was used for this as for particle size measurement i.e. Zetasizer Nano ZS 90 at 25 °C with a voltage of 4 mV. The samples were analysed at 25 °C at an angle of 173 to the laser beam. The intensity-weighted mean value was measured and the average of three measurements taken.

The measurement was conducted after filling 1 ml of each liposomal and phytosomal dispersion into the zeta-potential measurement capillary cell (DTS 1070), the capillary cells were thoroughly rinsed with deionized water before filling with liposomes or phytosomes solution to avoid any contamination. Three independent measurements for ten cycles were performed for each sample (Saoji *et al.*, 2016).

3.5.4 Percentage entrapment efficiency

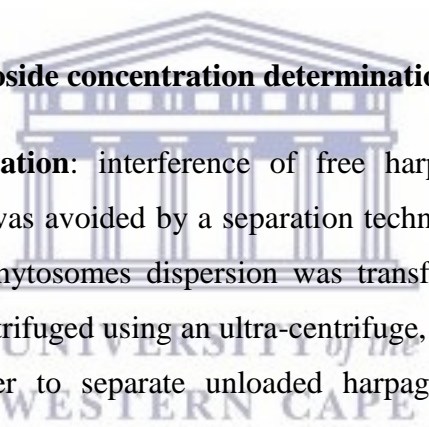
Encapsulation efficiency (% EE) was evaluated by determining the content of plant extract encapsulated (using harpagoside as the marker) into the liposomes and phytosomes. This

involved two steps (Begum *et al.*, 2012).

Step one: Harpagoside starting concentration determination

In case of liposomes, the starting concentration was determined by using a 1ml sample from the aqueous phase which consisted of plant aqueous solution dissolved in phosphate buffer before hydration, filtered through 0.45 μm nylon syringe filters (kimLab, India) with the sample analysed by UHPLC. In the case of phytosomes, because the crude extract is integrated in the thin film formation process, the phytosomes had to be disrupted for harpagoside detection. One millilitre of ethanol (Merck .SA) was added to 1 ml phytosomal suspension and sonicated for 3 min to break the phytosomes using a probe tip sonicator (Bandelin Sonoplus, Germany). This was followed by centrifugation using an ultra-centrifuge (Eppendorf 5417 R, Germany) at 10, 000 rpm for 5 min at 4 °C and filtration through 0.45 μm syringe filter. The sample was analysed using UHPLC.

Step 2: Encapsulated harpagoside concentration determination

- 
- a- Lipid vesicles purification:** interference of free harpagoside with encapsulated harpagoside detection was avoided by a separation technique. 1ml of *H. procumbens* loaded liposomes or phytosomes dispersion was transferred via pipette to a 2 ml eppendorf tube and centrifuged using an ultra-centrifuge, at speed of 10,000 rpm for 1 hour at 4 °C in order to separate unloaded harpagoside by the formation of supernatant and a pellet. The formed pellet which comprised the liposome or phytosomes was double washed with PBS, where 1 ml PBS was added to the pellet and vortexed for 20 seconds to disperse the vesicles and dissolve the free harpagoside in the PBS and centrifuged again at the same speed and time.
- b- Pellet lysing and content analysis:** after washing steps, 1 ml ethanol was added to the pellet to lyse the lipid vesicle to liberate the entrapped harpagoside. This mixture was sonicated by using a probe tip sonicator. The sonicator tip was inserted in the eppendorf tube and sonicated for 3 min at high intensity. The mixture was centrifuged and filtered using a 0.45 μm filter; the entrapped harpagoside was determined by UHPLC. The percentage encapsulation efficiency (% EE) was expressed as the percentage of the encapsulated harpagoside concentration to the total, as follows:

$$\% \text{ EE} = \frac{C_1}{C_2} \times 100. \quad \text{Eq 4.}$$

Where C_1 represents the drug content in the pellet, C_2 is the total drug content added to the formulation.

3.6 Preliminary study for determination of nano lipid vesicles formulation parameters

Preliminary studies were performed on the lipid vesicles to ensure vesicle formation, plant extract encapsulation and characterization. This was done before using experiment design software for optimized nano formulation.

3.6.1 Investigating the effect of lipid type on percentage encapsulation efficiency

Various trial batches of lipid vesicles were prepared as presented in table 3.1 with diversity in lipid type i.e. lecithin (Sigma aldrich) and L-a Soya phosphatidylcholine, on the basis of most commonly used, compatibility with plant extract, and lipid vesicle formation. Subsequent determination of percentage encapsulation efficiency was performed as stated in section 3.5.4.

Table 3.1: Lipid vesicles formulations with diversity in lipid type

Batch.no	Cholesterol	Lecithin	Plant extract	Phosphatidylcholine
	w/w	w/w	w/w	w/w
L1	1	/	5	9
L2	1	9	5	/

3.6.2 Investigating the optimal sonication time for vesicle disruption

Lecithin was excluded from further experiments as it demonstrated low percentage encapsulation efficiency from previous preliminary experiments and all further formulations were prepared with PC as the main lipid component in the formulation.

Lipid vesicles were formulated at a ratio of 5:9:01 w/w plant extract, cholesterol and PC, respectively. Four samples of 1ml each were centrifuged to pelletize the prepared vesicles, double washed with PBS and 1ml ethanol was added to each sample. Samples were sonicated using a probe tip sonicator, each of which was subjected to definite time of sonication 1, 2, 3,

4 min. The samples were centrifuged, filtered through 0.45 µm syringe filters and UHPLC analysed to determine harpagoside concentration after disruption with ethanol and sonication.

3.6.3 Investigation of the influence of lipid vesicle size reduction process on the percentage encapsulation efficiency

Lipid vesicles were formulated at a ratio of 5:9:01 w/w plant extract, cholesterol and PC, respectively. Three methods for vesicle size reduction were used i.e. probe sonication using a probe sonicator, water bath sonication using an ultra-sonic bath (Labotec, South Africa) and extrusion using an extruder. Samples from the 3 methods were analysed for particle size (section 3.5.2) and percentage encapsulation efficiency (section 3.5.4) by zeta-sizing and UHPLC, respectively.

3.6.4 Finding the appropriate plant extract ratio for appropriate percentage encapsulation efficiency

Lipid vesicles were prepared with different plant extract quantities to get an indication of the most suitable quantity to use for optimal percentage encapsulation efficiency. Various batches as demonstrated in table 3.2 were prepared and lipid vesicles were disrupted by adding ethanol and the percentage encapsulation efficiency was determined by applying the steps stated in section 3.5.4.

Table 3.2: Lipid vesicle formulations prepared with constant lipid phase content and variation in plant extract content for investigation of the percentage of encapsulation efficiency values divergence.

Lipid vesicle formulation	Plant extract: Phosphatidylcholine: Cholesterol
L1	2.5:9:01
L2	5:9:01
L3	10:9:01

3.7 RSM optimization process of nano lipid vesicles formulation by design of experiments

In the development of any pharmaceutical formulation an important issue is to design a formulation with optimized quality in a short time period and minimum number of trials. The response surface methodology has been commonly used for designing and optimization of

different pharmaceutical formulations, which requires minimum experimentation (Malakar *et al.*, 2012). Thus, it is less time-consuming and more cost-effective than the conventional methods of formulating dosage forms.

This methodology could be employed to optimize lipid vesicles formulations (liposome and phytosome) components for high encapsulation. RSM was used to optimize the particle size and percentage encapsulation efficiency of lipid vesicles using lipid content (PC and cholesterol) and vesicle type (liposome/phytosome) as effective variables.

3.7.1 Generating experimental matrix

RSM optimal design was employed for the optimization of *H. procumbens* plant extract nano formulation (liposome and phytosome) using Design-Expert[®] software version 8.0.7.1 (Stat Ease Inc., USA). Numerous variables may affect the response of the liposome formulations. It is practically very difficult to identify and control the small contributions from each one (Bezerra *et al.*, 2008). Therefore, three important process parameters including initial concentrations of PC (A), cholesterol (B), as well as vesicle type (liposome/ phytosome) (C) were used and optimized as input factors to obtain the best response of particle size (Y1_{PS}), polydispersity index (Y2_{PDI}) and the percentage encapsulation efficiency (Y3_{%EE}). These were used as output factors. The input factors were evaluated at two levels, the higher and lower levels of each factor are presented in table 3.3.

Table 3.3: The upper and lower levels of input factors set for optimization process.

Input factor	Name	Lower level	Upper level
A	Phosphatidylcholine (% wt)	10	80
B	Cholesterol (% wt)	5	40
C	Vesicle type	Liposome	phytosome

The RSM optimal design building outcome was 17 runs which varied between liposomes and phytosomes formulations with different composition as represented in table 3.4.

Table 3.4: Generated experimental matrix by RSM optimal design.

Std	Run	Factor 1 A:PC %	Factor 2 B:CHOL %	Factor 3 C:vesicle type material
1	1	80.00	40.00	liposome
3	2	45.00	40.00	phytosome
2	3	80.00	22.50	phytosome
6	4	10.00	5.00	phytosome
16	5	10.00	40.00	phytosome
10	6	80.00	5.00	liposome
14	7	80.00	5.00	phytosome
13	8	45.00	5.00	phytosome
11	9	45.00	22.50	liposome
5	10	10.00	22.50	phytosome
12	11	80.00	40.00	phytosome
8	12	10.00	40.00	liposome
4	13	45.00	22.50	liposome
9	14	10.00	5.00	liposome
7	15	45.00	22.50	liposome
15	16	45.00	5.00	liposome
17	17	45.00	22.50	liposome

3.7.2 Lipid vesicle characterization of RSM generated experiments

The 17 different runs of liposomes and phytosomes were carried out according to the components ratio proposed by the design software using thin lipid film hydration technique as described in section (3.4.2 and 3.4.3). Liposomal and phytosomal preparations were characterized for vesicle size, polydispersity index and percentage encapsulation efficiency. After this the experimental results for each output factor were fitted in the design matrix.

3.7.3 RSM Data analysis and evaluation of the fitted response surface models

The output variables were fitted to a second order model in order to correlate the output and input variables. The general form of the second polynomial equation is as follows:

$$y = b_0 + b_1A + b_2B + b_3C + b_4A^2 + b_5B^2 + b_6C^2 + b_7AB + b_8AC + b_9BC. \quad \text{Eq 5.}$$

Where, y is the output variable, b_0 is an intercept and b_1 – b_9 are the regression coefficients. A, B and C represent the main effects, A^2 , B^2 and C^2 the quadratic effect, and AB, AC, and BC are the interaction effect.

Regression analysis of the data was carried out using the Design-Expert® software version 8.0.7.1 (Stat Ease Inc., USA). One-way ANOVA was applied to estimate the significance of the model ($P < 0.05$) for individual output parameters. After ANOVA analysis, the Y3 full model was found not to be significant and the model was reduced using the model reduction method. ANOVA was also performed to identify the significance of single factors in relation to their influence on the responses. Each factor was considered to be significant when the p value was < 0.05 . The adequacy of model was checked by accounting for R^2 , adjusted- R^2 and comparing lack of fit p - values for each response.

3.7.4 Formulation optimization using desirability function

The desirability function approach is a technique for the simultaneous determination of optimum settings of input variables that can determine optimum performance levels for one or more responses (Mourabet *et al.*, 2014). In this study, the numerical optimization technique which represents the closeness of a response to its ideal value (Raissi *et al.*, 2009) was adapted to optimize the process conditions of formulation variables (A; particle size, B; polydispersity index and C; percentage encapsulation efficiency) that provide desired outcomes for all responses. The desired goals known as constraints for each output and input factors were chosen along with the weighting and importance allocated for each goal as illustrated in table 3.5. All the independent variables were kept within range while the responses were either maximized or minimized.

Table 3.5.: Desirability specifications of numerical optimization for *H. procumbens* nano formulation.

Name	Goal	Lower limit	Upper Limit	Lower weight	Upper weight	Importance
Phosphatidylcholine (% wt)	is in range	10	80	1	1	/
Cholesterol (% wt)	is in range	5	40	1	1	/
Vesicle type	is in range	liposome	phytosome	1	1	/

Vesicle size (nm)	minimize	207.8	608.7	1	1	**
Polydispersity index	minimize	0.18	0.593	1	1	**
Percentage encapsulation efficiency (%)	maximize	2	31.25	1	1	****

3.7.5 Validation of optimized condition

The optimum values of the selected formulation and its predicted output factors values were verified experimentally. Four replicates of the optimized phytosomes formulation were produced and the output factor values (particle size, polydispersity index, and percentage encapsulation efficiency) were experimentally determined. The model predicted values were compared with actual ones obtained from experimentation and the percentage error was calculated by using the following formula (Ghanbarzadeh *et al.*, 2013):

$$\% \text{ Error} = \frac{\text{Predicted} - \text{observed}}{\text{Observed}} \times 100 \quad \text{Eq 6.}$$

3.8 Characterization of selected optimized RSM formulation

3.8.1 Particle size and polydispersity index

The optimized RSM phytosomes formulation was characterized for mean particle size and polydispersity index using the Zetasizer Malvern instrument as per method in section 3.5.2.

3.8.2 Zeta Potential Analysis

The optimized RSM phytosomes formulation was also characterized for zeta potential although it was not one of the output factors as per method in section 3.5.3.

3.8.3 Surface Morphology

The Scanning Electron Microscope (SEM) was utilized to study the external morphology of the phytosomes produced from the optimized formulation. Approximately 5µL of the phytosomal suspension was placed on double-sided carbon conductive adhesive tape fixed on SEM aluminium stubs. The samples were allowed to dry at room temperature. The phytosomes were then sputter-coated with a thin layer of gold in vacuum for 30 seconds at 20 mA using a coating unit (Emitech K550X, England) to make it electrically conductive. The

surface morphology of the coated samples was viewed and photographed using an Auriga HR-SEM F50 scanning electron microscope (Zeiss, Germany) (El-Gazayerly *et al.*, 2014).

3.8.4 Apparent solubility study

To determine the change in solubility due to complexation, a protocol reported by Tan *et al.*, (2012) was followed. Solubility characteristics of *H. procumbens* extract and prepared *H. procumbens* phytosomes were determined by adding excess of the samples to 6 ml of water and n-octanol in a sealed glass container at room temperature. The liquids were shaken for 24 hours and centrifuged at 4000 rpm for 10 min. The supernatant was filtered through a 0.45 µm syringe filter, and analysed using UHPLC.

3.8.5 FTIR spectroscopy

To study the possible interactions between plant extract and phospholipids, IR spectrums of freeze dried *H. procumbens* plant extract, empty phytosomes, loaded *H. procumbens* phytosomes, were recorded in range of 4000 – 650 cm⁻¹ using a Fourier transform infrared spectrometer (Perkin-Elmer Spectrum-400, USA) equipped with a diamond attenuated total reflectance (ATR) accessories with a diamond crystal.

After fresh preparation of the phytosomal suspensions (empty and loaded), the residual moisture in the samples was removed by subjecting the samples to vacuum drying using a vacuum oven before obtaining any spectra (Niive, Iasec, South Africa). A small quantity of the sample was placed on the crystal, pressure applied and scanned at 2 cm⁻¹/sec 4 times at a resolution of 4 cm⁻¹/sec, the obtained IR spectra were interpreted for functional groups at their respective wave number (cm⁻¹). The analysis of the spectra was done using spectrum software version 6.3.5.

3.8.6 Stability in simulated gastric fluid (SGF) pH 1.2

The selected optimized *H. procumbens* phytosomes formulation was evaluated for *in vitro* physicochemical stability after exposure to simulated gastric fluid (SGF; pH 1.2) by monitoring the physicochemical properties (particle size, polydispersity index, and zeta potential) of the prepared phytosomes and compared with the initial values and physical changes (aggregation and precipitation) that were seen with *H. procumbens* phytosomes.

3.8.6.1 Preparation of simulated GI media

Simulated intestinal fluid and gastric fluid as media were used to conduct the stability study as per WHO (WHO, 2012) guidelines. The simulated gastric fluid (SGF) was prepared by dissolving 2.0 g of sodium chloride in 7.0 mL of hydrochloric acid (420 g/l) and made up to 1000 ml with water. SLS (0.1 %) was added as surfactant to simulate the gastric conditions. This test solution had a pH of 1.2.

3.8.6.2 Method

Physical changes of *H. procumbens* phytosomes in simulated GI media and the possible corresponding correlation of these changes with the phytosomes stability was investigated. The method reported by Freag *et al.*, (2013) was used with some modifications. *H. procumbens* phytosomes were prepared and purified by the centrifugation technique as stated in section (3.5.4, step 2 a). One millilitre of the phytosomal formulation was added to 2 ml SGF at pH 1.2 in 10 ml glass vials tightly closed with plastic caps. The vials were incubated for 2 hours. The samples were thereafter mildly agitated at 75 rpm on a digital multi-position magnetic stirrer (VELP Scientifica, Europe), and heated at 37 °C in the circulating thermostatic bath (Julabo5B, Germany). Empty phytosomes were prepared following the same steps and exposed to SGF. This served as the control.

At two hour intervals, samples of empty and loaded phytosomes were assessed for the physicochemical properties such as particle size, zeta potential as well as polydispersity index and harpagoside content in the medium, using the Zetasizer and UHPLC. Experiments were performed in duplicate.

3.9 Phytosomes in alginate system

One of the key features of an oral delivery system for *H. procumbens* phytosomes should be the ability to transit through stomach with minimal impact from the adverse gastric environment.

3.9.1 Preparation of the alginate coated *H. procumbens* phytosomes

The alginate coated *H. procumbens* phytosomes were prepared using the inotropic gelation technique by the syringe method as reported by Bansal *et al.*, (2016) with slight modifications, in attempt to increase the *H. procumbens* phytosomes stability in the gastric environment.

i. Preparation of sodium alginate stock solution

Concentrated sodium alginate was prepared by weighing the corresponding amount (1, 2 and 4 mg) of sodium alginate powder (Merck, South Africa) and dissolved by sprinkling the powder in a 200 ml beaker with 90 ml distilled water. This was placed on a magnetic stirrer (500 rpm) at 60 °C for 2 hours to ensure complete dissolution of the powder. The solution was left to cool to room temperature (Abdalla *et al.*, 2015).

ii. Preparation of Calcium Chloride Solution (cross linking agent)

Calcium chloride solution was prepared by mixing (2 and 4 mg) (Merck, South Africa) in 100 ml of distilled water and stirred until complete solution.

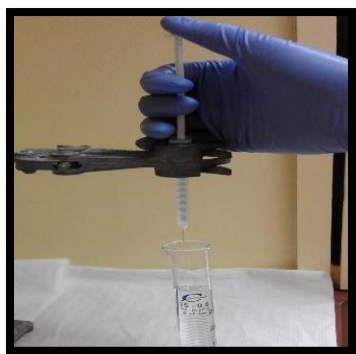
iii. Addition of *H. procumbens* phytosomes to the alginate solution

Freshly prepared *H. procumbens* phytosomes were pelleted by centrifugation, washed twice to separate un-encapsulated plant extract and re-suspended in distilled water. Ten millilitres of pure *H. procumbens* phytosomal suspension was mixed with 90 ml sodium alginate to obtain a final concentration of (1, 2 and 4 %). The dispersion was then stirred slowly for 10 min for equal dispersion of the phytosome in the polymer (sodium alginate) solution.

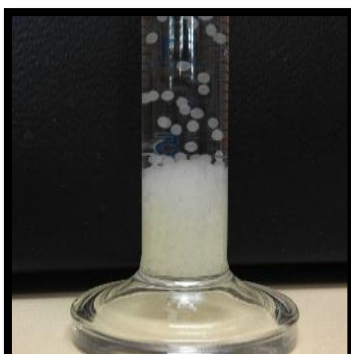
iv. Dropping of *H. procumbens* phytosomes - alginate solution into CaCl₂ solution

Bubble free *H. procumbens* phytosomes-alginate solution was added drop wise in a 50 ml measuring cylinder had 50 ml of aqueous calcium chloride solution (cross-linking agent), via an insulin syringe filled by 5 ml syringe with sodium alginate-phytosomes solution, kept at 25 °C and stirred slowly at 400 rpm for 15 min, to enhance the rigidity, mechanical strength of the beads and also to prevent aggregation of the formed beads. The distance of the needle from the cross linking solution was 5 cm, the droplets from the drug-polymer dispersion instantaneously gelled upon contact with the calcium chloride solution which acts as a cross-linking agent and small beads formed as shown in figure 3.2.

After 15 min of curing, the obtained beads were harvested by filtering through a Whatman[®] filter paper, washed thoroughly with distilled water to remove any traces of crosslinking agent from the beads. The beads were collected on a petri-dish and air dried for 36 hours at room temperature and stored in an air-tight container.



A) Dropping



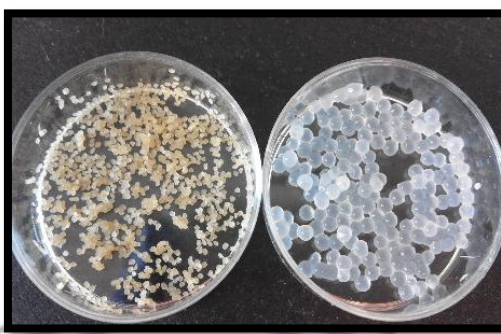
B) Curing



C) Washing



A) Washing



B) Obtained dried - fresh beads

Figure 3-2: Preparation of alginate coated *H. procumbens* phytosomes beads by ionotropic gelation method.

3.9.2 Process variables and optimization

The ability of beads to entrap the phytosomes is the determining factor for selection of composition of the beads. Accordingly, preliminary work on the preparation of alginate beads was performed to investigate the contribution of formulation parameters on the bead size and ease of preparation, entrapment efficiency and release profile of *H. procumbens* phytosomes from alginate beads (output factors). Input factors such as concentration of sodium alginate and of calcium chloride were chosen to optimize the beads composition because they play a vital role in achieving high entrapment efficiency, proper particle size, swelling behaviour, and surface morphology (Patel *et al.*, 2016).

Six sets of empty and alginate coated *H. procumbens* phytosomes were prepared using different sodium alginate and calcium chloride concentrations. The sodium alginate factor was evaluated at three different concentrations (Singh *et al.*, 2012) and calcium chloride at two concentrations (table 3.6). The other variables that are thought to have effect on the bead

character such as, stirring speed of the cross linking solution, was kept constant at 400 (Alkassas *et al.*, 2007). The needle distance from the cross linking solution was 5 cm (Jahan *et al.*, 2010). The volume of cross linking solution was kept constant to exclude any source of variability. Formulations were analysed for all determined output factors.

Table 3.6: Composition of alginate coated *H. procumbens* phytosomes formulations

Batch Code	Sodium Alginate	Calcium Chloride
	(%w/v)	(%w/v)
F1	1	2
F2	2	2
F3	4	2
F4	1	4
F5	2	4
F6	4	4

3.9.3 Characterization of alginate coated *H. procumbens* phytosomes

3.9.3.1 Particle size measurements

The particle size of empty and alginate coated *H. procumbens* phytosomes was measured using a light microscope (Nikon, Japan). Randomly selected beads were placed on a clean glass slide. The diameter of 10 randomly selected beads was measured at a 40X magnification. The instrument eyepiece was calibrated at 1 unit equal to 0.0256 mm. The average sizes of 10 beads were determined for each formulation using the calibration factor; all measurements were in triplicate the average diameter of the beads was calculated using the following formula (Patel *et al.*, 2016).

$$X = \sum (X_i) / N \quad \text{Eq 7.}$$

Where, X = Average particle diameter, X_i = individual diameter of beads and N = number of beads.

3.9.3.2 Percentage encapsulation efficiency determination

Alginate coated *H. procumbens* phytosomes (100 mg) were dispersed in a glass vial containing 2 ml PBS (pH 7.4) and sonicated for 10 min. The mixture was vigorously stirred

at 1000 rpm for 4 hours with a magnetic stirrer to break down the alginate coating (Nayak *et al.*, 2011). One ml of ethanol was added and the mixture was probe sonicated for 3 min to lyse the *H. procumbens* phytosomes liberated from lysed alginate beads. The mixture was centrifuged for 5 min, filtered through 0.45 µm syringe filter and analyzed using UHPLC. Observations were recorded in triplicate and the beads percentage encapsulation efficiency was calculated using following formula (Kassem *et al.*, 2012):

$$\text{Percentage encapsulation efficiency} = \frac{\text{Entrapped drug}}{\text{Initial drug}} \times 100 \quad \text{Eq 8.}$$

3.9.3.3 Alginate coated *H. procumbens* phytosomes erosion study

An erosion study was performed to determine how alginate and calcium chloride concentration affects the time needed for alginate beads to swell, disintegrate and release their encapsulated phytosomes. Equal amounts of dried alginate beads were dispersed in glass vials containing phosphate buffer solution pH 7.4 in equal volumes and placed in multi positions of a magnetic stirrer water bath at 37 °C and 100 rpm for 2 hours. Alginate coated *H. procumbens* phytosomes integrity was visual inspected and released plant extract was detected by UHPLC at time interval of 1, 2, 4, 6 & 8 hours.

3.9.3.4 Morphology and surface assessment of selected alginate coated *H. procumbens* phytosomes

Morphological examination of the surface of the dried alginate coated *H. procumbens* phytosomes was carried out using a scanning electron microscope. Randomly selected beads were placed on double-sided copper conductive tape fixed on aluminium stubs. The beads were then sputter-coated with a thin layer of gold in a vacuum for at 20 mA using a coating unit to make it electrically conductive and was analyzed with a SEM instrument.

3.9.3.5 Phytosomes- polymer compatibility study

H. procumbens phytosomes- alginate polymer interactions in the formulation were studied by the use of the Fourier Transform Infrared (FTIR) spectrometer. Empty and loaded alginate beads (alginate-coated *H. procumbens* phytosome) were prepared and air dried. *H. procumbens* phytosomes were prepared and dried in a vacuum oven at room temperature.

The samples were put on the small diamond crystal and pressure was applied by ATR accessory and scanned 4 times at 2 cm⁻¹/sec at a resolution of 4 cm⁻¹/sec within the wave number range of 4000 cm⁻¹-650 cm⁻¹. Drug polymer interaction was studied by comparing the IR spectra of *H. procumbens* phytosomes and empty alginate beads with *H. procumbens* phytosomes loaded alginate beads. The analysis of the spectra conducted used spectrum software version 6.3.5.

3.9.3.6 Swelling index study

This study was conducted to estimate the percentage swelling of the alginate beads. This is responsible for leaching of the phytosomes into the gastric and intestinal fluids. The beads swelling extent in the dissolution medium was determined by following described methods by Patel *et al.*, (2016; Nayak *et al.*, (2011). The extent of swelling was measured in terms of % weight gain by beads. The swelling behaviour of dried beads in gastric and intestinal simulated fluids (SGF; pH 1.2, SIF; pH 7.4) was tested. Simulated gastric fluid prepared as prescribed in section (3.8.6.1), simulated intestinal fluid (SIF) was prepared as per WHO (WHO, 2012); 6.8 g of potassium dihydrogen phosphate was dissolved in 250 ml of water and 190 ml sodium hydroxide (0.2 mol/l) and 400 ml water. The resulting solution was adjusted with sodium hydroxide (0.2 mol/l) to a pH of 7.5 ± 0.1 and diluted with sufficient water up to 1000 ml.

In this test 3.4 mg of optimized alginate-coated *H. procumbens* phytosomes formulation was transferred to a glass vial containing GSF. The samples were stirred at 60 rpm speed in a multi stirrer water bath and allowed to swell for 2 hours at 37 ± 0.5 °C in simulating the gastric medium. The same experiment was repeated in SIF. At the end of 2 hours, the beads were withdrawn, placed on tissue paper to remove moisture adhering to the surface and immediately weighed. The swelling behaviour of beads was expressed as the ratio of initial weight of beads to the final weight of swollen beads as a function of time.

The % weight gain by the beads (swelling index) was calculated by the following formula:

$$\text{Swelling index (SI)} = \left[\frac{W_t - W_0}{W_0} \right] \times 100. \quad \text{Eq 9.}$$

Where, W_t = Mass of swollen beads at time t and W_0 = Mass of dry beads at $t = 0$.

3.9.3.7 Invitro drug release in GIT fluids

The release study was performed at different pH (SGF; 1.2, SIF; 7.4), simulating transition of beads in GIT; the media of pH 1.2 was representing the gastric condition pH 7.4 was representing the intestinal condition.

Accurately weighed 10 mg of alginate coated *H. procumbens* phytosomes was dispersed in a 10 ml glass vial containing 2 ml simulated intestinal fluid (SIF) and placed in a multi stirrer water bath its temperature was adjusted to 37 °C and 200 rpm. The experiment was conducted for 8 hours. One vial was used for each time point. (1, 2, 4, 6, and 8 hours). At the determined time interval the vial was removed from the water bath and the solution was transferred by pipette to eppendorf tubes. This was centrifuged for 30 min at 14,000 rpm. The supernatant was filtered through 0.45 µm syringe filter and UHPLC was used for the analysis to quantify the harpagoside released from alginate coated *H. procumbens* phytosomes. The experiment was repeated using simulated gastric fluid (SGF) as release medium for 4 hours, The experiments were done in duplicate (Shazly *et al.*, 2008) with slight modification.

3.9.3.8 Release profile determination

The drug release study was performed by using the dispersion method reported by Shazly *et al.*, (2008) with slight changes on selected optimized *H. procumbens* phytosomes formulation, alginate coated *H. procumbens* phytosomes formulation and freeze dried extract to compare the release pattern in PBS pH 7.4 as release medium. Five mg of freeze dried *H. procumbens* extract was placed in 10 ml glass vials containing 2 ml release medium. These were placed in a circulating thermostatic water bath on digital multi-position magnetic stirrer. The temperature was set at 37 °C and stirring speed of 200 rpm for 8 hours. A different vial was used for each time interval. After the specific time interval, a vial was removed; the solution filtered, and analyzed using UHPLC, to quantify harpagoside concentration in the release medium. Experiments were performed in duplicate. The same steps were applied for the *H. procumbens* phytosomes and alginate coated phytosomes, but firstly the phytosomes were purified by centrifugation as mentioned in section (3.5.4) to prevent un-encapsulated harpagoside from being present in the release medium and influencing the result. The purified phytosomes were re-suspended in PBS and used to conduct the release study.

3.9.3.9 Mechanism of release

The analysis of the mechanism of drug release from the pharmaceutical dosage form is an important process. In order to understand the mechanism and kinetics of drug release, the drug release data of the in-vitro study was fitted to various kinetic equations such as zero-order, first-order, Higuchi and the Korsmeyer and Peppas equation (Mello *et al.*, 2011) The DDSolver 1.0 software was used for the linear regression analysis. It features 40 models that can be used to directly calculate the parameters and the appropriateness of each model. Correlation coefficient correlation values were calculated for the linear curves obtained with regression analysis. The value of the release exponent (n) of the Korsmeyer–Peppas equation was determined and used to indicate different release mechanisms. The highest values of regression coefficient (R²) were selected as the best fit model. The equations used for calculating the release kinetics are as follows:

➤ **Zero Order model:** $F = k_0 * t$ Eq.10

Where F denotes fraction of drug released up to time t, k₀ is the zero-order rate constant expressed in units of concentration/time, t is the time in hours.

➤ **First Order model:** $F = 100 * [1 - e^{(-k_f * t)}]$ Eq.11

Where k_f is the constant of mathematical model.

➤ **Higuchi's model** $F = k_H * t^{1/2}$ Eq.12

Where k_H is the constant reflecting the design variable of the system.

➤ **Korsmeyer-Peppas model:** $F = k_{K-P} * t^n$ Eq.13

Where k_{K-P} is the rate constant and n is the release exponent.

3.9.3.10 Effect of storage temperature on *H. procumbens* phytosomes and alginate coated phytosomes.

Phytosomes were stored for 30 days at 4-8 °C (refrigerated temperature), 25 °C, and 37 °C. Freshly prepared phytosomes were purified to separate of non-entrapped harpagoside by centrifugation method. Purified phytosome formulations were placed in glass vials, tightly sealed and parafilmed. Sample aliquots were withdrawn periodically at 1, 7, 14, 30 days. Particle size, polydispersity index, zeta potential and harpagoside leakage analysis were evaluated using a zetasizer and UHPLC as the method described by Muppidi *et al.*, (2012).

For leakage analysis samples were centrifuged and the supernatant was injected into UHPLC to detect and quantify the harpagoside leaked from phytosomes.

For alginate coated *H. procumbens* phytosomes, the method reported by Kashid *et al.*, (2016) was used with slight modifications. These were also tested for stability. A 50mg of dried alginate coated *H. procumbens* phytosomes were transferred to air tight containers, parafilmed and stored at 4-8 °C, 25 °C and 37 °C for 30 days. At predetermined time of 1, 7, 14, 30 days samples were analysed for particle size to check for possible changes in the bead size due to temperature variation. The samples were tested for harpagoside leakage. Samples were transferred to 2 ml tubes; 1ml ethanol was added and stirred slowly for 10 min. The ethanol was added to dissolve any phytosomes which may have migrated from the alginate core to the shell. Ethanol does not affect the alginate bead integrity.

3.10 Statistical analysis of data

All results were expressed as mean values \pm standard deviation (SD). The results were evaluated and analyzed statistically with the GraphPad InStat[®] software (version 6, Graph Pad Software San Diego, California, USA). Analysis of variance (ANOVA) was used to assess regression analysis R^2 (correlation coefficient) and linear regression to measure linearity. Data was analyzed for one and two way analysis of variance (ANOVA). One-way ANOVA analysis was followed by the Tukey's multiple comparison test. A probability factor of less than 0.05 ($P < 0.05$) was considered to represent statistically significant difference, whereas $P < 0.001$ was considered extremely significant.

Design-Expert[®], version 8.0.7.1 software (Stat-ease Inc., USA) was used for performing experimental design, polynomial fitting and ANOVA results.

DDsolver software for model fitting for release study data and evaluation of release kinetics was obtained according to exponent release value.

Chapter 4

Results and discussion

4.1 *H. procumbens* plant extract preparation

Freeze dried *H. procumbens* plant extract was prepared by maceration of coarse plant powder in water followed by freeze-drying and solvent elimination under reduced pressure. This produced a light-brown, powdery crude extract which was stored in the freezer at -20 °C in an air tight container.

4.2 Identification of harpagoside biomarker in *H. procumbens* plant extract

4.2.1 LC/MS

The detection was performed by means of electrospray ionization mass spectrometry in negative and positive ion mode. Positive identification of harpagoside in plant extracts was accomplished by analysis of peaks using mass spectrometry (MS)-detection. Figure 4.2, 4.4 show the full scan mass spectra obtained by direct infusion of the test sample solution in the electron spray ionization (ESI) positive and negative ion mode respectively, following careful comparison of harpagoside ESI /MS spectra in *H. procumbens* plant extract with pure standard harpagoside (figure 4.1, 4.3). In the ESI negative ion mode, the fragmentation pathways are different from those obtained in the positive ion mode.

In the positive ion mode, as can be seen in figure 4.1, the pure standard harpagoside spectrum characterized by the presence of fragment ion of 517 $[M+Na]^+$ corresponding to sodium ion adduction as the base peak of harpagoside and the same corresponding fragment ion at m/z 517 was seen in *H. procumbens* extract as demonstrated in figure 4.2 (the arrow refers to the harpagoside fragment ions).

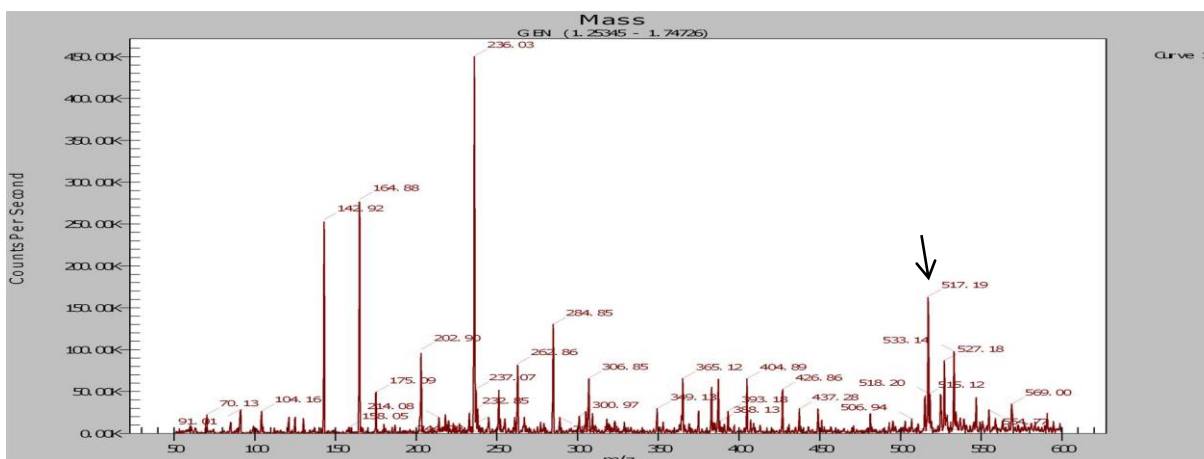


Figure 4-1: full scan MS spectrum of pure standard harpagoside in positive ion mode showing $[M+Na]^+$ Ion of harpagoside at m/z 517.

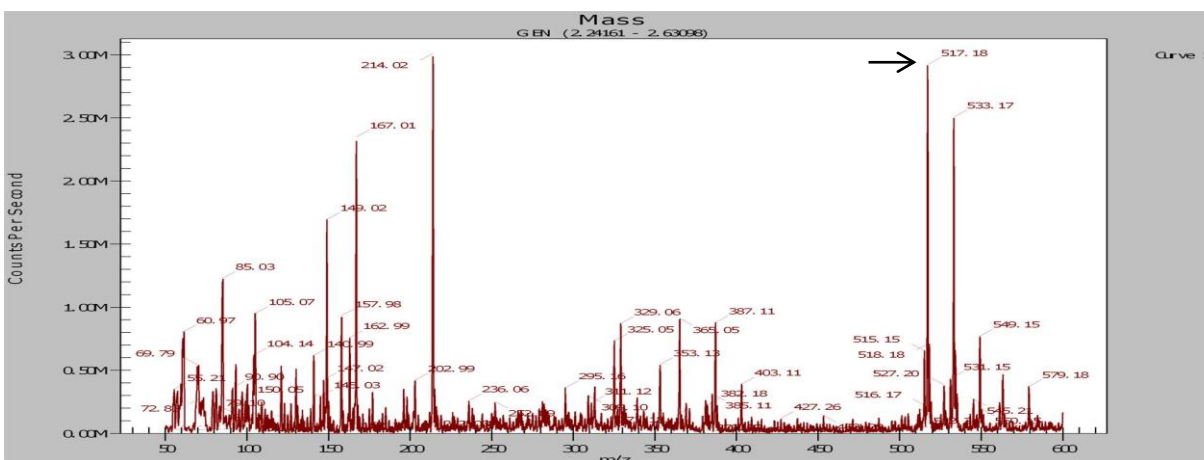


Figure 4-2: full scan MS spectrum of plant extract in positive ion mode showing $[M+Na]^+$ Ion of harpagoside at m/z 517.

In the negative ion mode, as can be seen in figure 4.3; the pure standard harpagoside spectrum was observed as molecule with attached negative formic acid ions $[M+HCOO]^-$ at m/z 539.23 as the base peak of harpagoside and the same corresponding fragment ion at m/z 517 was seen in *H. procumbens* extract as demonstrated in figure 4.4 (the arrow refer to the harpagoside fragment ions). Karioti et al. demonstrated $[M+HCOO]^-$ ion for harpagoside at m/z 539.23 in the negative mode and fragment ions of 517 $[M+Na]^+$ for harpagoside in the positive mode (Karioti *et al.*, 2011).

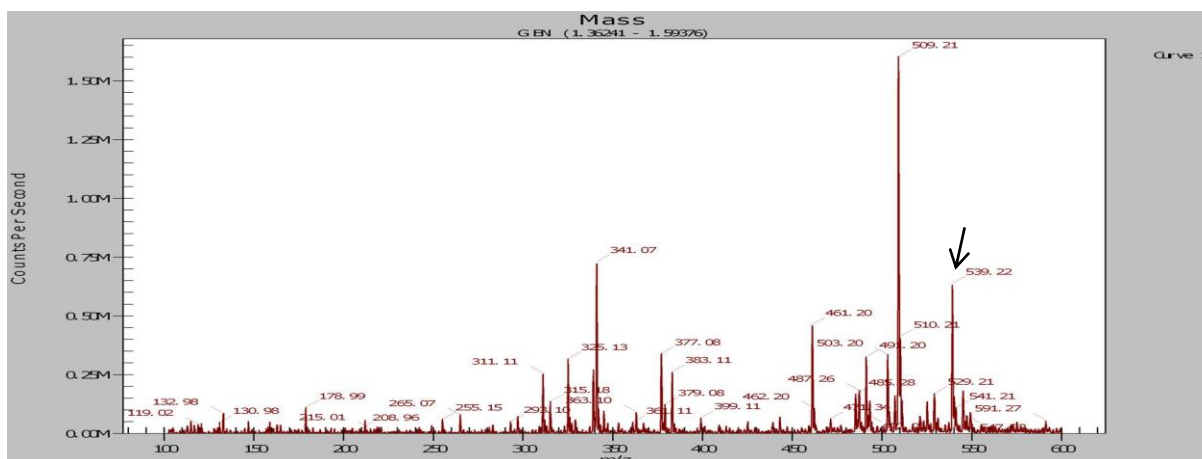


Figure 4-3: full scan MS spectrum of pure standard harpagoside in negative ion mode showing $[M+HCOO]^-$ Ion of harpagoside at m/z 539.23.

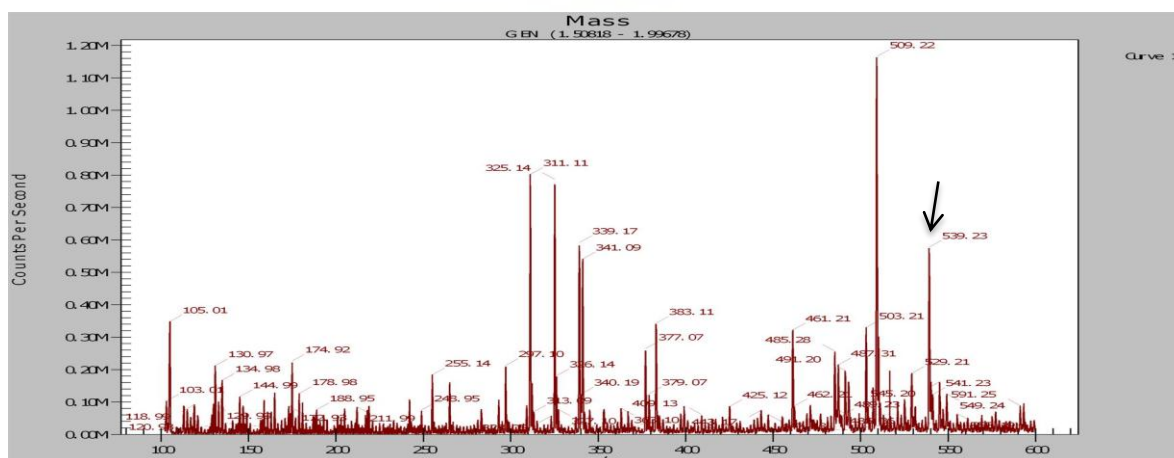


Figure 4-4: full scan MS spectrum of plant extract in negative ion mode showing $[M+HCOO]^-$ Ion of harpagoside at m/z 539.23.

4.2.2 UHPLC

For confirmative identification of harpagoside in plant extract, UHPLC was performed. Pre analysed plant extract sample represented in figure 4.5.1 was spiked with pure standard harpagoside; the blue peak demonstrates the harpagoside peak in *H. procumbens* plant extract before spiking.

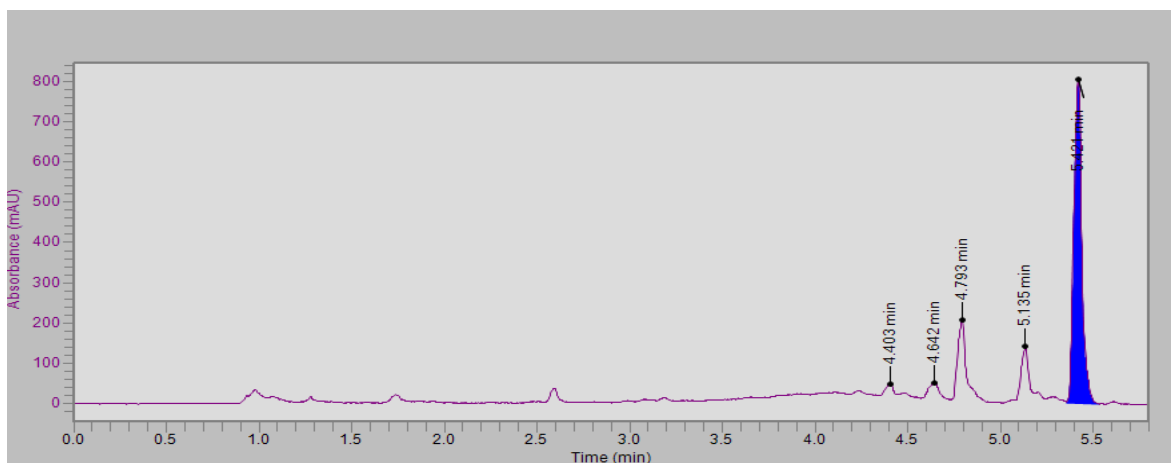


Figure 4-5-1: Harpagoside chromatogram in plant extract before spiking.

Figure 4.5.2; represents the increasing harpagoside peak i.e. the blue peak height in the shown UHPLC chromatogram of plant extract after being spiked with pure standard harpagoside confirming the identity of the compound in the crude plant extract. The UHPLC method was used for identification and quantification of harpagoside in this thesis.

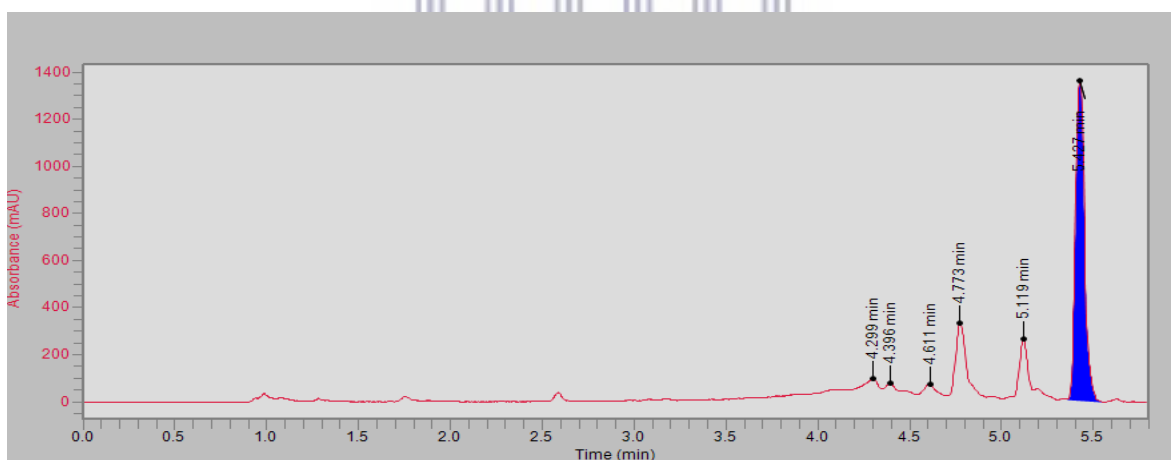


Figure 4-5-2: Harpagoside chromatogram in plant extract after spiking.

UV spectrum analysis was performed for pure standard harpagoside in figure 4.6 (top) and the corresponding UV spectrum was obtained, which confirmed the identification of the harpagoside peak as depicted in figure 4.6 (bottom) when compared to harpagoside reference spectra from literature.

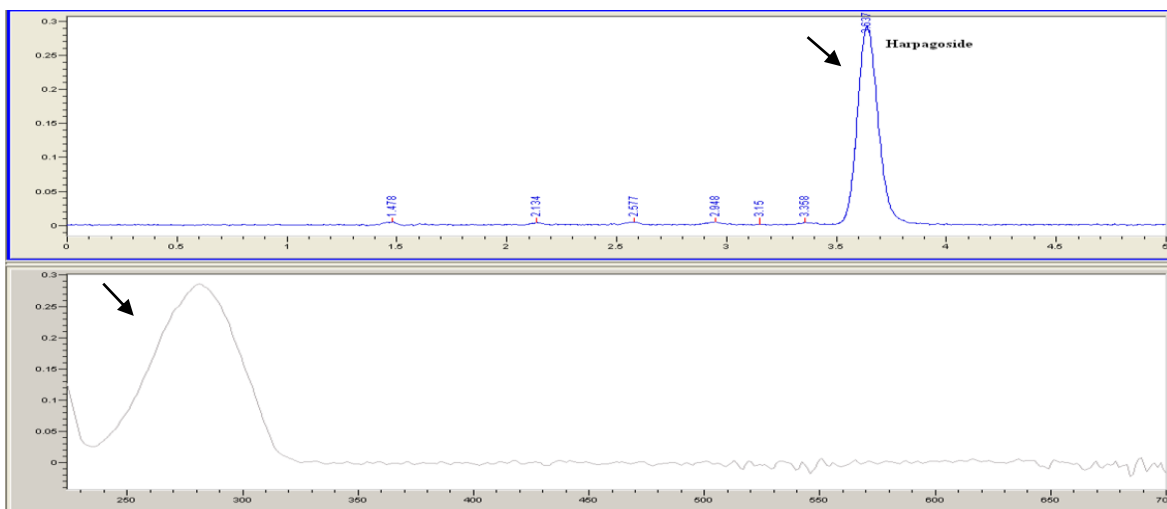


Figure 4-6: Spectra for pure standard harpagoside peak at 278 nm indicating harpagoside identity and no co elution with harpagoside from other plant extract components.

4.2.2.1 Development of an UHPLC method for harpagoside assay

Utilizing the chromatographic conditions in the method mentioned in the experimental section produced peak eluted at 3.6 min retention time in a run time of 5 min as can be seen in figure 4.7 (blue peak represent harpagoside peak).

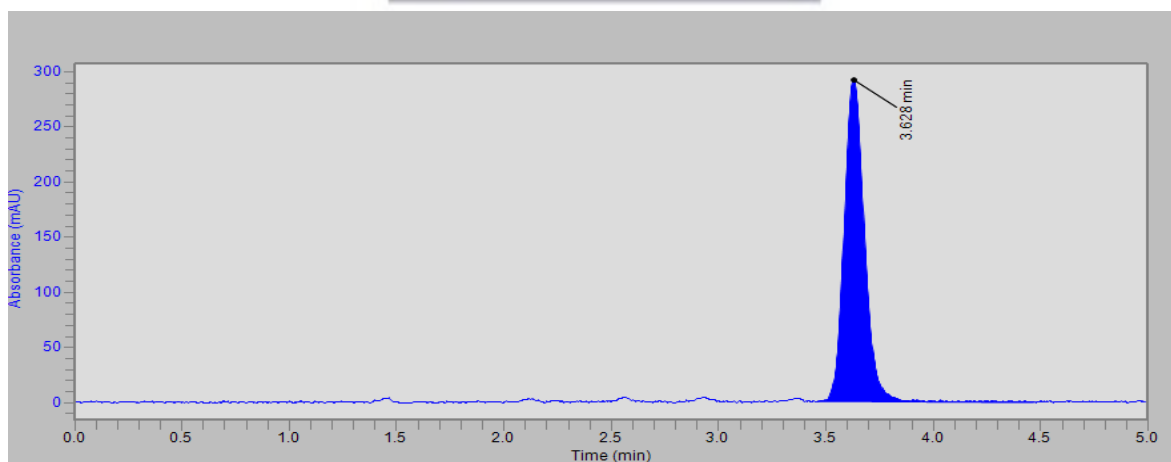


Figure 4-7: UHPLC chromatogram of pure harpagoside. Mobile phase (methanol: water; (60:40v/v).

These optimal chromatographic conditions were employed for *H. procumbens* plant extract and produced the same peak at same retention time (3.6 min) as the pure harpagoside (figure 4.7) with good resolution and selectivity of harpagoside in plant extract as indicated in figure 4.8 (The blue peak indicating harpagoside peak).

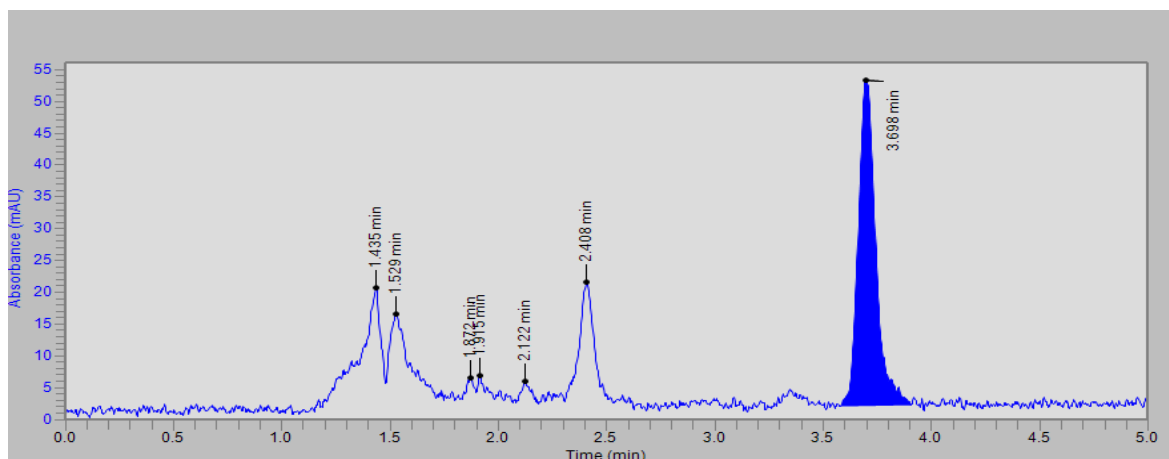


Figure 4-8: UHPLC chromatogram of harpagoside in *H. procumbens* plant extract.

The corresponding UV spectrum of the harpagoside peak in *H. procumbens* plant extract at retention time of (3.6 min) recorded at absorption maximum (278 nm) is represented in figure 4.9 (arrow - harpagoside peak and corresponding UV spectrum).

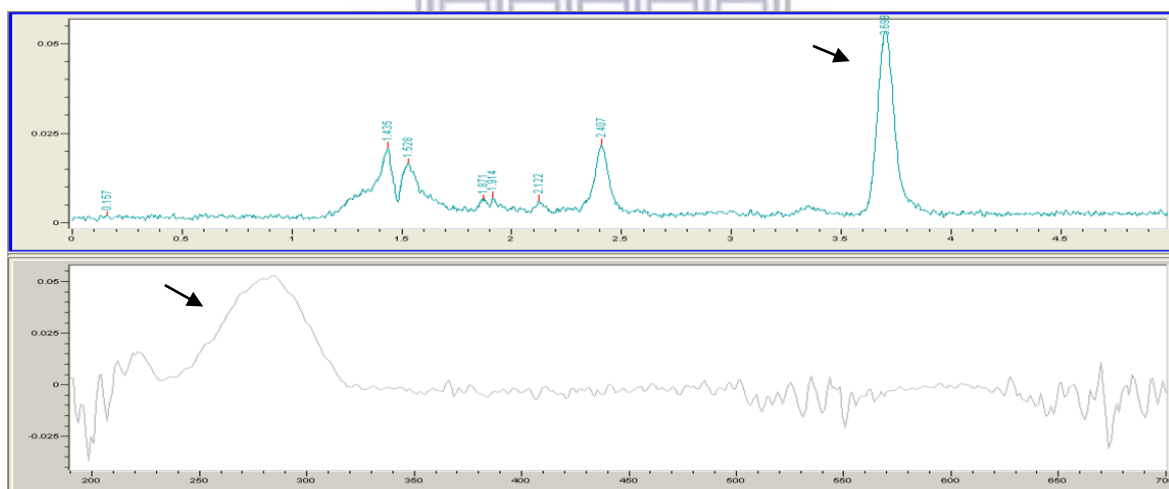


Figure 4-9: Identical spectra (bottom) acquired across the harpagoside peak in plant extract (top) indicate a pure peak of harpagoside at 3.6 min and showing no co elution with harpagoside at 278 nm from other plant extract components.

The UV spectrum of harpagoside in the extract and that of the standard harpagoside was the same and in agreement to the UV spectrum reported by Li *et al.*, (1999) and Wagner *et al.*, (2011).

4.2.2.2 Validation UHPLC method of harpagoside

1. Specificity

Analysis of mobile phase did not create any interference with harpagoside elution, as demonstrated in figure 4.10.1 which is methanol chromatogram indicating that there was no peak eluted at harpagoside retention time (3.6 min) and figure 4.10.2 which is deionized water chromatogram showing also no peak eluted at harpagoside retention time (3.6 min). From this result it was found that suitability of mobile phase system to perform UHPLC analysis for harpagoside.

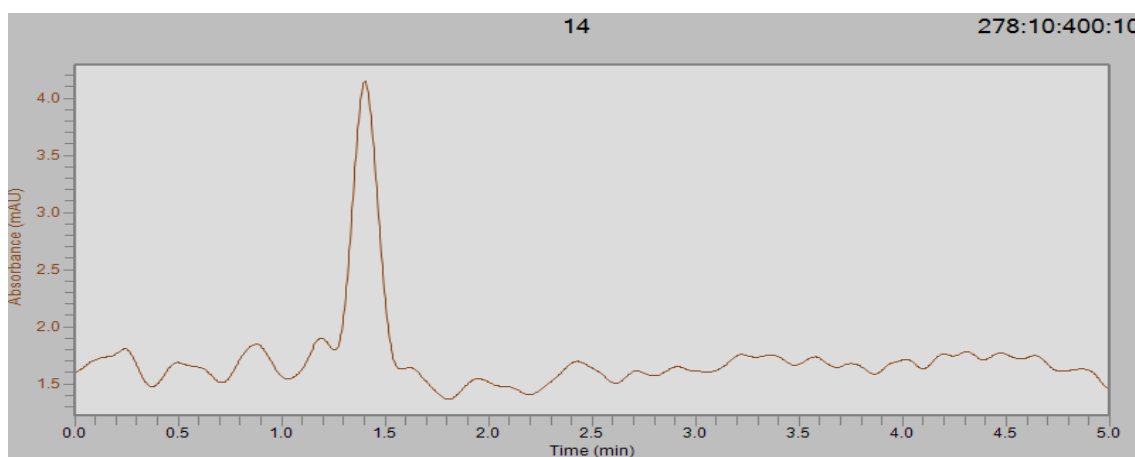


Figure 4-10-1: Mobile phase component (methanol) chromatogram.

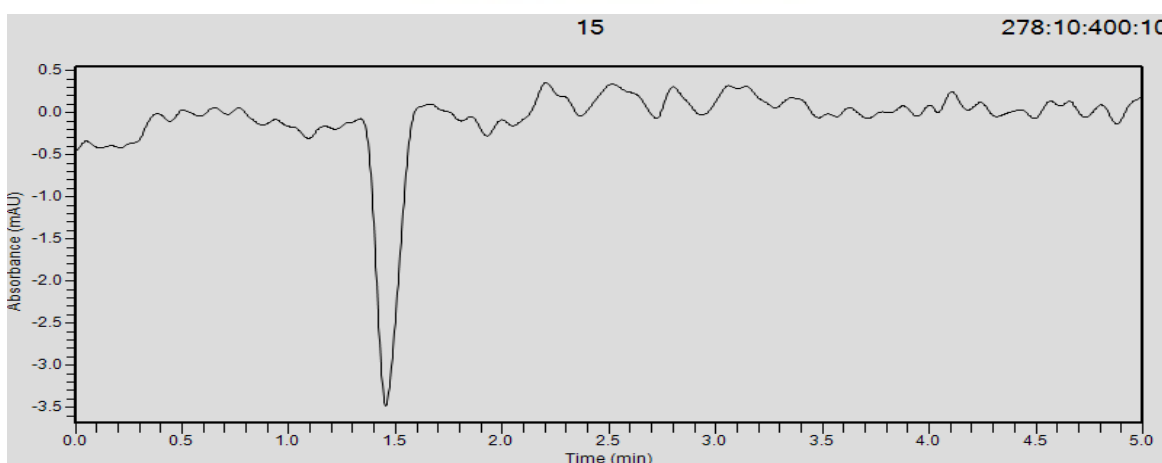


Figure 4-10-2: Mobile phase component (deionized water) chromatogram.

To ensure specificity of the method the harpagoside was placed in 0.1 M sodium hydroxide. This degraded sample of harpagoside reflected a lower harpagoside peak height due to decrease in the analyte concentration as a result of degradation compared with non-degraded harpagoside sample peak, which illustrate the specificity of the method to detect the harpagoside even when it is degraded. Figure 4.11.1 illustrates non-degraded harpagoside (blue peak) and figure 4.11.2 illustrates degraded harpagoside (blue peak). The proposed method passed the specificity test successfully.

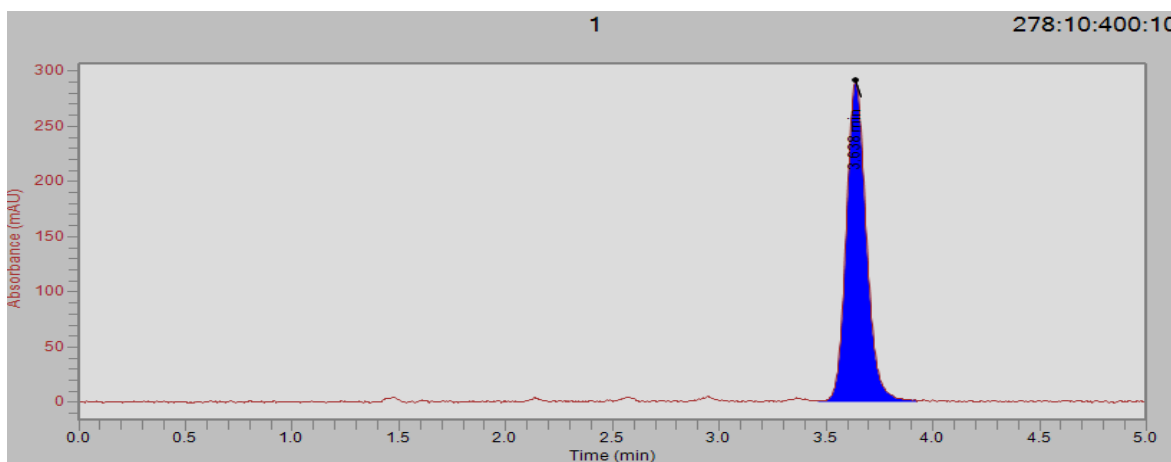


Figure 4-11-1: UHPLC chromatogram of pure standard non-degraded harpagoside.

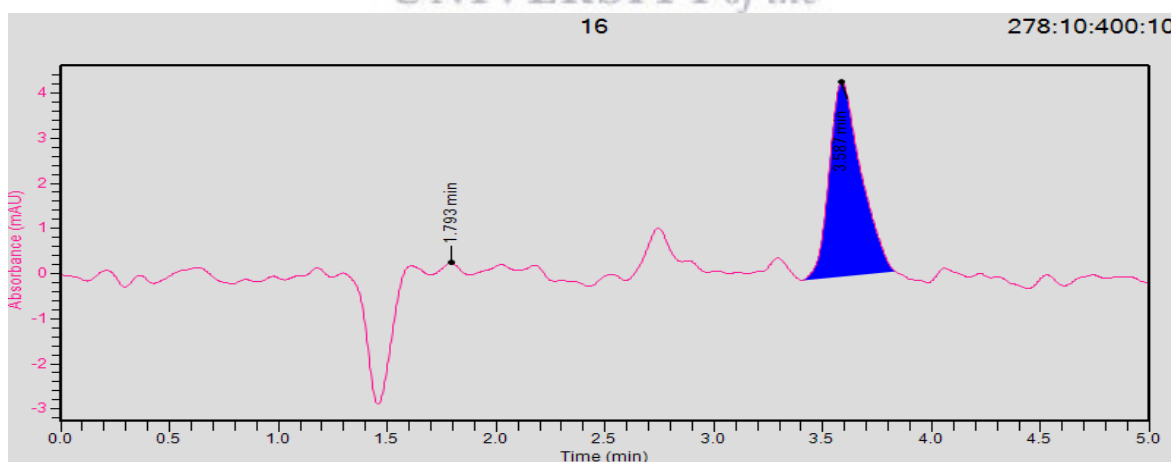


Figure 4-11-2: UHPLC chromatogram of the forced degradation harpagoside sample in NaOH.

2. Linearity

Linearity was measured using calibration plot of peak area against harpagoside concentration in a concentration range of 0.250 (100 %), 0.125 (50 %), 0.0625 (25 %), 0.03125 (12.5 %), 0.0039 mg/ml (1.56 %) as depicted in figure 4.12.1. The slope, Y-intercept and correlation coefficient of the calibration curve were calculated by analysis of the regression line and the linear graph with linear equation $Y = 7.849e + 006 X - 135.3$ was obtained. X is the concentration in mg/ml and Y is the peak area in absorbance units. A correlation coefficient of 0.9995 was obtained indicating good linearity correlation between the concentration peak area in the proposed range as it meets the acceptance criteria for linearity which is not less than 0.990 (Al-Rimawi, 2014).

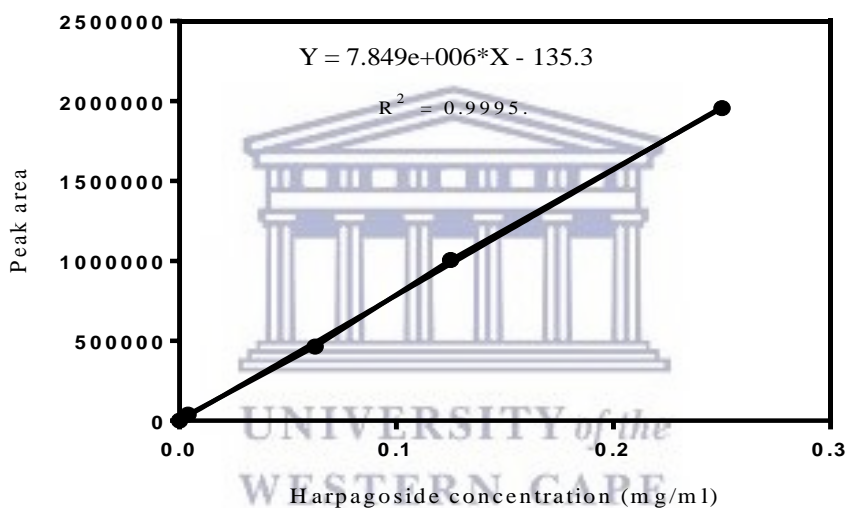


Figure 4-12-1: Linearity plot of harpagoside dissolved in methanol.

Another calibration curve was performed of harpagoside utilizing the same concentrations and different solvent of phosphate buffer (PBS) solution. It was used for harpagoside concentration calculation when the sample matrix is PBS. The linear equation of $Y = 8.062e + 006X - 995.8$ was obtained for this calibration curve and had a correlation coefficient of 0.9992 which indicates the acceptable linearity between the concentration and peak area in the proposed range as represent in figure 4.12.2.

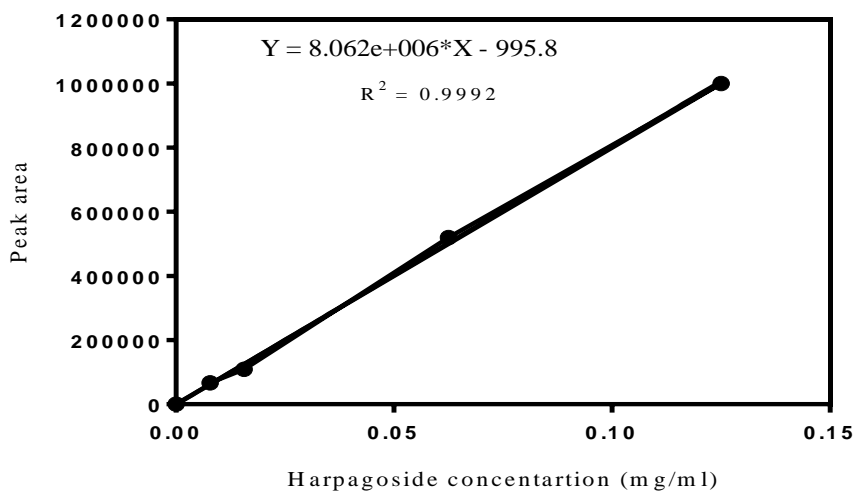


Figure 4-12-2: Linearity plot of harpagoside dissolved in phosphate buffer solution, pH 7.4.

3. Intra-day precision (repeatability)

Six harpagoside standard samples were used for this test each containing 62.5 µg/l. The percentage relative standard deviation was calculated and the results of the precision study are tabulated in table 4.1.

Table 4-1: Intra-day precision (repeatability)

Sample	Peak area
1	510971.39
2	527050.87
3	509822.10
4	514614.35
5	511100.73
6	508643.31
Average	513700.46
SD	6839.4681
% RSD	1.3314117

The predetermined criterion for intra-day and inter-day precision is the percentage relative standard deviation of areas from 6 preparations. The precision level should not be more than 2.0 %

(Venhatesh *et al.*, 2010). The obtained result (1.33 %) was within this specification that indicates the analytical method is precise within the tested range.

4. Intermediate precision

Intermediate precision of the method was evaluated by calculating the percentage recovery of harpagoside at 3 concentration levels (0.125, 0.0625, 0.03125 µg/ml), over 3 days. The percentage relative standard deviation was calculated and the results of study are tabulated in table 4.2.

Table 4-2: Intermediate precision

	0.125 mg/ml	0.0625 mg/ml	0.03125 mg/ml
Day1	1010935.1	510971.4	336194.28
Day2	1008195.7	529051.46	326897.81
Day3	1005117	514470.47	324072.35
Average	1008082.6	518164.44	329054.8
SD	2910.6984	9589.3844	6342.302
% RDS	0.2887361	1.8506450	1.92743

The low % RSD of the 3 concentrations were (0.28, 1.85 and 1.92) which demonstrated that the UHPLC method is precise as the results were not more than 2 % (Venhatesh *et al.*, 2010).

5. Accuracy

Accuracy was calculated by the recovery method from 6 replicates at the concentration level of 0.0625 mg/ml. Accuracy was based on ratio of the measured quantity to the calculated quantity. The percentage relative standard deviation was calculated and the results are tabulated in table 4.3.

Table 4-3: Percentage recovery of the harpagoside

Measured conc. (mg/ml)	Calculated conc. (mg/ml)	Recovery %
0.0625	0.0642	103.44
0.0625	0.0662	105.93
0.0625	0.0645	103.21
0.0625	0.0651	104.19
0.0625	0.0646	103.47
0.0625	0.0643	102.97
Average	0.0649	103.87

As per International Council for Harmonisation (ICH, 2005) guidelines, pre-specified limits recovery should be within 95 % - 105 %. In the present study the percentage mean recovery of the 6 replicates of test concentration was (103.87 %) and therefore passed the accuracy test (Venkatesh *et al.*, 2010).

6. Specificity:

Limit of detection and Limit of quantification of harpagoside investigated in this study using the current method were found to be low i.e. 0.0057 µg/ml and 0.0120 µg/ml, respectively. This shows the detection and quantitation of this compound at low concentration levels.

7. Robustness

Robustness of the method was studied by variation in temperature and wavelength by a 2 % change while other chromatographic conditions are kept constant. When wavelength changed by 278 ± 2 nm no variation in peak retention time compared with the retention time of harpagoside peak at 278 nm which eluted at 3.6 min. Moreover, the results demonstrate that during temperature variance conditions, the retention time of the peak was slightly affected and shifted to 3.7 min with low % RSD and it was in accordance with that of actual harpagoside peak at 278 nm which eluted at 3.6 min. The results are indicated in table 4.4.

Table 4-4: method robustness

Parameter	Retention time		% RSD
	(min)	Mean, n = 3	
Temperature (25 ± 2 °C)	23	3.720	0.282
	27	3.779	0.687
Wavelength (278 ± 2 nm)	276	3.720	1.023
	280	3.687	1.351

Percentages RSD of peak areas were evaluated and all changes showed % RSD of less than 2 % (Venhatesh *et al.*, 2010). Hence the analytical method would be concluded as robust.

8. System suitability

System suitability parameters were analyzed to check the system performance consistency and the resulted values are tabulated in table 4.5.

Table 4-4: System suitability

Parameter	Average, n=3	Criteria
Theoretical Plates	5821.667±3.90	> 2000
Tailing Factor	1.137±3.16	< 2
Peak Purity	8.976667±1.20	> 0.98
RT (min)	3.865333±1.17	Not applicable

Theoretical plates indicates column efficiency with values more than 2000 reflecting good separation of peaks. The harpagoside peak gave a value of 5821. Tailing factors for most peaks were < 2, with a value of 1.137 indicating a perfectly symmetrical peak. Here, the peak purity was 8.97, which is in the system required suitability range (> 0.98). There was no interference or

co-eluting along with harpagoside at this retention time. All system suitability parameters met the acceptance criteria as shown in table 4.5 (Shabir, 2003).

4.3 Quantitative determination of harpagoside constituent in plant extract

The harpagoside yield in the crude *H. procumbens* extract was 2.6 %. This result was in line with the range reported in other studies (1.355 %; Poukens-Renwart *et al.*, 1996, 1.62 %; Karioti *et al.*, 2011 and 2.35 %; Boje *et al.*, 2003). According to the standard set by the European and British Pharmacopoeias, the harpagoside content is required to be at least 1.2 % (dried drug) (Mncwangi *et al.*, 2014). Hence the harpagoside content in the prepared *H. procumbens* extract was suitable to formulate the plant extract.

4.4 Lipid vesicles preparation and characterization

Lipid vesicles were successfully prepared with the thin film hydration method. Figure 4.13 is a photomicrograph of lipid vesicles captured under a microscope confirms the formation of the phospholipid vesicles on hydration of thin lipid film formed by the rotary evaporator.

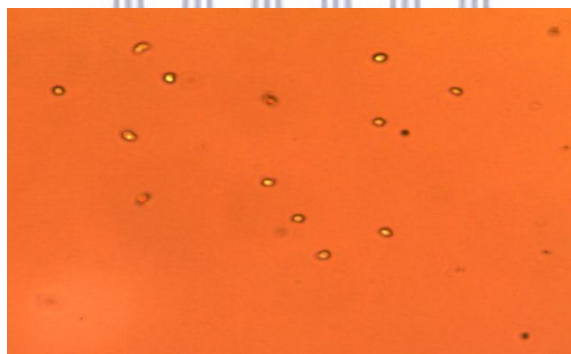


Figure 4-13: Microscopic images of lipid vesicles.

4.5 Preliminary study for determination of nano lipid vesicles formulation parameters

Preliminary studies were conducted to ensure lipid vesicles formation and plant extract encapsulation in the vesicles. This included the selection of the phospholipid, method for size reduction, vesicles disruption and sonication time required for vesicle disruption. These methodical parameters were determined before the statistical response surface methodology (RSM) optimization of nano lipid vesicles was implemented.

4.5.1 Investigating the effect of lipid type on percentage encapsulation efficiency

Soy L- α -PC and lecithin were utilized in the formulation as the lipid phase. From the results, the type of lipid used for the preparation of lipid vesicles appeared to affect the incorporation of the drug as differences in percentage encapsulation efficiency values were observed. High percentage encapsulation efficiency values were obtained when PC was utilized in the formulation as the lipid component and low values were obtained when Lecithin was utilized as represented in figure 4.14.

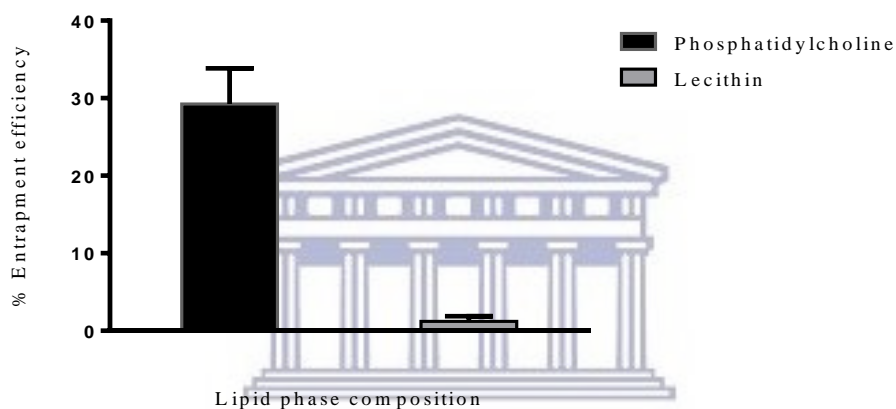


Figure 4-14: Histogram illustrating lipid type on percentage encapsulation efficiency.

The lower percentage encapsulation efficiency demonstrated by lecithin may be due to the presence of other components like phospholipids, glycolipids and complex carbohydrates such as sucrose, raffinose and stachyose (van Nieuwenhuyzen *et al.*, 2008). It could be that some of these impurities formed micelles rather than bilayer-lipid formations or interfered with the plant extract resulting in a decrease in % encapsulation efficiency. Imura *et al.* demonstrated high percentage encapsulation efficiency of liposome made from Lecinol S-10EX. This contains 95 % PC with low % encapsulation efficiency while liposome made from Lecinol S-10 contains 32 % PC. Based on these preliminary experiments PC was selected to formulate the lipid vesicle formulations due to its higher percentage encapsulation efficiency (Imura *et al.*, 2003).

4.5.2 Investigating the optimal sonication time for vesicle disruption

The optimal sonication time for the disruption of lipid vesicles was investigated. Prepared lipid vesicles were disrupted via sonication for different time periods. With increase in sonication time more harpagoside was released. The release at 3-5 min was similar as depicted in figure 4.15.

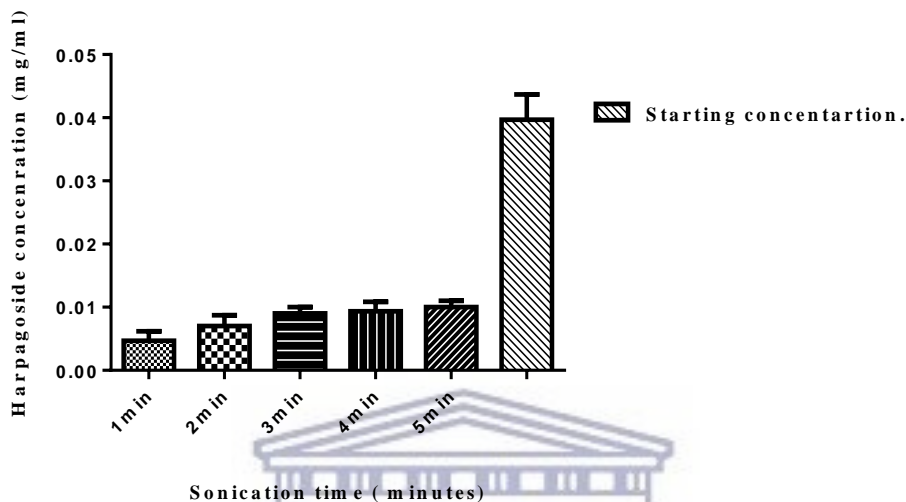


Figure 4-15: Sonication time for disrupt of lipid vesicles to release maximum amount of loaded drug.

There was an increase in the release of harpagoside between 1 and 3 min but increasing the sonication time from 3 to 5 min did not cause any further appreciable increase. Sonication time of 3 min was selected to disrupt the prepared lipid vesicles. In addition, although the 5 min time interval resulted in a slightly higher breakdown of vesicles, the 3 min interval was selected due a decreased possibility of ethanol loss due to heat generated evaporation with increased sonication time.

4.5.3 Investigating the influence of the lipid vesicle size reduction method on percentage encapsulation efficiency.

Water bath sonication, probe sonication and extrusion method were applied to reduce lipid vesicle size. Each method displayed characteristic particle size and percentage encapsulation efficiency values. Encapsulation efficiency dropped from probe sonication > extrusion > water bath sonication. This is demonstrated in table 4.6.

Table 4-5: Influence of vesicles sizing down method on the percentage of encapsulation efficiency.

Size reduction method	Particle Size mean \pm SD	% EE mean \pm SD
Probe sonication	103.66 \pm 7.45	2.933 \pm 1.3
Water bath sonication	1066.36 \pm 13.71	34.76 \pm 5.67
Extrusion	347.53 \pm 17.15	15.95 \pm 3.10

The probe tip sonication method caused size reduction and low percentage encapsulation efficiency (2.9 %). The decrease may be due to the disruption of lipid vesicles as a result of subsequent heat build-up. Ding *et al.* (2009) reported that the decrease in encapsulation efficiency of ferrous glycinate liposomes with increasing of sonication strength, may be attributed to the high input of energy resulted in overheating ferrous glycinate leaking from the liposomes (Ding *et al.*, 2009). Although, the energy was low because low intensity was utilized, it can be destructive to phospholipid molecules (Ong *et al.*, 2016). Therefore, probe sonication was not the method of choice for size reduction.

The water bath sonication method did not reflect reduction in particle size and the percentage encapsulation efficiency was high, as these were micro units sized particles. Work done by Perkins *et al.*, (1993; Muppidi *et al.*, (2012) shows that percentage encapsulation efficiency increase with particle size increases.

The extrusion method exhibited appropriate particle size reduction with relatively lower percentage encapsulation efficiency compared to the water bath sonication method but higher than the probe sonication method. This might be as result of decrease in particle size of the lipid vesicles resulting in lower the drug loading (Ong *et al.*, 2016). Therefore a balance needs to be obtained between the size reduction required and the drug loading for practical application. Thus, the extrusion method was used as size reduction method for all further experiments.

4.5.4 Finding the appropriate plant extract ratio for appropriate percentage encapsulation efficiency

The percentage encapsulation efficiency of prepared lipid vesicle batches with constant PC and cholesterol ratio and different plant extract ratio was 13.92 ± 1.007 at 2.5 mg/ml, 11.76 ± 0.46 at 5 mg/ml and 15.04 ± 0.60 at 10 mg/ml as represented in the following figure 4.16.

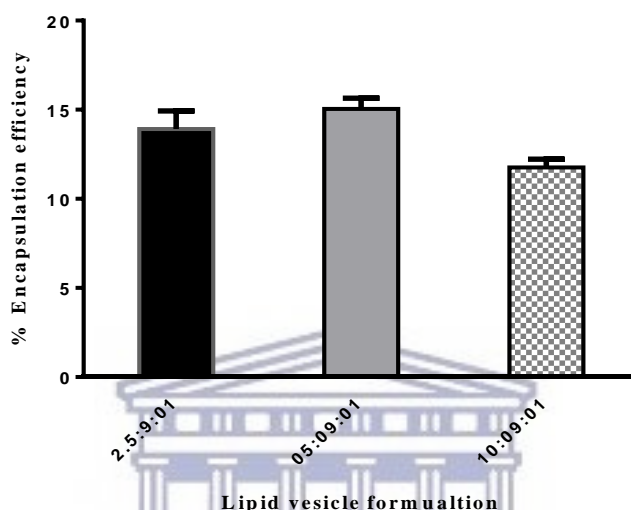


Figure 4-16: Effect of variation in plant extract content on the percentage encapsulation efficiency of lipid vesicle formulations prepared with constant lipid phase content (plant extract: PC: cholesterol).

When the plant extract concentration was increased from 2.5 to 5 %, there was no significant increase in percentage encapsulation efficiency, in contrast, when increased above 10 a % decrease in percentage encapsulation efficiency was observed. In the light of these results it was shown that using a fixed amount of lipid and different amounts of crude plant extract did not increase the percentage encapsulation efficiency significantly ($p > 0.05$). It might correspond to saturation of the lipid portion. These findings are similar to those reported previously by Singh *et al.*, (2015). In their study there was a slight increase in percentage encapsulation efficiency when the drug - lipid molar ratio changed from 1:2 to 2:2. Carafa *et al.* (2010) found that an increase in drug content from 6 to 60 mM, the drug loading decreased from 87 % to 79 % (Carafa *et al.*, 2010). Kan *et al.* (2010) reported that encapsulation efficiency was maintained even though the drug: phospholipid molar ratio was increased (Kan *et al.*, 2010). Hence, in our study (2.5 mg/ml)

plant extract concentration was used in the optimization process with RSM. Beyond this ratio there was no change but a decrease in percentage encapsulation efficiency was observed.

4.6 Response Surface Methodology (RSM) optimization process of nano lipid vesicles formulation

4.6.1 Design of experiments

Response surface methodology has been established as a convenient method for developing optimum processes with precise conditions and has also minimized the cost of production of many a process with efficient screening of process parameters (Francis *et al.*, 2003).

4.6.2 Generating experimental matrix

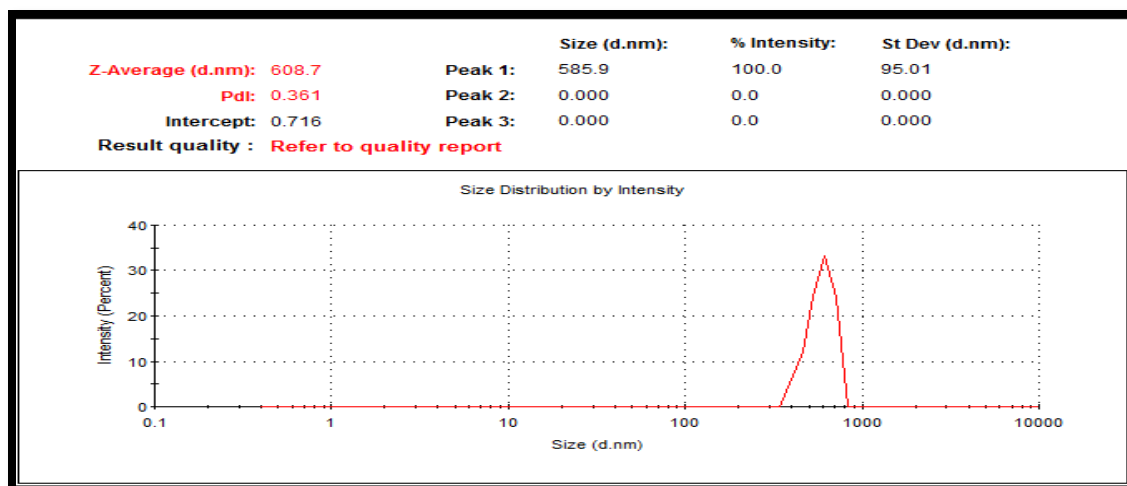
For the optimization study, the output factor surface methodology (RSM) IV-optimal design was adopted to optimize experimental parameters and explore the effect of input factors. These were PC content; (X1), cholesterol content; (X2) and the type of the lipid vesicle; (X3). The output factors viz. particle size; (Y1_{PS}), polydispersity index; (Y2_{PDI}) and percentage entrapment efficiency; (Y3_{%EE}). The software generated design matrix with 17 experiments as refelected in table 4.7. These 17 experiments were performed as generated by the RSM matrix. The results of the output factors as per expermental runs were populated in table 4.7 as response 1, 2 and 3.

Table 4 -6: Experimental matrix of RSM optimal design.

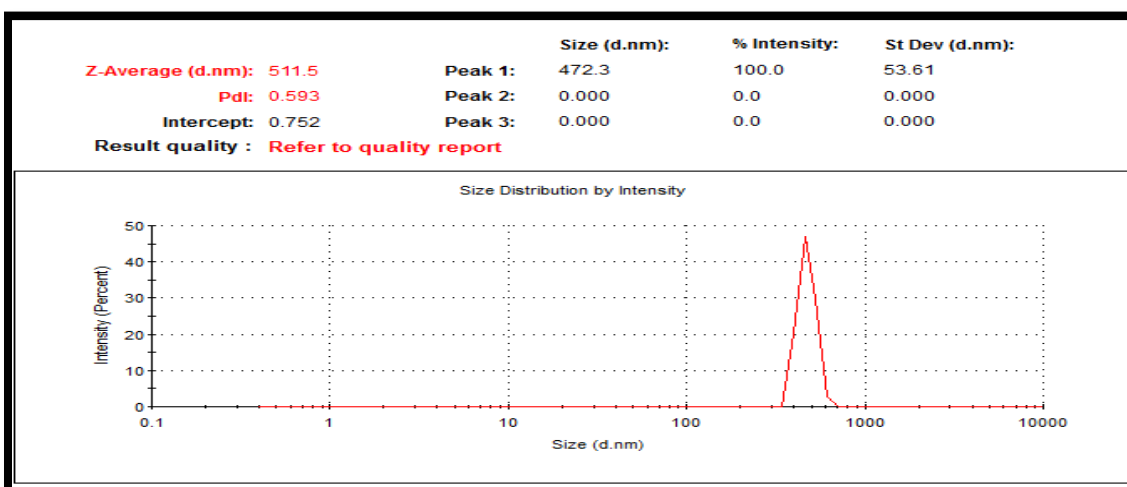
Std	Run	Factor 1 A:PC %	Factor 2 B:CHOL %	Factor 3 C:vesicle type material	Response 1 Size nm	Response 2 PDI /	Response 3 EE %
1	1	80.00	40.00	liposome	608.7	0.361	14.6
3	2	45.00	40.00	phytosome	531.1	0.547	19.51
2	3	80.00	22.50	phytosome	596.4	0.369	30.95
6	4	10.00	5.00	phytosome	328	0.272	9.52
16	5	10.00	40.00	phytosome	434.6	0.379	15.38
10	6	80.00	5.00	liposome	546	0.18	21.2
14	7	80.00	5.00	phytosome	527.8	0.182	27.02
13	8	45.00	5.00	phytosome	587.5	0.375	24.4
11	9	45.00	22.50	liposome	474.8	0.353	17.7
5	10	10.00	22.50	phytosome	207.8	0.288	2.6
12	11	80.00	40.00	phytosome	587.1	0.479	31.25
8	12	10.00	40.00	liposome	437.5	0.528	2.38
4	13	45.00	22.50	liposome	446.9	0.414	12.5
9	14	10.00	5.00	liposome	491.7	0.558	2
7	15	45.00	22.50	liposome	382.6	0.268	15.83
15	16	45.00	5.00	liposome	496.9	0.418	23.4
17	17	45.00	22.50	liposome	511.5	0.593	13.95

4.6.3 Lipid vesicle characterization of RSM generated experiments

The generated design matrix consisted of 17 experiments with different composition varied for liposome and phytosomes formulations. Particle size, polydispersity index and percentage encapsulation efficiency were measured and the results are depicted in table 4.7. The size range obtained varied between 208 nm and 609 nm. The polydispersity index values of the formulations were between 0.18 and 0.593 revealing that the particle polydispersity index was homogeneous in some formulations and hererogeneous in some. The percentage encapsulation efficiency of the lipid vesicles formulations was calculated and within the range of 2 % - 31.25 %. Phytosomes, prepared with the same formulation as the liposomes demonstrated lower particle size and higher percentage encapsulation efficiency compared with liposomes, this can be seen when experiment 1, 12, 14 (liposomes formulations) were compared to 11, 5, 4, (phytosomes formulations) respectively. The variation in output values is believed to be due to variation in formulation composition. The following figure 4.17 shows the particle size and polydispersity index curve of two randomly selected formulations from those proposed by RSM.



Formulation 1



Formulation 17

Figure 4-17: illustration of particle size of two randomly selected formulations (formulation 1 and 17) of according to RSM.

4.6.4 Analysis of RSM data and evaluation of the fitted output factor surface models

The experimentally obtained output factor values of 17 experiment were fitted to various models namely linear, 2FI (2 factor interaction), quadratic and cubic by using Design Expert software to determine the data suitability model. A suitable model was selected based on lack of fit p-value and R^2 values. The different model fitting values are shown in table 4.8.

Table 4- 7: Estimation of regression model, fit summary of the output factors $Y1_{PS}$, $Y2_{PDI}$ and $Y3_{\%EE}$, respectively.

Source	Sequential p-value	Adjusted R-Squared	Predicted R-Squared	Adequate precision	
Y_1					
Linear	0.3317	0.0449	-0.3272	1.40	
2FI	0.9309	-0.1900	-1.2363	2.28	
<u>Quadratic</u>	<u>0.0065</u>	<u>0.810</u>	<u>0.737</u>	<u>7.027</u>	<u>Suggested</u>
Cubic	0.2449	0.7787			Aliased
Y_2					
Linear	0.0945	0.2337	-0.0425	4.62	
2FI	0.2028	0.3588	0.3034	3.11	
<u>Quadratic</u>	<u>0.047</u>	<u>0.5571</u>	<u>0.5178</u>	<u>5.710</u>	<u>Suggested</u>
Cubic	0.9875	-0.0241			Aliased
Y_3					
<u>Linear</u>	<u>0.0001</u>	<u>0.7397</u>	<u>0.6234</u>	<u>12.556</u>	<u>Suggested</u>
2FI	0.4049	0.7438	0.3588	9.626	
Quadratic	0.1190	0.8119	0.4724	6.215	
Cubic	0.1263	0.9398			Aliased

The value of correlation coefficient (R^2) is also an indication of the appropriateness of the selected model. From the table, the predicted and adjusted R^2 of all models are in reasonable agreement with the adjusted R^2 . They are within 0.20 of each other (Jaafarzadeh *et al.*, 2016) and is an indication of appropriateness of the selected models which are quadratic for $Y1_{PS}$ and $Y2_{PDI}$ and linear for $Y3_{\%EE}$. Adequate precision measures the signal to noise ratio and compares the range of the predicted values at the design points to the average prediction error (Mourabet *et al.*, 2014). The ratio greater than 4 is desirable and indicates this model can be used to navigate the design space according to the software. In this study, the ratio is found to be 7.02 for particle size, 5.71 for polydispersity index and 12.55 for percentage encapsulation efficiency. This indicates the adequateness and the reliability of the experiment data and this model can be used to navigate the design space.

The statistical validity of the selected models was further established by ANOVA. The insignificant coefficients were eliminated after examining the coefficients, and the models were finally refined. Results of the ANOVA for all model selected for $Y1_{PS}$, $Y2_{PDI}$ and $Y3_{\%EE}$ are summarized in table 4.9, 4.10 and 4.11, respectively.

Table 4-8: Statistical parameters obtained from the ANOVA for the selected regression model of Y_{1PS} generated from RSM software.

ANOVA for Response Surface Reduced Quadratic Model						
Analysis of variance table [Partial sum of squares - Type III]						
Source	Sum of Squares	df	Mean Square	F Value	p-value Prob > F	
Model	1.572E+005	5	31446.77	6.08	0.0061	significant
<i>A-PC</i>	13053.77	1	13053.77	2.52	0.1405	
<i>B-CHOL</i>	7.92	1	7.92	1.531E-003	0.9695	
<i>C-vesicle type</i>	30153.75	1	30153.75	5.83	0.0343	
A^2	40302.32	1	40302.32	7.79	0.0175	
B^2	1.000E+005	1	1.000E+005	19.33	0.0011	
Residual	56900.66	11	5172.79			
<i>Lack of Fit</i>	48013.41	8	6001.68	2.03	0.3034	not significant

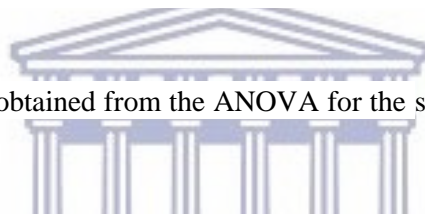


Table 4-9 : Statistical parameters obtained from the ANOVA for the selected regression model for Y_{2PDI} generated from RSM software.

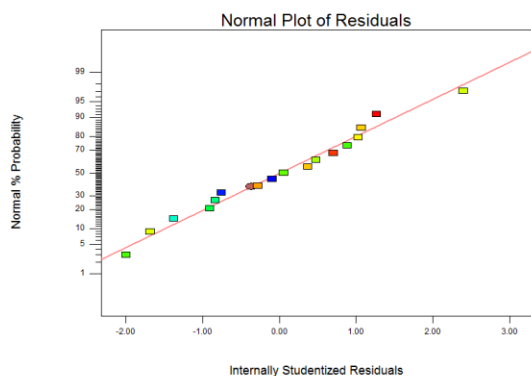
ANOVA for Response Surface Quadratic Model						
Analysis of variance table [Partial sum of squares - Type III]						
Source	Sum of Squares	df	Mean Square	F Value	p-value Prob > F	
Model	0.23	8	0.029	3.52	0.0472	significant
<i>A-PC</i>	0.057	1	0.057	6.98	0.0296	
<i>B-CHOL</i>	0.055	1	0.055	6.70	0.0322	
<i>C-vesicle type</i>	0.015	1	0.015	1.86	0.2099	
<i>AB</i>	0.020	1	0.020	2.45	0.1561	
<i>AC</i>	0.033	1	0.033	4.08	0.0780	
<i>BC</i>	6.063E-003	1	6.063E-003	0.74	0.4149	
A^2	0.038	1	0.038	4.68	0.0625	
B^2	0.034	1	0.034	4.11	0.0773	
Residual	0.066	8	8.200E-003			
<i>Lack of Fit</i>	8.716E-003	5	1.743E-003	0.092	0.9875	not significant

Table 4.11: Statistical parameters obtained from the ANOVA for the selected regression model for Y3_{%EE} generated from RSM software.

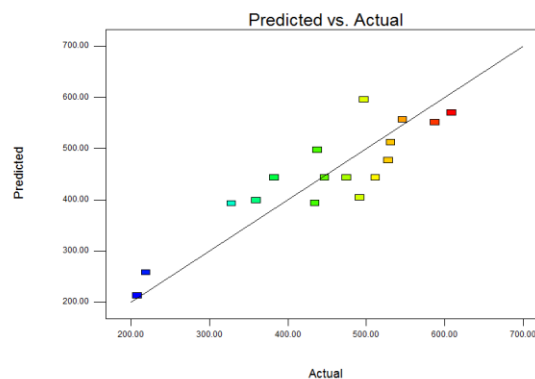
Response	3	EE				
ANOVA for Response Surface Linear Model						
Analysis of variance table [Partial sum of squares - Type III]						
	Sum of		Mean	F	p-value	
Source	Squares	df	Square	Value	Prob > F	
Model	1070.91	3	356.97	16.15	0.0001	significant
A-PC	867.51	1	867.51	39.25	< 0.0001	
B-CHOL	32.64	1	32.64	1.48	0.2459	
C-vesicle type	180.41	1	180.41	8.16	0.0135	
Residual	287.30	13	22.10			
Lack of Fit	271.97	10	27.20	5.32	0.0978	not significant

ANOVA analysis was performed to choose a significant model and insignificant lack of fit for each output factor depends on p value. From the ANOVA analysis it is observed that models chosen for output factors (Y1_{PS}, Y2_{PDI} and Y3_{%EE} had) had p value 0.006, 0.047 and 0.0001 respectively. The very small probability values of the selected model of each output factor reflected that the model was significant for data set ($p < 0.05$). Moreover, the selected model had an insignificant ($p \text{ value} > 0.05$) lack of fit p value = 0.303, 0.987 and 0.097, respectively. That confirms the adequacy of the model fit and demonstrated that the models were valid for the present work. A significant lack of fit ($p < 0.05$) is an undesirable property (according RSM) because it suggests that the model does not fit the data well and hence should not be used for further predictions.

A normal probability plot indicates whether the residuals follow a normal distribution. The residual and corresponding normal probability plots of actual and predicted values for Y1_{PS}, Y2_{PDI} and Y3_{%EE} are demonstrated in figure 4.18.1, 4.18.2 and 4.18.3, respectively. Residual plots indicate errors in the model are normally distributed with respect to run order as the data points on the plot lie close to a straight line. The normal probability plot of residuals for output factor Y2_{PDI} demonstrated all the points are close to the straight line except for two points which illustrate significance of those terms interactions (as per software).

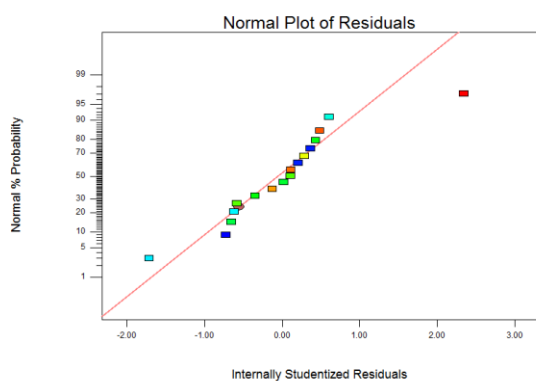


(a)

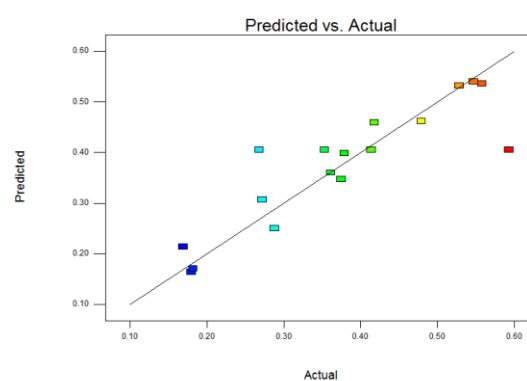


(b)

Figure 4-18-1: Normal plot of residuals (a), normal probability plot of actual and predicted values (b) of particle size ($Y1_{PS}$).



(a)



(b)

Figure 4-18-2: Normal plot of residuals (a), normal probability plot of actual and predicted values (b) of polydispersity index ($Y2_{PDI}$).

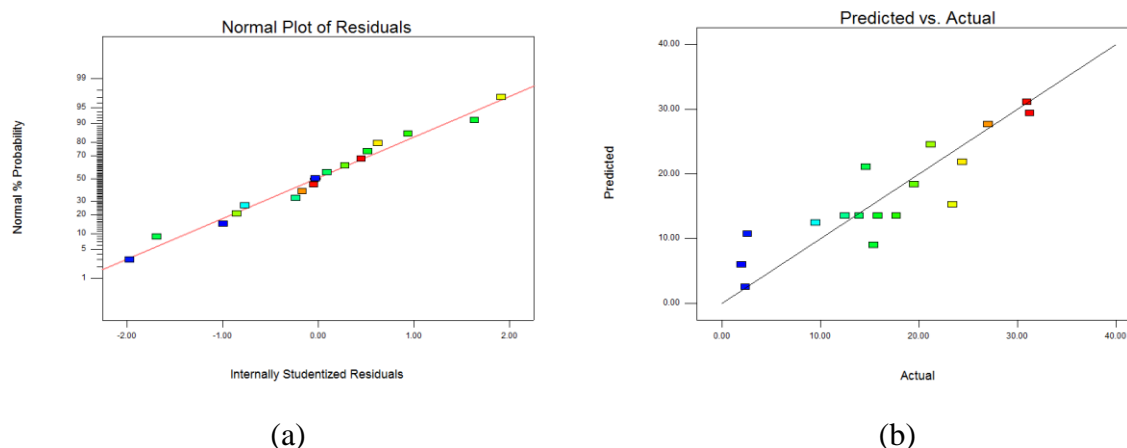


Figure 4-18-3: Normal plot of residuals (a), normal probability plot of actual and predicted values (b) of percentage encapsulation efficiency ($Y3_{\%EE}$).

For normal probability plot of actual and predicted values the actual results are shown on the vertical axis while the results predicted by the RSM model are along the horizontal axis. This will be the same for all of the following normal probability plots. The majority of points cluster around the diagonal line indicated a satisfactory correlation between the observed and predicted output factor values because minor departures from normality are acceptable (Alshamrani, 2017) and further shows a good fit of the model.

4.6.5 Effect of input factor on output factor $Y1_{PS}$ (particle size)

One of the most important parameters, which need to be monitored during lipid vesicles preparation, is the vesicle size and the polydispersity index. It is evident that the particle size and polydispersity index of the liposomes determine their *in vitro* or *in vivo* performance (Ghanbarzadeh *et al.*, 2013). The particle sizes of lipid vesicles were in a range of 382.6 to 608.7 nm for liposomes and for phytosomes in a range of 207.8 to 596.4 nm. The particle size values of liposomes and phytosomes formulation generated by RSM are represented in the following table 4.12.

Table 4.12: Particle size of liposomes and phytosomes formulation (extracted from table 4.7)

F. code	Factor 1; PC %	Factor 2; Chol%	Factor 3; Vesicle type	Response 1 Particle size (nm)
1	80	40	liposome	608.7
2	45	40	phytosome	531.1
3	80	22.5	phytosome	596.4
4	10	5	phytosome	328
5	10	40	phytosome	434.6
6	80	5	liposome	546
7	80	5	phytosome	527.8
8	45	5	phytosome	587.5
9	45	22.5	liposome	474.8
10	10	22.5	phytosome	207.8
11	80	40	phytosome	587.1
12	10	40	liposome	437.5
13	45	22.5	liposome	446.9
14	10	5	liposome	491.7
15	45	22.5	liposome	382.6
16	45	5	liposome	496.9
17	45	22.5	liposome	511.5

The table shows that particle size (Y_{1PS}) increased as PC and cholesterol quantities increase for liposome and phytosomes. This is due to phospholipids constituting the lipid vesicle membrane and PC concentration directly affects the particle size of the lipid vesicle (Ma *et al.*, 2012), cholesterol also increases the thickness of phospholipid bilayer (Hung *et al.*, 2007). This vesicle size increase was demonstrated by Song *et al.* (2008) with silybin-phospholipid complex. Similar observations were reported with ketotifen liposomes and quercetin liposomes with increasing PC and cholesterol respectively (Yas, 2014 and Rasaie *et al.*, 2014). This is also confirmed from the resulted RSM regression model:

$$Y_{1PS} = 396.00 + 36.13 A + 0.86 B - 44.65 C - 111.35 A^2 + 175.41 B^2. \quad \text{Eq 14.}$$

From the equation it can be seen that the input factor PC content (A) and cholesterol content (B) had positive (+) values. They had positive effects on particle size i.e. an increase in their concentrations led to an increased particle size. This can be seen for PC effect when compare the experiments (1, 12 and 6, 14) for liposomes and (3, 10 and 2, 11) for phytosomes with constant plant extract and cholesterol content and different PC content, and for cholesterol effect can be

seen when compare the experiments (16-17 and 4,5) for liposomes and phytosomes ,respectively in table 4.8.

For a better explanation of the input factors and their interactive effects on the particle size, three-dimensional (3D) surface plots were generated using equation 14. These are represented in figure 4.19.1. Flatness of surface suggested that interaction between factors was weak (Zhao *et al.*, 2014). The plot shows that the particle size increases as PC content increases and does not change as much as cholesterol content changes.

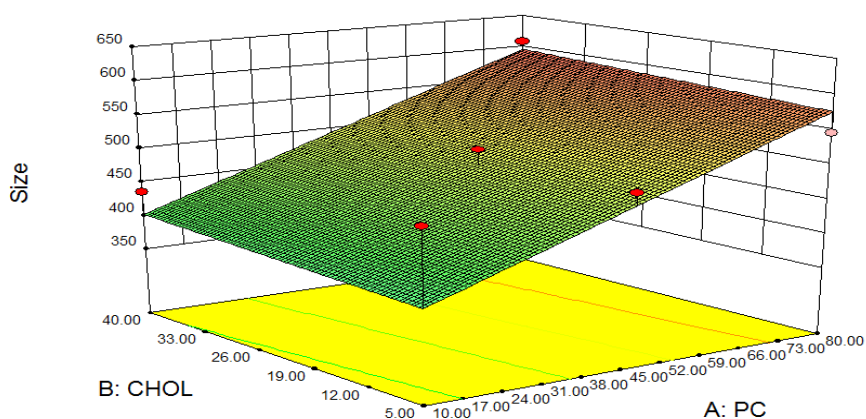


Figure 4-19-1: Three-dimensional (3D) surface plot showing the effect of P and cholesterol content on particle size; Y_{1PS} .

4.6.6 Effect of input factors on output factor Y_{2PDI} (polydispersity index)

The polydispersity index of liposomes and phytosomes formulations generated by RSM was evaluated and tabulated in the following table (table 4.13).

Table 4.13: Polydispersity index of liposomes and phytosomes formulation (extracted from table 4.7).

F. code	Factor 1; PC %	Factor 2; Chol %	Factor 3; Vesicle type	Response 2 PDI
1	80	40	liposome	0.361
2	45	40	phytosome	0.547
3	80	22.5	phytosome	0.369
4	10	5	phytosome	0.272
5	10	40	phytosome	0.379
6	80	5	liposome	0.18
7	80	5	phytosome	0.182
8	45	5	phytosome	0.375
9	45	22.5	liposome	0.353
10	10	22.5	phytosome	0.288
11	80	40	phytosome	0.479
12	10	40	liposome	0.528
13	45	22.5	liposome	0.414
14	10	5	liposome	0.558
15	45	22.5	liposome	0.268
16	45	5	liposome	0.418
17	45	22.5	liposome	0.593

The design matrix (table 4.9) shows that PDI decreases as PC concentration increases, indicating complete complexation. Reduction in PDI of phytosomes containing diosmin was similarly reported by Freag *et al.*, (2013). Generally, PDI was higher (broad polydispersity index) when the vesicles type were liposomes. Moreover, in equation 15, increasing the PC concentration displayed a minus (-) value, resulting in a decrease in the polydispersity index, which is desirable.

$$Y_{2PDI} = 0.37 - 0.077 A + 0.072 B - 0.032 C + 0.050 AB + 0.059 AC + 0.024 BC - 0.11A^2 + 0.10 B^2. \quad \text{Eq 15}$$

This can be seen when compare liposomes formulations for example (14, 16) and phytosomes formulations (7, 8) with constant plant extract and cholesterol quantity and different PC quantity and in case of cholesterol the equation represent the cholesterol had negative effect as it had minus value, which means increase its concentration leads to increase in PDI, this can be seen when compare experiments (1, 6) in case liposomes and (3, 7, 11 and 2, 8- 4, 5) in case of phytosomes.

The relationship between the input and output factors was further elucidated using surface plots in figure 4.19.2. Which represent that polydispersity index for different formulations decrease with increasing in PC content.

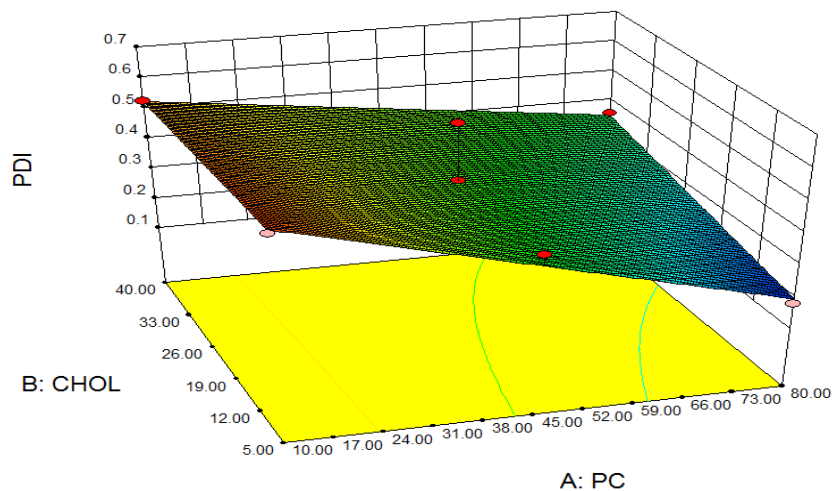


Figure 4-19-2: Three-dimensional (3D) surface plot showing the effect of PC and cholesterol content on polydispersity index (Y_{2PDI}).

4.6.7 Effect of input factors on percentage encapsulation efficiency Y3_{%EE} (percentage encapsulation efficiency)

The percentage encapsulation efficiency of liposomes and phytosomes formulation generated by RSM are evaluated and represented in the following table 4.14.

Table 4.14: Percentage encapsulation efficiency of liposomes and phytosomes formulations (extracted from table 4.7).

F. code	Factor 1; PC %	Factor 2; Chol %	Factor 3; Vesicle type	Response 3 %EE
1	80	40	liposome	14.6
2	45	40	phytosome	19.51
3	80	22.5	phytosome	30.95
4	10	5	phytosome	9.52
5	10	40	phytosome	15.38
6	80	5	liposome	21.2
7	80	5	phytosome	27.02
8	45	5	phytosome	24.4
9	45	22.5	liposome	17.7
10	10	22.5	phytosome	2.6
11	80	40	phytosome	31.25
12	10	40	liposome	2.38
13	45	22.5	liposome	12.5
14	10	5	liposome	2
15	45	22.5	liposome	15.83
16	45	5	liposome	23.4
17	45	22.5	liposome	13.95

The design matrix shows a higher percentage encapsulation efficiency when lipid vesicles type was phytosomes and the percentage encapsulation efficiency increased as PC was increased and this can be seen when compare between experiment 1 and 12 for liposomes, and 4 and 7 in the case of phytosomes. This increase can be attributed to the vesicles having sufficient PC molecules to self-assemble into phytosomes, and as a result more plant extract molecules become favourably entrapped in the phytosomes rather than in bulk solution (Abdelkader *et al.*, 2016). Further, from model regression equation 16, one observes that the PC concentration and cholesterol concentration have a positive effect, as they had a positive (+) value, which reflected in an increase in their concentrations lead to increase percentage encapsulation efficiency of lipid vesicles.

$$Y_{3\% EE} = 16.81 + 9.31 A + 1.73 B + 3.27 C.$$

Eq 16.

Ghanbarzadeh *et al.* (2014) reported that increase in PC led to increasing encapsulation efficiency of naproxen nano liposomes. Similarly, Ma *et al* (2012) reported that encapsulation efficiency of lactoferrin nano-liposomes increased as PC increased.

As for cholesterol effect, its high ratio led to higher percentage encapsulation efficiency as observed in (3, 7 and 4, 5), although its effect was negative in some experiments viz. (4, 10) which may be due to its critical level, hence, at higher concentrations cholesterol can form crystal habits (Mohammed *et al.*, 2004) that may start to disrupt the bilayer structure, leading to the loss of drug entrapment levels. Ding *et al.* (2009) and Agarwal *et al.* (2001) reported that decreasing entrapment efficiency with further increasing cholesterol ratio beyond a certain limit. Figure 4.19.3 indicates the surface plot of the percentage encapsulation efficiency along with cholesterol and PC content. This shows that the high PC content and the high percentage encapsulation efficiency. The plot demonstrates that PC had more effect than cholesterol.

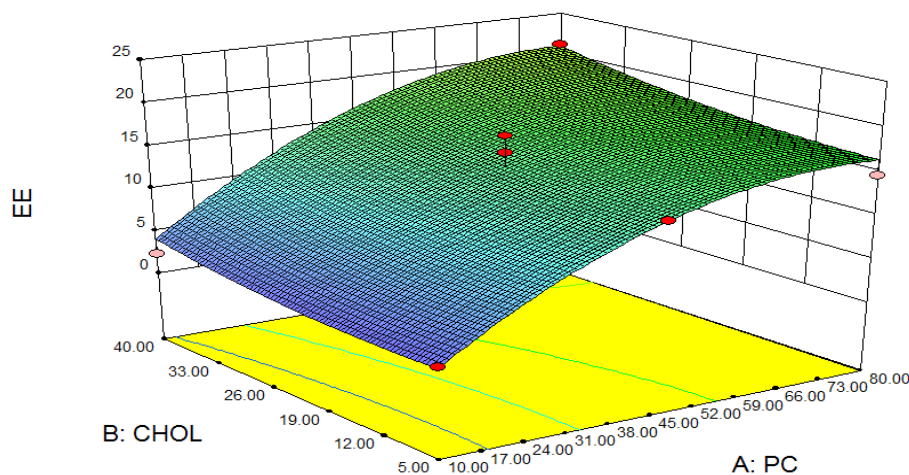


Figure 4-19-3: Three-dimensional (3D) surface plot showing the effect of PC and cholesterol content on percentage encapsulation efficiency.

4.6.8 Formulation optimization using desirability function

After the establishment and analysis of appropriate models for individual output factors, the simultaneous optimization of multiple output factors was carried out using Design Expert software to find a combination of factor levels that simultaneously satisfy the requirements placed on each of the output factors and input factors.

In this step, the optimal conditions such as minimum particles size, polydispersity index as well as maximum percentage encapsulation efficiency was determined by using the desirability function approach. The optimization step generated 6 checkpoint scenarios. The highest with a desirability factor of 0.774 was selected as the most desirable optimized formulation. The desirability ramp in figure 4.20 represents the various input and output parameters generated for this formulation which consists of PC concentration 80 %, cholesterol concentration 5 % and the type of lipid vesicle prepared phytosome with predicted small particle size range 531.29 nm, small polydispersity index range 0.230, and percentage encapsulation efficiency 31.12 %.

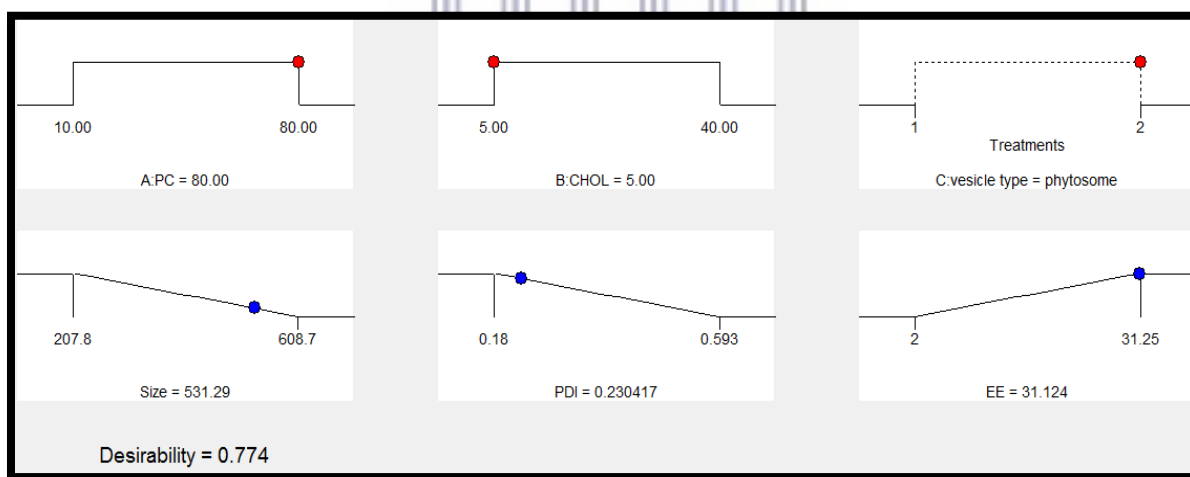


Figure 4-20: Desirability ramp for the optimization process.

4.6.9 Verification of optimized condition

The optimized formulation values were further validated by carrying out the experiment at 4 replicates and values of output were determined experimentally. The average values after experimentation were compared to the model predicted values which are 531.29 nm particle size,

0.230 polydispersity index and percentage encapsulation efficiency 31.12 %. Figure 4.21 shows particle size, polydispersity index and percentage encapsulation efficiency of this comparison. The verified particle size was 509.97 ± 29.9 nm, polydispersity index was 0.213 ± 0.03 and percentage encapsulation efficiency was 28.60 ± 2.4 %. The average percent errors are found to be -9.82 ± 6.7 % for percentage encapsulation efficiency, -4.01 ± 4.8 % for particle size and -7.06 ± 13.9 % for polydispersity index. These percentage error values are sufficiently low to confirm the high predictive power of the RSM (Bassi *et al.*, 2015). The figure indicates good agreements between the experimental and predicted values.

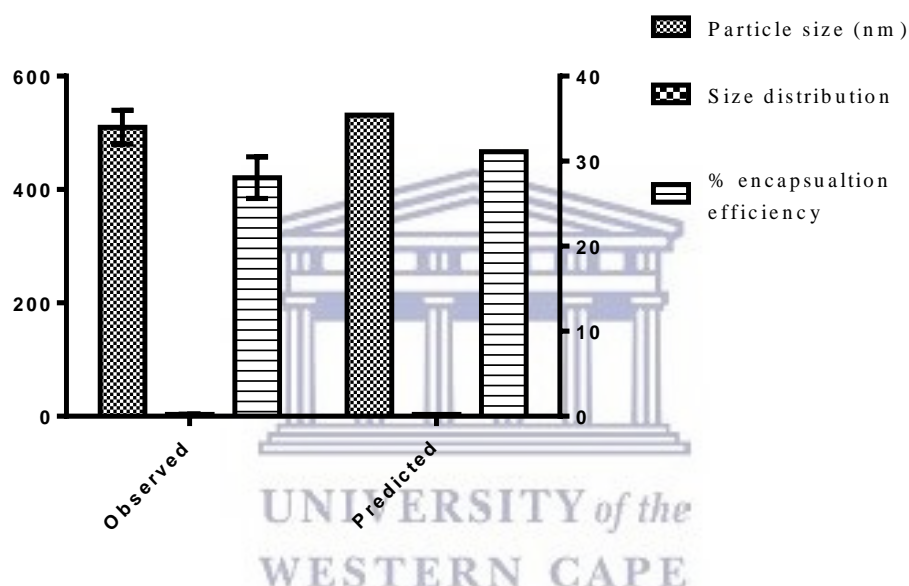


Figure 4-21: Observed values of optimized formula (particle size, polydispersity index and % encapsulation efficiency) in comparison with proposed optimized formulation of RSM.

4.7 Characteristics of selected optimised formulation

Based on the above findings, a phytosome formulation containing 80 % PC and 5 % cholesterol was selected as the final optimized formulation.

4.7.1 Particle size and polydispersity index

Figure 4.22 demonstrates the 4 replicates of the optimised formulation with a mean particle diameter of 509.97 ± 29.9 nm indicating LUV as the lipid vesicle type because the particle size was more than 100 nm (Pattni *et al.*, 2015). It also has a polydispersity index of 0.21 ± 0.036

which indicates narrow polydispersity index and homogeneity of lipid vesicles which is desirable in the manufacture of phytosomes (de Sousa *et al.*, 2013).

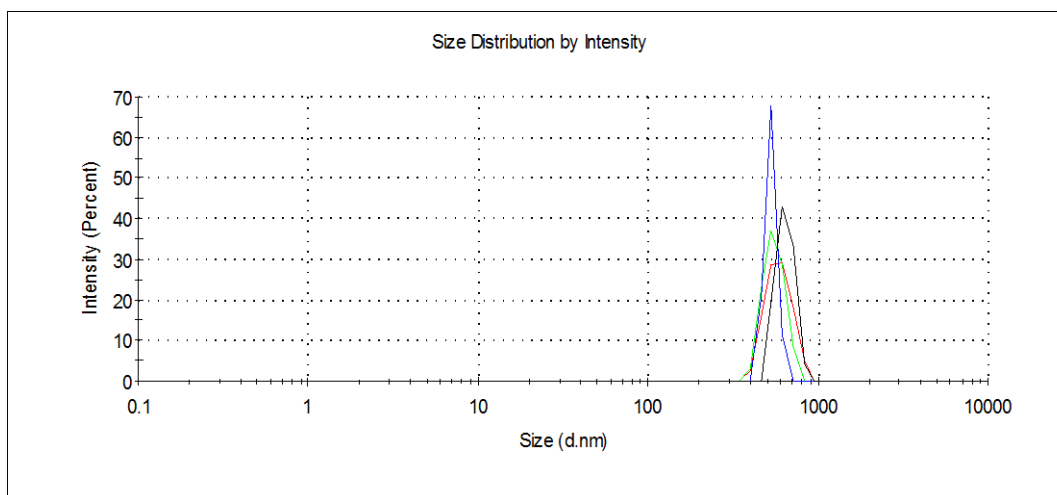


Figure 4-22: Particle size for final optimized phytosomes formulation.

4.7.2 Zeta Potential Analysis

The optimized phytosome formulation carries a low negative charge (-8.3 ± 0.72 mV). These findings are in agreement with the finding of Freag *et al.* who reported the lyophilized diosmin phytosomes manufactured from soya PC carried low negative charge (-6 mV) (Freag *et al.*, 2013). The low optimized phytosomes formulation zeta potential value indicates stability possible problems with stability (Thassu *et al.*, 2012).

The mean of zeta potential values of all the liposomes and phytosomes formulations proposed by RSM were also investigated using the Zetasizer, although it was not one of the dependant factors. The results are displayed in table 4.15.

Table 4 -15: Zeta potential results of proposed formulation by RSM

F. code	Factor 1; PC %	Factor 2; Chol%	Factor 3; Vesicle type	Zeta potential (mv) (mean±sd, n=3)
1	80	40	liposome	-5.14
2	45	40	phytosome	-3.26
3	80	22.5	phytosome	-4.55
4	10	5	phytosome	-0.19
5	10	40	phytosome	-0.54
6	80	5	liposome	-6.64
7	80	5	phytosome	-6.78
8	45	5	phytosome	-4.47
9	45	22.5	liposome	-2.59
10	10	22.5	phytosome	-1.08
11	80	40	phytosome	-7.73
12	10	40	liposome	-0.26
13	45	22.5	liposome	-3.27
14	10	5	liposome	-0.51
15	45	22.5	liposome	-5.26
16	45	5	liposome	-4.18
17	45	22.5	liposome	-2.89

As can be observed from the table that all vesicles displayed a negative surface charge (-7.7 to -0.2 mV) due to the presence of the phosphate group of PC at neutral pH (Allam *et al.*, 2015).

Zeta potential is an index commonly used to assess the stability of the lipid vesicles. The zeta potential indicates the degree of repulsion between, similarly charged particles in dispersion. Zeta potential values beyond +30 mV or below -30 mV are generally considered to be an indication of stability through strong repulsion forces among particles to prevent aggregation (Haidar *et al.*, 2008). When the potential is low it leads to attrition of particles and the dispersion will break and flocculate (De *et al.*, 2012).

These results obtained for the zeta potential was out of the recommended charge range, therefore the need arose to search for a way to increase the surface charge in an attempt to increase the stability of lipid vesicles. Stearic acid has been used as charge inducer (Sudhakar *et al.*, 2014). Stearic acid, a charge inducer component was included to the optimized *H. procumbens* phytosomes formulation to improve the zeta potential. The formulation was tested for particle

size, polydispersity index and zeta potential. The results were compared with the optimized formulation without stearic acid. The results are represented in figure 4.23.

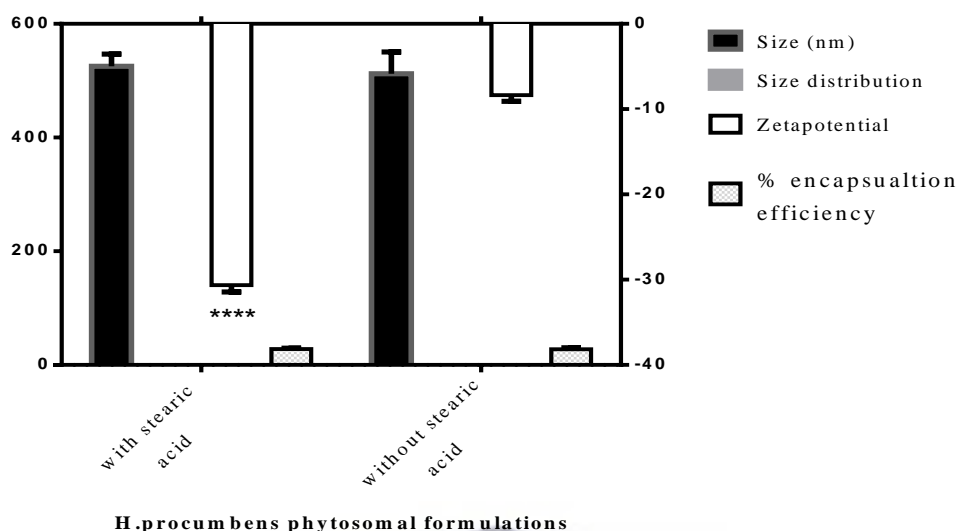


Figure 4-23: Incorporation of stearic acid as charge inducer significantly ($p < 0.05$) enhances the zeta potential of the phytosome optimized formulation.

The zeta potential was significantly ($p < 0.05$) improved when stearic acid was added to the optimized formulation. Results revealed that zeta potential of the empty phytosomes was -1.34 ± 1.14 mV and the loaded optimized phytosomes formulation was -8.3 ± 0.72 mV, and when the stearic acid was included the zeta potential became -30.6 ± 0.80 mV (figure 4.24) due to the surface charge imparting nature of stearic acid (Sudhakar *et al.*, 214). This may serve as a partial indicator of physical stability to ensure creation of a high-energy barrier against rupture or coalescence of the formed globules.

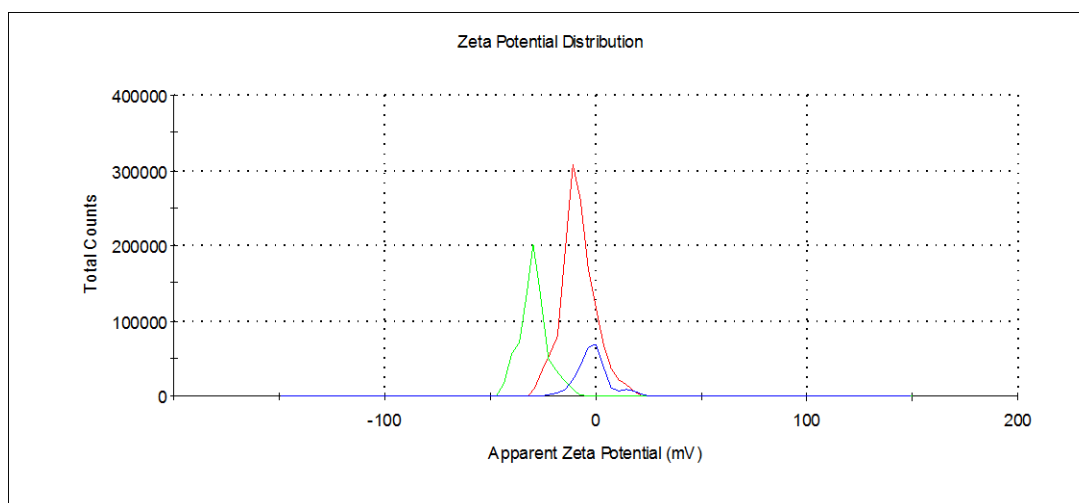


Figure 4-24: Zeta potential of empty phytosomes (blue peak), loaded *H. procumbens* phytosomes (red peak), and loaded *H. procumbens* phytosomes including stearic acid (green peak).

There was small change in phytosomes particle size changing from 525.5 ± 21.12 to 512.3 ± 38.17 and the encapsulation efficiency changed from 28.01 ± 1.51 to 27.58 ± 2.75 , which is considered statistical insignificant. Similarly reported by Marsanasco *et al.* they demonstrated that the addition of stearic acid to liposomes produced slight changes in particle size and liposome encapsulation efficiency when working with vitamin loaded liposomes (Marsanasco *et al.*, 2011). The all next characterization and investigation studies were performed on optimized phytosomes formulation included stearic acid.

4.7.3 Scanning Electron Microscopy (SEM)

Morphological characteristics were observed by SEM. The photomicrography provided evidence of vesicle formation and also showed the shape. Their morphology evaluation demonstrated that phytosomes were discrete and spherically shaped as depicted in figure 4.25.

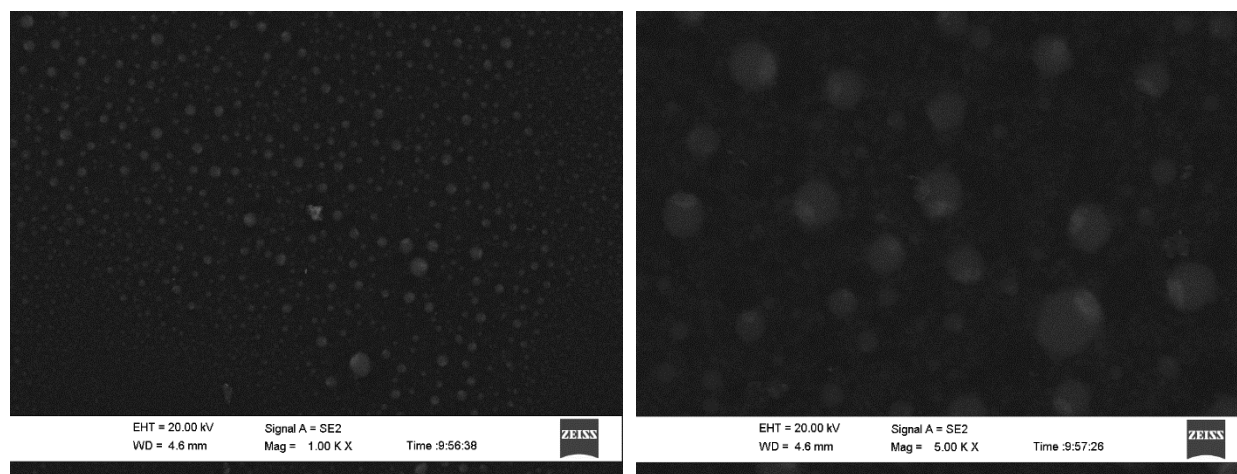


Figure 4-25: Representative SEM micrograph of optimized *H. procumbens* phytosomes at two different magnifications.

4.7.4 Solubility

Figure 4.26 indicates the measured solubility of *H. procumbens* plant extract and phospholipid complex (phytosomes) in water and n-octanol, respectively. The plant extract had a low lipid solubility of 0.002829 ± 0.0005 mg/ml, and a relatively higher aqueous solubility of 0.559008 ± 0.002 mg/ml, indicating a hydrophilic nature. The prepared *H. procumbens* phytosomes demonstrated an increase of 0.05297 ± 0.001268 mg/ml in the lipid solubility compared to the plant extract. This form could improve the passage of the plant extract across the lipid-rich cell membranes of the intestine wall (lipid diffusion) and increase its absorption.

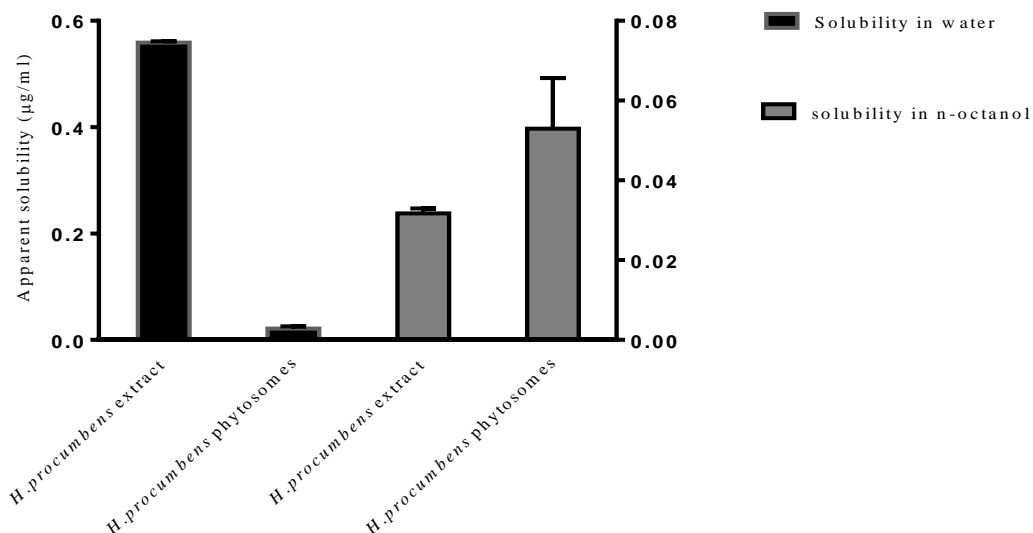


Figure 4-26: Represents the apparent solubility of *H. procumbens* extract and phytosomes in water and n-octanol.

The overall amphiphilic nature of the prepared *H. procumbens* phytosomes can be attributed as the main reason for this observed increase in lipid solubility. Vankudri *et al.*, (2016) reported that rutin-phospholipid complex increased the solubility of rutin in n-octanol more than in water. The results for *H. procumbens* phytosomes assumes absorption and therefore bioavailability because it possesses both hydrophilic and lipophilic qualities which offers better dissolution in the GI fluid and also better absorption through the lipophilic membrane or tissue system.

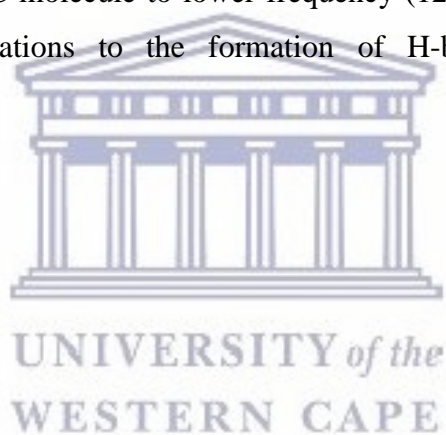
4.7.5 FTIR study

To detect the possible interaction between the plant extract and PC in the phospholipid complex FTIR was completed. The IR spectrum figure 4.27 of the empty phytosomes showed characteristic absorption bands at 3373.52 cm^{-1} for a hydroxyl (-OH) group and C-H stretching bands of a fatty acid chain at 2924.43 and 2854.18 cm^{-1} , carbonyl stretching band at 1734.02 cm^{-1} in the fatty acid ester, at 1466.34 cm^{-1} for C-H bending, P=O stretching band at 1238.67 cm^{-1} , P-O-C stretching band at 1087.51 cm^{-1} and choline N-(CH³)³ stretching at 969.49 cm^{-1} . These results of FTIR are well supported by the previous work by Zhang *et al.*, (2016) with non-considerable shifting. Their study indicated that PC demonstrated characteristic peaks at 3384.1 cm^{-1} (Hydroxyl stretching); 2925.2 and 2854.2 cm^{-1} (C-H stretching of long fatty acid chain);

1736.4 cm^{-1} (carbonyl stretching of the fatty acid ester); 1466.1 cm^{-1} (C-H bending); 1242.9 cm^{-1} (P = O stretching band); 1090.0 cm^{-1} (P-O-C stretching) and 968.4 cm^{-1} ($\text{N}^+(\text{CH}_3)_3$ stretching).

The *H. procumbens* extract exhibited a characteristic band at 3293.83 cm^{-1} for a hydroxyl (-OH) group and at 2926.43 cm^{-1} (for C-H stretching) and 1627.82 cm^{-1} . This indicates the presence of a carbonyl (C=O) group and 1346.36 cm^{-1} for (C-H bending) and 991.68 for (C-O group).

The FT-IR spectrum of the complex (phytosomes), showed significant changes. The absorption peak of hydroxyl (O-H) stretching of empty phytosomes shifted to lower wave number at 3352.62 cm^{-1} in complex. This could indicate the interaction of plant extract to polar end of the PC through formation of strong hydrogen bonding between hydroxyl groups of phospholipid and extract phytoconstituents in phytosomes (Vankudri *et al.*, 2016; Singh *et al.*, 2013). Shifting of the P=O absorption band of PC molecule to lower frequency (1235.92 cm^{-1}) further indicates the sensitivity of these vibrations to the formation of H-bonds (Süleymanoglu, 2009)



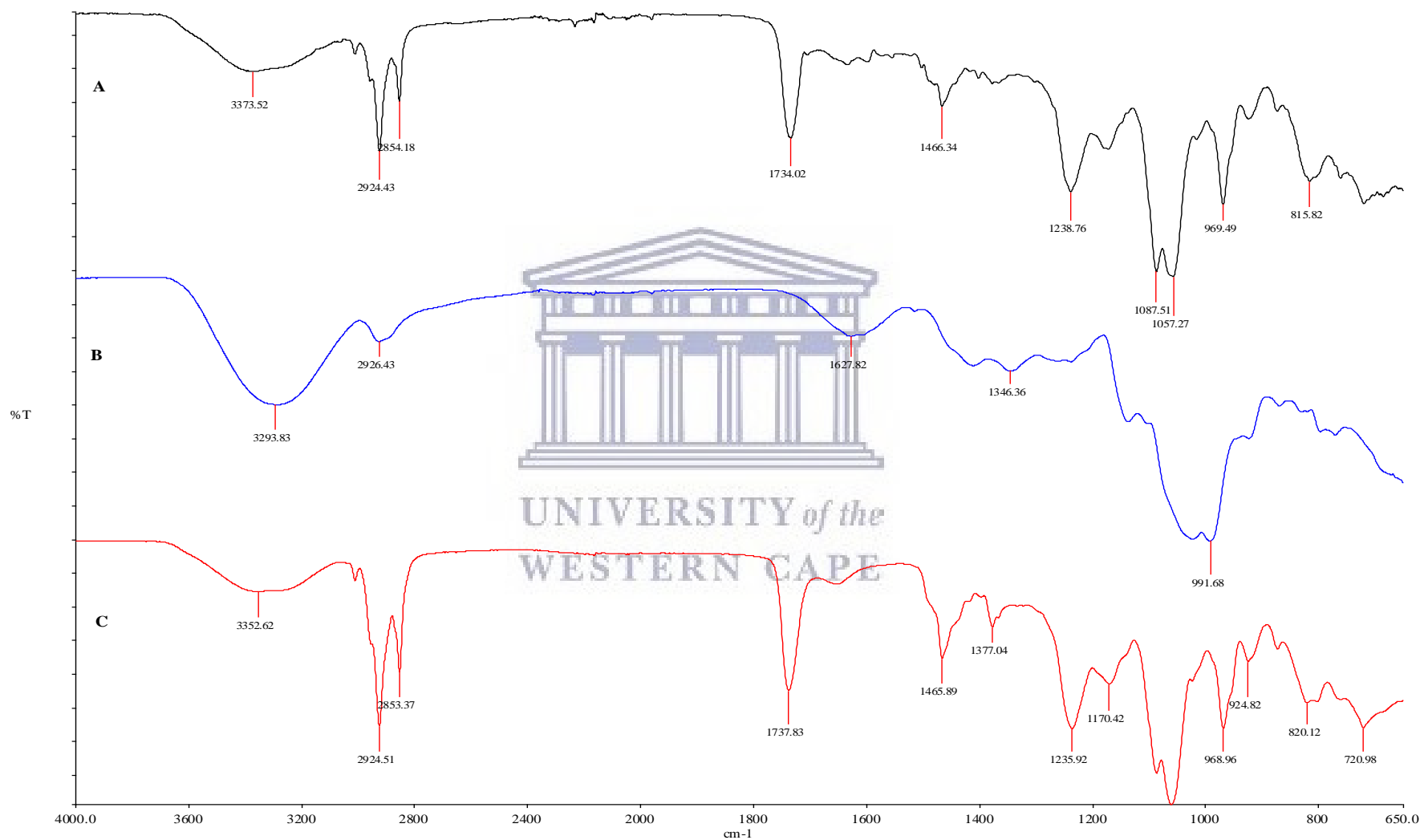


Figure 4-27: FTIR spectra of (A) empty phytosomes, (B) *H. procumbens* plant extract and (C) *H. procumbens* loaded phytosomes.

These results are in good agreement with those of (Dhase *et al.*, 2015) who reported shifting of the hydroxyl group (OH) to a lower frequency in the spectra of phytosomes (3625cm^{-1} to 3560cm^{-1}). They indicated the formation of strong hydrogen bonding between the hydroxyl group of the phospholipid and leaves of *Aegle marmelos* (Bael) extract phytoconstituents during complex formation.

4.7.6 Stability in simulated gastric fluid (SGF) pH 1.2.

The effect of gastric pH on *H. procumbens* phytosomes integrity was evaluated to mimic the stability range of these lipid vesicles after oral administration. The physicochemical characteristics of the phytosomes formulation were investigated:

1) Phytosomes particle size

The results of the *in vitro* stability study investigation of the *H. procumbens* loaded phytosomes and the control (empty phytosomes) in SGF are illustrated in figure 4.28.1. This shows an increase in particle size of loaded phytosome and the control after 2 hours incubation with the SGF (pH 1.2). This increase continued significantly ($p < 0.05$) after 4 hours from 481.75 ± 7.36 nm to 570.95 ± 4.03 nm in case of loaded phytosomes and increased also statistically significantly ($p < 0.05$) from 473.65 ± 47.44 to 522.95 ± 10.53 for empty phytosomes.

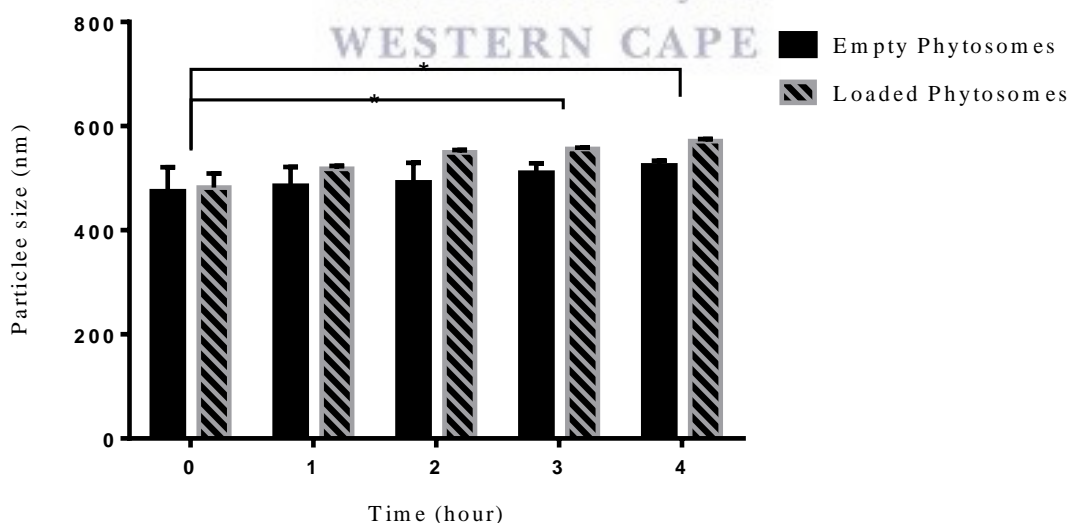


Figure 4-28-1: Particle size of empty and loaded *H. procumbens* phytosomes against simulated gastric fluid (SGF) 37 °C for 4 hours (mean ±sd, n =2).

The possible explanation for size increase is that it may be due to vesicle aggregation. Channarong *et al.*, 2011 reported an increase in polyplex liposomes particle size in low pH medium. Similarly, Ramana *et al.*, 2010 reported an increase in the size of nevirapine liposomes in acidic media. This change in particle size is an indication of the instability of phytosomes in acidic medium (gastric environment).

2) Phytosomes polydispersity index (PDI)

The results obtained from PDI analysis of empty and loaded phytosomes can be seen in figure 4.28.2, The PDI changed from the initial value of 0.27 ± 0.03 to 0.38 ± 0.01 after 4 hours for empty phytosomes and for loaded *H. procumbens* phytosomes, the PDI changed from 0.25 ± 0.01 to 0.45 ± 0.12 . This is a further indication of instability of phytosomes in acidic medium.

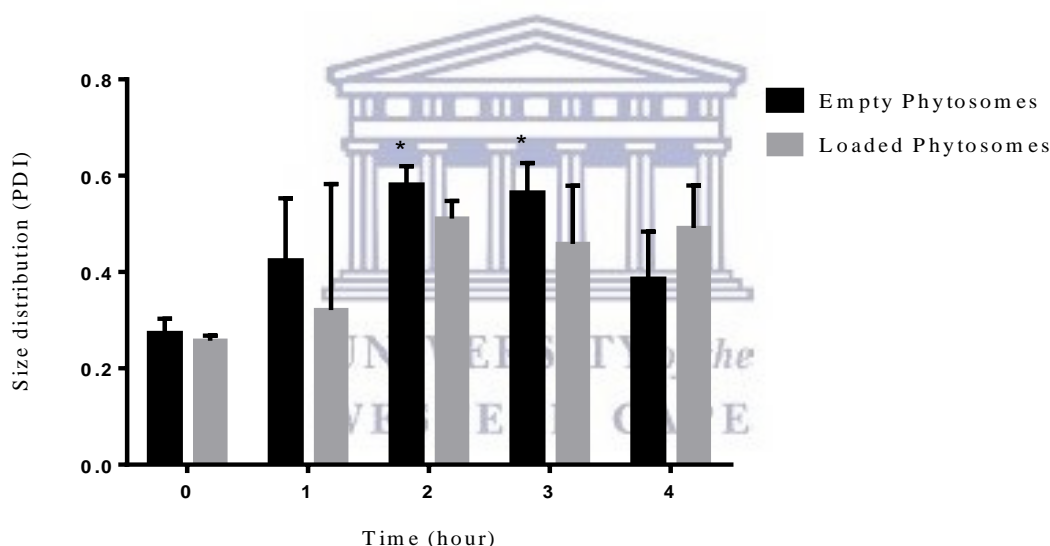


Figure 4-28-2: Polydispersity index of empty and loaded *H.procumbens* phytosomes against simulated gastric fluid (SGF) at 37 °C for 4 hours (mean \pm sd, n=2).

3) Phytosomes zeta potential

The results obtained from the zeta potential analysis for empty and loaded phytosomes are shown in figure 4.28.3.

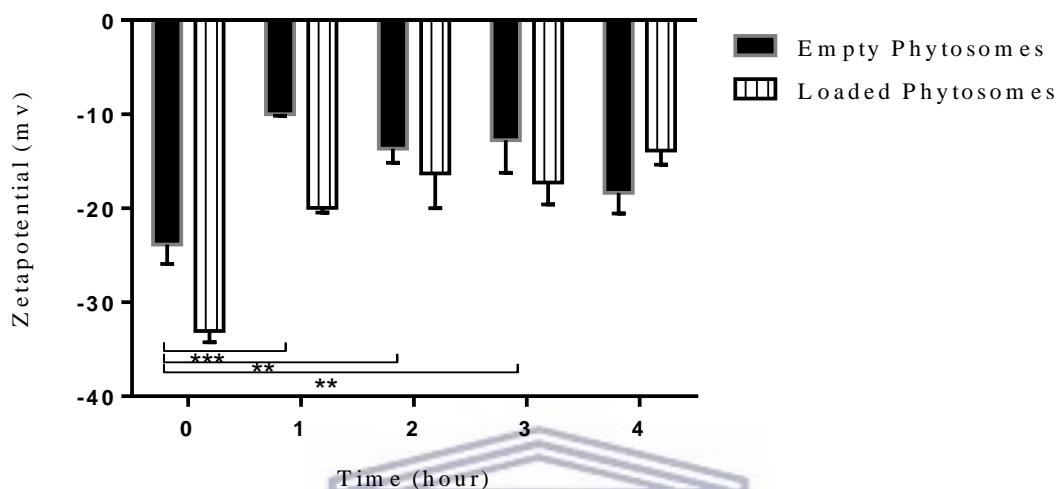


Figure 4-28-3: Zeta potential of empty and loaded *H. procumbens* phytosomes against simulated gastric fluid simulated gastric fluid at 37 °C for 4 hours (mean±sd, n=2).

The results reveals a statistically significant ($p < 0.05$) decrease in the initial zeta potential (-23.85 ± 2.05 mV) of the empty phytosomes at 4 hours (-18.35 ± 2.19 mV). For loaded *H. procumbens* phytosomes the zeta potential decreased (statistically significant) from (-33.05 ± 1.20 mV) to (-13.85 ± 1.48 mV). This decrease in charge is possibly due to neutralization and ionization of phosphate polar head group of the PC in the acidic medium (Channarong *et al.*, 2011). The zeta potential decreasing was further indication phytosome instability in gastric medium.

4) *H. procumbens* phytosomes release study in SGF

A burst release in the first hour was observed for the *H. procumbens* phytosomes in SGF, followed by a steady release for 4 hours. The phytosomes demonstrated release of 40.44 ± 1.55 % in SGF after 4 hours (figure 4.28.4).

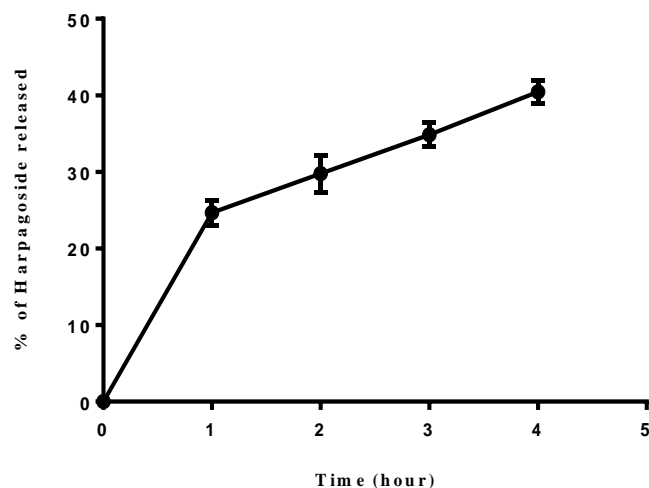


Figure 4-28-4: Harpagoside release from *H. procumbens* phytosomes in simulated gastric fluid (SGF) (mean±sd, n=3).

The release of the contents from these phytosomes could occur when the excess hydrogen ions present in the SGF, diffuse in the inner space of the *H. procumbens* phytosomes. It competes with plant extract to combine with the anionic phosphate groups of PC and disturb the weak interaction balance of the phytosomes, leading to the plant extract release from the *H. procumbens* phytosomes (Yu *et al.*, 2016). The same trend was reported by Zhang *et al.*, (2014) who found 55 % of insulin released in SGF from liposomes made from soybean PC. This is the same phospholipid type used in our study. Release of plant extract from the phytosomes in gastric medium is not desirable because it indicates phytosomes instability in this this medium. To protect the plant extract from the gastric environment and enhance its absorption in the intestinal region, the phytosomes should be keeping intact in the gastric environment. We therefore suggest that coating the phytosome with the alginate polymer will prevent it from releasing the plant extract early in the acidic (gastric) environment.

4.8 Phytosome - alginate system

4.8.1 Preparation of the alginate coated *H. procumbens* phytosomes

Alginate coated- *H. procumbens* phytosomes were successfully prepared by ionotropic gelation technique by using sodium alginate and calcium chloride as a cross-linking agent. The colour of

alginate coated - *H. procumbens* phytosomes crosslinked with calcium chloride was relatively opaque white and changed to yellowish brown after drying as indicated in figure 4. 29.

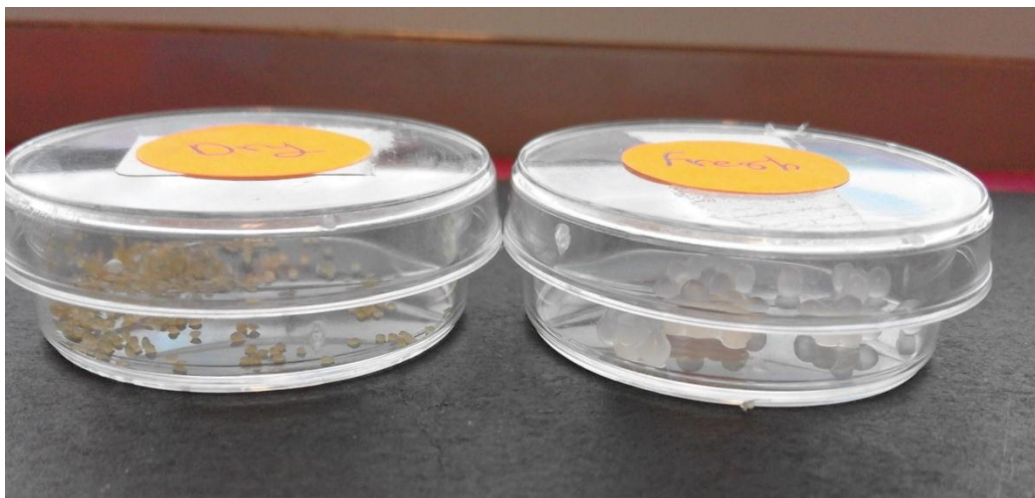


Figure 4-29: dry and freshly prepared alginate coated *H. procumbens* phytosomes.

4.8.2 Process variables and process optimization

Different variables, i.e. concentrations of sodium alginate and of calcium chloride were investigated for their effect on particle size, percentage encapsulation efficiency and disintegration time and release behaviour.

4.9 Characterization of alginate coated *H. procumbens* phytosomes

4.9.1 Particle size

Bead size was measured using a light microscope and found to be within a narrow size range of 1.19 ± 0.06 mm and 2.24 ± 0.07 mm. The mean particle size differed between the formulations with varying concentrations of alginate and calcium chloride as represented in figure 4.30. There was an increase in the average diameter of particles with an increase in the concentration of sodium alginate polymer. No statistical difference between empty and loaded beads size was detected.

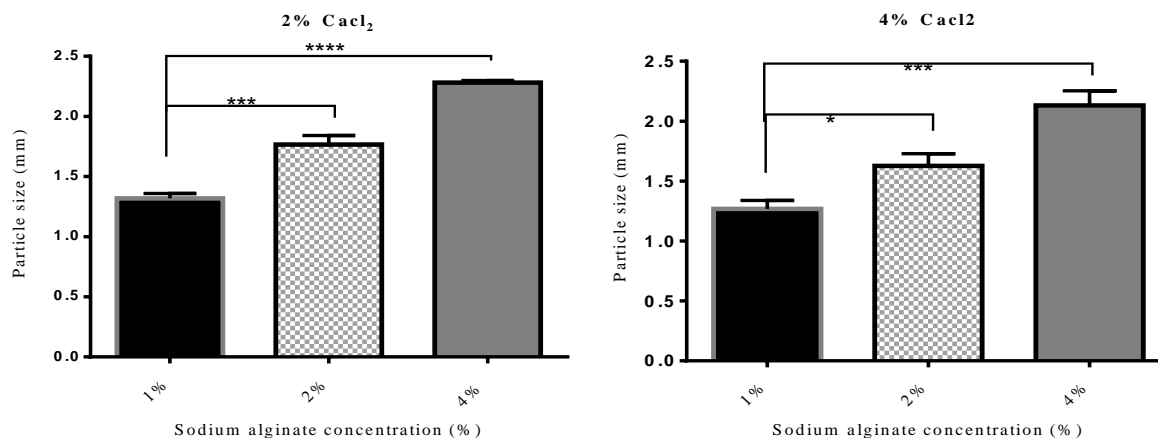


Figure 4-30: Alginate coated *H. procumbens* phytosomes particle size as a function of different alginate and calcium chloride concentrations (mean±sd, n=3).

It is worth noting that sodium alginate polymer content had significant ($p < 0.05$) effect on beads size. Larger beads were obtained when concentration of sodium alginate was increased. This was probably due to larger drops dispersed from the syringe during the bead formation process as a result of increased viscosity of the alginate solution. Similarly, it has been reported that large tinidazole alginate beads were prepared with alginate concentration above 3% (Singhal *et al.*, 2010). Studies by (Patil *et al.*, 2014; Das *et al.*, 2007; Manjanna, 2009) further support this findings. It was also observed that at high sodium alginate concentration the beads maintained their form integrity whereas at lower concentrations the beads deformed and lost their shape after drying. The same trend was reported by Singh *et al.*, (2012).

As depicted in the figure, the beads particle sizes decreased [not statistically significant ($p > 0.05$)] when calcium chloride concentration was increased from 2 % (w/v) to 4 % (w/v). This decreased bead size is due to a high degree of crosslinking causing shrinkage of the beads (Abdalla *et al.*, 2015). This result was similar to studies performed by (El-Kamel *et al.*, 2010; Nayak *et al.*, 2011; Bansal *et al.*, 2016).

4.9.2 Percentage encapsulation efficiency of alginate coated *H. procumbens* phytosomes

The alginate coated *H. procumbens* phytosomes percentage encapsulation efficiency of 1 %, 2 % and 4 % was investigated and the results represented in figure 4.31. The percentage encapsulation efficiency was between 12.80 ± 2.51 % and 57.79 ± 6.74 %.

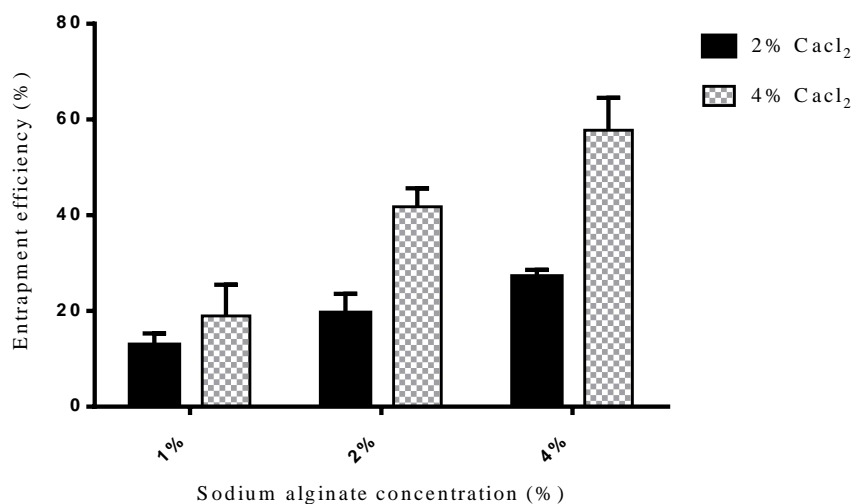


Figure 4-31: Alginate coated *H. procumbens* phytosomes percentage entrapment efficiency at different alginate and calcium chloride concentrations (mean \pm sd, n=3).

The results indicate the higher the concentration of alginate and calcium chloride the higher the capacity of beads to hold the phytosomes. The highest being 57.79 % \pm 6.74. The lower percentage encapsulation efficiency observed at lower alginate concentrations may be due to the phytosomes not encapsulated completely because of less available active calcium-binding sites in the polymeric chains and, consequently, a lower degree of cross-linking with the gelling agent leading to the formation of lower strength matrix structure (Thomas *et al.*, 2011). The increase in percentage encapsulation efficiency at higher alginate concentration is attributed to the increase in viscosity at a higher concentration of sodium alginate due to the formation of a denser matrix structure (Patel *et al.*, 2016).

The percentage encapsulation efficiency increased significantly ($P < 0.05$) when calcium chloride concentration was increased from 2 % - 4 % w/v. The percentage encapsulation efficiency increase may be attributed to the greater availability of active calcium binding sites in the polymeric chains resulting in better cross-linking reactions and compactness of the formed insoluble dense matrices (Suruse, 2014). This is similar to results observed by Takka, (1999) for nicardipine calcium alginate beads and by Manjanna *et al.*, (2013) for aceclofenac sodium microbeads.

Higher percentage encapsulation efficiency depends on both the concentration of sodium alginat

and calcium chloride in the formulation. These findings are in agreement with (Vinod *et al.*, 2013) who reached the higher entrapment efficiency based on the concentration of sodium alginate and the ability of the calcium ions to crosslink with sodium alginate.

4.9.3 Alginate coated *H. procumbens* phytosomes erosion and release study

Short erosion and release study in PBS was performed to determine the time period for alginate coated *H. procumbens* phytosomes to disintegrate and release the phytosomes. The rate of release of the formulations was between 26.11 ± 2.42 and 4.14 ± 2.37 as shown in figure 4.32.

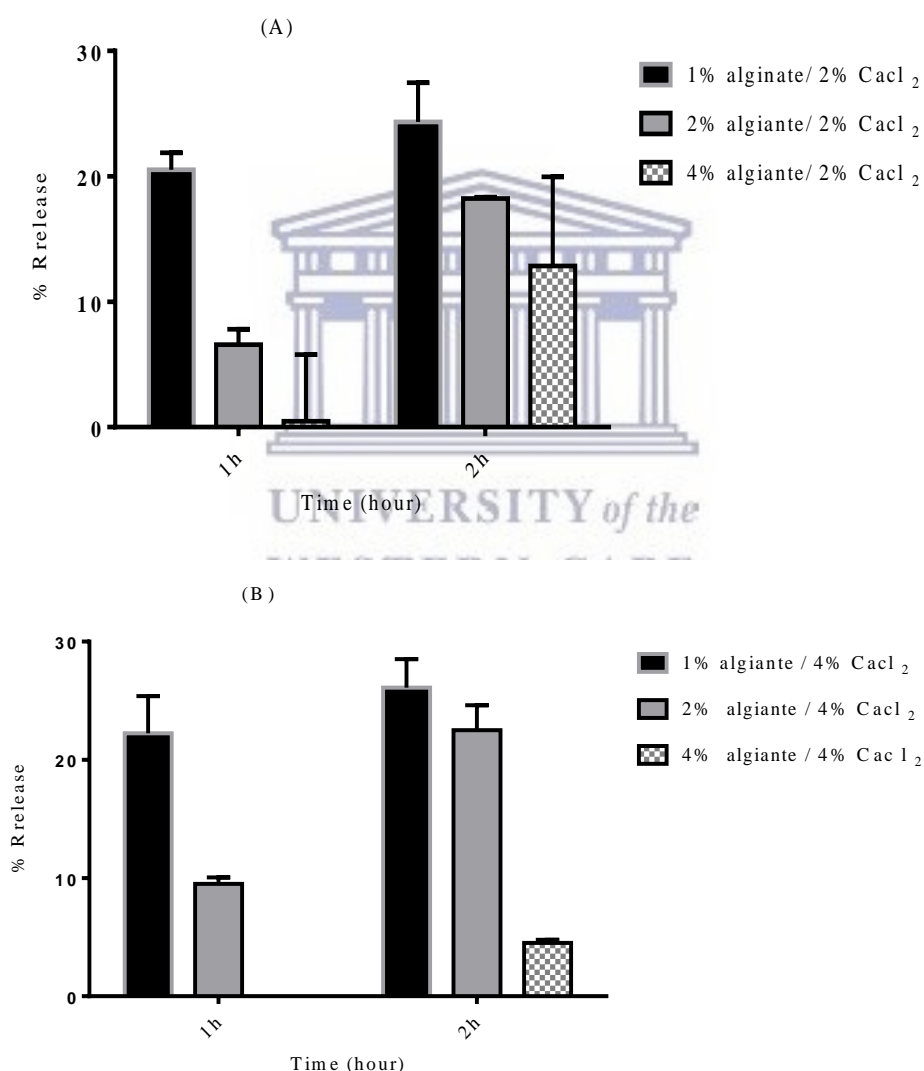


Figure 4-32: Erosion and release from alginate coated *H.procumbens* phytosomes at different sodium concentrations; (A) 2% calcium chloride (B) 4% calcium chloride as cross linking solution (mean±sd, n=3).

Figure 4 shows that a decrease in polymer ratio, decreased the time for bead erosion. The presence of lower amounts of sodium alginate produces a highly porous matrix structure having low gel strength; this resulted in rapid diffusion of the drug from the matrix (Thomas *et al.*, 2011). Similar results were observed for trimetazidine alginate beads, the lower concentrations of sodium alginate led to faster trimetazidine release (Mandal *et al.*, 2010). The results show no appreciable ($p > 0.05$) difference between the releases rates of the formulation with different calcium chloride concentrations (2 % and 4 %). These results are in agreement with Thomas *et al.* (2011) who reported that increasing the concentration of CaCl_2 produced a non-significant effect on dissolution behaviour.

In the case of formulations prepared with a high content of sodium alginate, the erosion time increased, alginate coated *H. procumbens* phytosomes expanded but did not erode in 2 hours. This is illustrated in figure 4.33. The decreased release of entrapped phytosomes is related to high crosslinking delaying alginate gel disintegration (Chowdhury *et al.*, 2011).

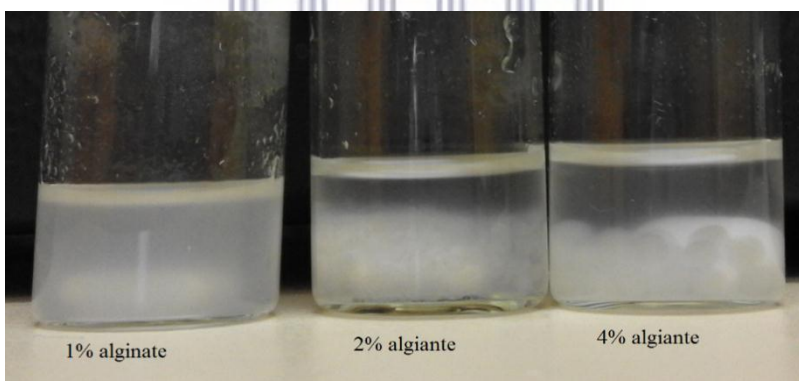


Figure 4-33: Pictures of alginate coated *H. procumbens* phytosomes in PBS 7.4 at different sodium alginate concentrations formulation and 4% CaCl_2 during erosion study.

Overall, considering the beads size, percentage encapsulation efficiency, erosion and release characteristics of alginate beads, it was found that optimum concentration of sodium alginate (2 %), calcium chloride (4 %). This formulation was selected and subjected for further investigation.

4.9.4 Shape and surface assessment of selected alginate coated *H. procumbens* phytosomes

The shape of visually dry and freshly prepared alginate coated *H. procumbens* phytosomes was examined. The dried alginate coated *H. procumbens* phytosomes were seen to be spherically shaped as demonstrated in figure 4.34.1.

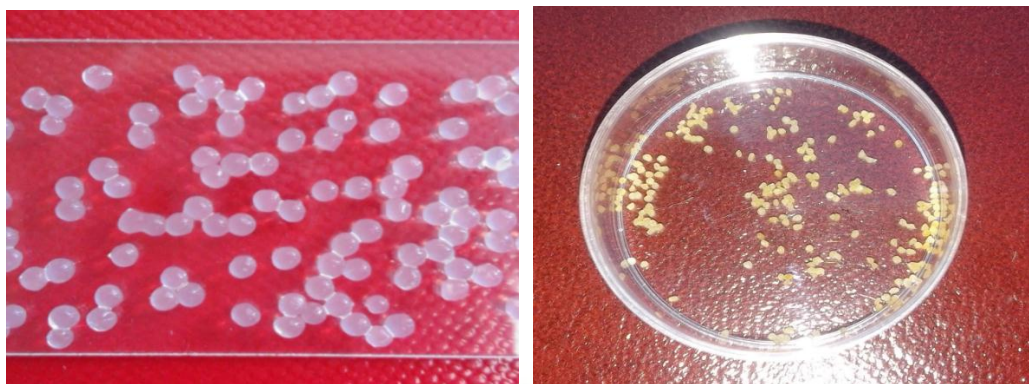


Figure 4-34-1: Spherical shape of dry and freshly prepared alginate coated *H. procumbens* phytosomes.

Examination of the surface structure are depicted in figure 4.34.2 reveals small cracks on the surface probably caused by partial collapsing of the alginate polymer network during the dehydration process.

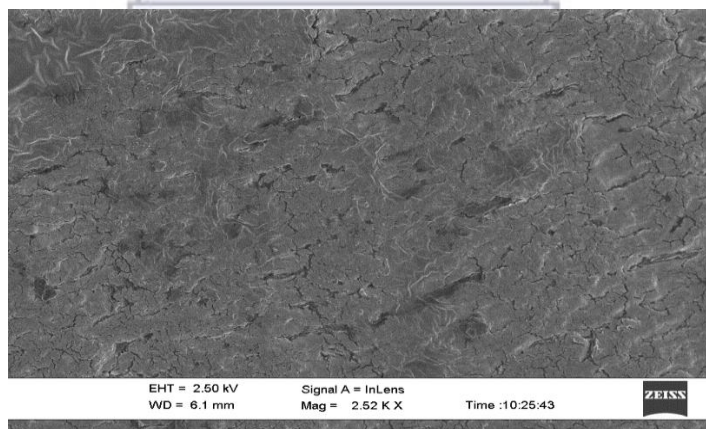


Figure 4-34-2: SEM micrograph of surface microstructure of the dried alginate coated *H. procumbens* phytosomes.

4.9.5 Phytosomes- polymer compatibility study

H. procumbens phytosomes - alginate compatibility studies were done using a FTIR spectrometer. The spectra of sodium alginate powder, empty alginate beads and alginate coated *H. procumbens* phytosomes are represented in (Figure 4.35).

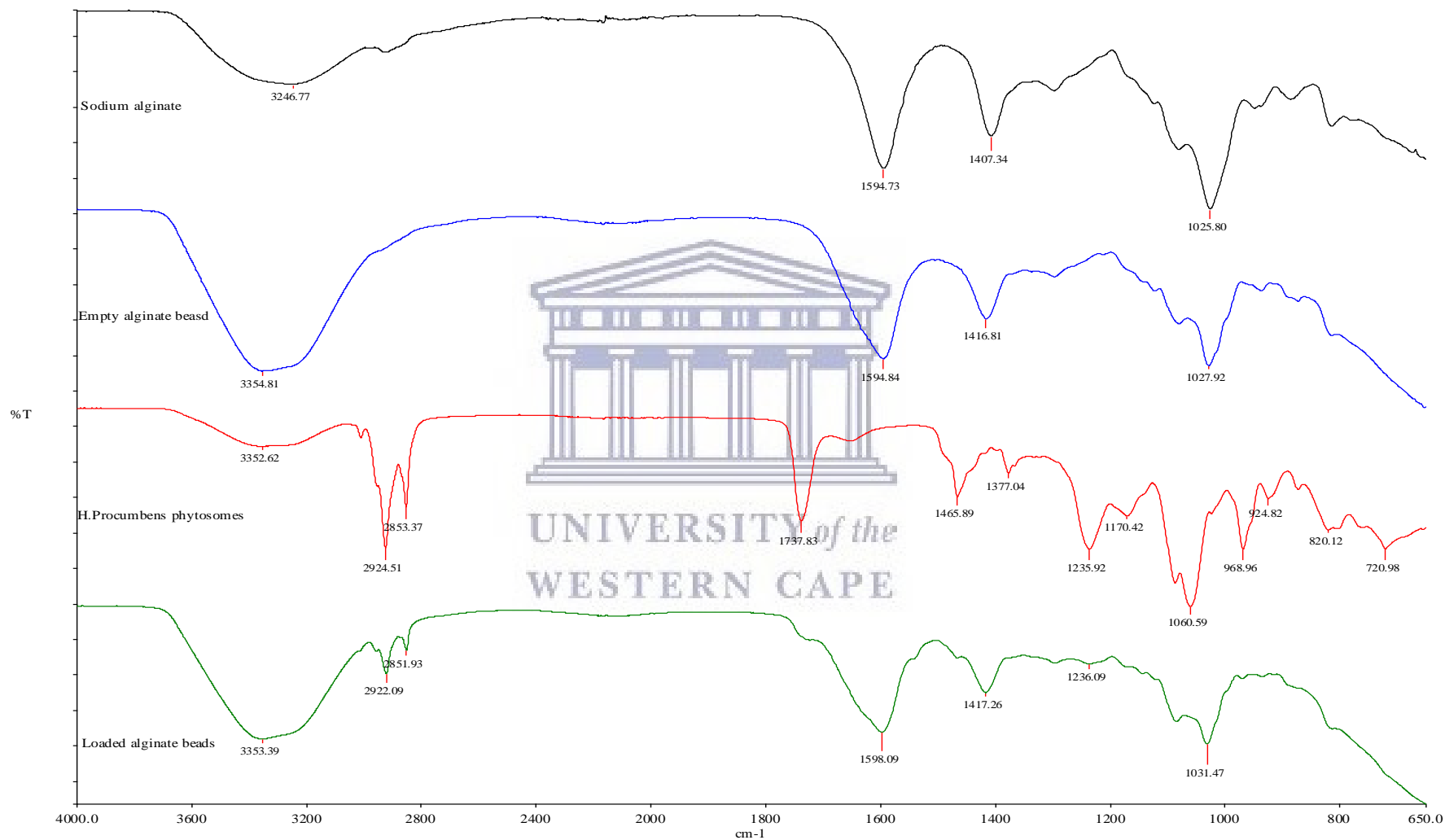


Figure 4-35: FTIR spectra of sodium alginate, empty alginate coated phytosomes, *H. procumbens* phytosomes and alginate coated *H. procumbens* phytosomes

Sodium alginate demonstrated a characteristic broad peak for – OH because alginate is a carbohydrate polymer, which has OH groups in their structure (Saleem *et al.*, 2012), confirmed by the broad peak at 3246.77 cm^{-1} . The two band peaks at 1594.73 cm^{-1} and 1407.34 cm^{-1} were identified as the asymmetric and symmetric stretching vibrations of the C–O bond of the COO group, respectively, and the peak at 1025.80 cm^{-1} indicates stretching vibrations of the C–O of the glucourinic unit. These peak bands were in line with the neglectable shift with the alginate bands findings of Mohandas *et al.*, (2015) who represented three distinct peaks for alginate bandage ($1,593\text{ cm}^{-1}$, $1,409\text{ cm}^{-1}$ and $1,026\text{ cm}^{-1}$ respectively).

The empty alginate beads spectrum demonstrated broad and strong –OH bending occurred at 3354.81 and some distinct peaks such as carboxyl group demonstrated strong absorption bands at 1594.84 cm^{-1} and 1416.81 cm^{-1} due to carboxyl anions asymmetric and symmetric stretching vibrations. The stretching vibrations of the C–O of the glucourinic unit occurred at 1027.92 cm^{-1} .

In the spectra of empty alginate beads, the shift in the peaks of empty alginate beads vs. sodium alginate indicated the involvement of the COO group in the Ca^{2+} mediated processes of alginate reticulation and egg-box-structure formation, and replacement of the Na^+ in the uronic-acid residues by Ca^{2+} i.e. confirming crosslinking. This is in agreement with the study of ultra-high concentration calcium alginate beads, where the representative peaks at 1594 and 409 shifted to 1593 and 1417 , respectively (Voo *et al.*, 2015)

Alginate-coated *H. procumbens* phytosomes (loaded alginate beads) demonstrated almost the same peaks of empty alginate with no appreciable shift i.e. 3353.39 cm^{-1} , 1598.09 cm^{-1} , 1417.26 cm^{-1} and 1031.47 cm^{-1} . Moreover, it demonstrated three peaks 2922.09 cm^{-1} , 2851.93 cm^{-1} and 1236.09 cm^{-1} which correspond to *H. procumbens* phytosomes as represented in the figure, which elucidates no significant chemical reaction occurred between *H. procumbens* phytosomes and alginate polymer, confirming compatibility of the polymer with the phytosomes and the phytosomes is present in unchanged form.

The results indicate that the main characteristic peaks of *H. procumbens* phytosomes are present in the combination spectrum, which reflects it does not significantly compromise the chemical composition and structural integrity of the *H. procumbens* phytosomes. This suggests chemical compatibility of the phytosomes with the alginate polymer.

4.9.6 Swelling index

The swelling study of the prepared alginate beads was performed in both SGF pH 1.2 and SIF pH 7.5. The swelling ratio of alginate beads was 18.96 ± 5.85 % in SGF and 92.45814 ± 0.80 % in SIF (figure 4.36).

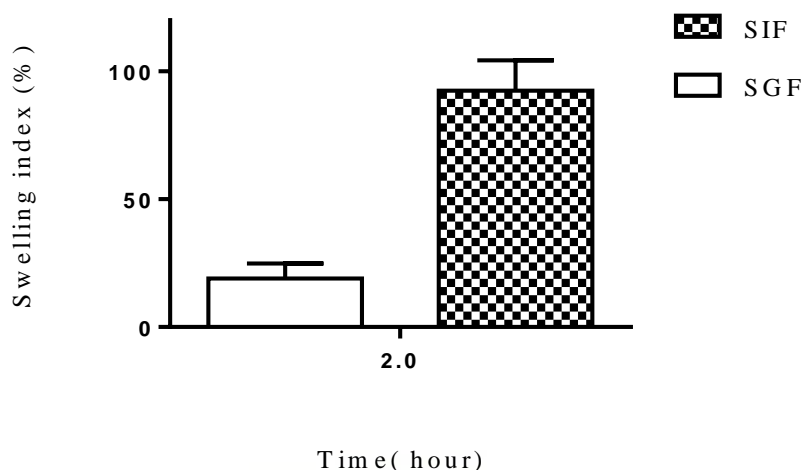


Figure 4-36: Swelling Index of alginate coated *H. procumbens* phytosomes in simulated gastric fluid (SGF) and simulated intestinal fluid (SIF).

At pH 1.2 (SGF), the low swelling degree of the alginate coated *H. procumbens* phytosomes could be due to the reduced chemical potential of the network resulted from protonation of the carboxyl group (Sathali *et al.*, 2012).

At pH 7.4 (SIF), the swelling degree of the alginate coated *H. procumbens* phytosomes was high and found to be statistically significant ($p < 0.05$). After the alginate coated *H. procumbens* phytosomes swelled, there was structural breakdown. This result is in agreement with Sankalia *et al.*, (2005) and Tous *et al.* (2014) reported alginate beads did not undergo swelling in the acidic environment, whereas they swell and disintegrate in intestinal fluid.

The swelling mechanism at pH 7.4 could be explained by the exchange of ions between the calcium ion of alginate beads and the sodium ions present in SIF, under influence of calcium-sequestrant phosphate ions (Nayak *et al.*, 2011) This ultimately results in a loose structure and hence the beads take up more water until bursting of the beads take place and start to disintegrate (Pasparakis *et al.*, 2006).

The result obtained for the swelling test is of importance to our study as it demonstrates negligible swelling in the SGF maintaining phytosomes integrity in gastric environment that

could affect and deform the phytosomes that entrap and protect the *H. procumbens* plant extract. Further, swelling takes place in the intestinal environment which increases phytosome release from alginate matrix which could phytosomal intestinal absorption.

4.9.7 Release study in GIT fluids

Release study of harpagoside from phytosome-alginate beads was performed in SGF and SIF environments. The release profiles are shown in figure 4.37.

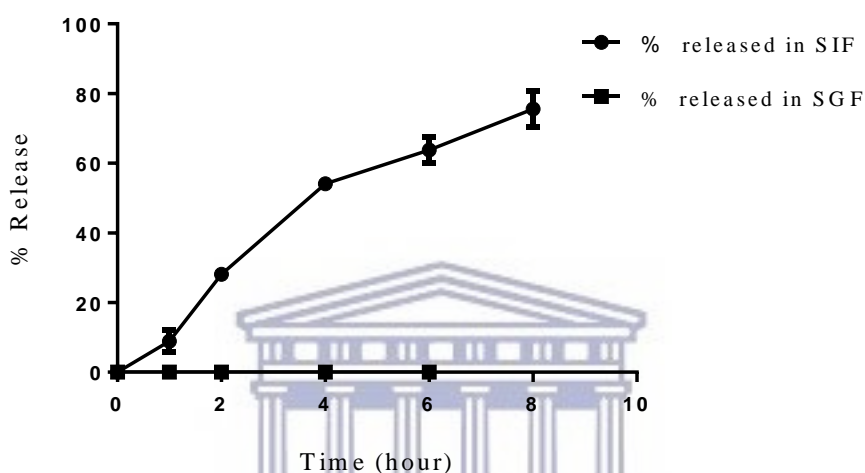


Figure 4-37: Release profile of *H. procumbens* phytosomes in simulated gastric fluid (SGF) and simulated intestinal fluid (SIF).

The drug release from the alginate beads is dependent on the penetration of the dissolution medium into the beads, swelling and dissolution of the alginate matrix, followed by the dissolution of the drug subsequent to leaching through the swollen matrix (Mandal *et al.*, 2010; Patel *et al.*, 2016).

In case of SGF, the alginate beads demonstrated no release at 4 hours and there was no sign of bead disruption and it maintained shape even after 4 hours as depicted in figure 4.38. The absence of the release the compounds from alginate beads could be related the low swelling ability (Shi *et al.*, 2006). Similar finding was reported by Tous *et al.*, (2014) who indicated that beads kept their intact form for up to 4 h in acidic pH; with no change in sphericity and low % release (4 %) of sodium diclofenac from sodium diclofenac loaded sodium alginate beads was observed in simulated gastric fluid (Saha *et al.*, 2013).



Figure 4-38: intact alginate coated *H. procumbens* phytosomes in SGF and eroded alginate coated *H. procumbens* phytosomes in SIF.

In contrast to SGF, *H. procumbens* phytosomes beads demonstrated a release of 54.05 ± 1.28 % at 4 hours and 75.55 ± 5.22 % in SIF at 8 hours. This value is the release of the *H. procumbens* from the alginate bead as well as the phytosome as it has to be released from the phytosome in order to be detected.

The lack of release in simulated gastric medium indicates that sodium alginate– *H. procumbens* phytosomes complex is capable of preventing release of phytosomes in the physiological environment of the stomach. In addition, the beads release the phytosomes in the intestinal environment making it available for intestinal absorption.

4.9.8 Release profile determination

Coated and un coated *H. procumbens* phytosomes formulations were subjected to release study and compared with the conventional plant extract release. The role of the carrier is of particular importance since it must efficiently release the drug and facilitate drug transport across the intestinal wall. The release profile for coated and un coated *H. procumbens* phytosomes and freeze dried plant extract were constructed and are shown in figure 4.39.

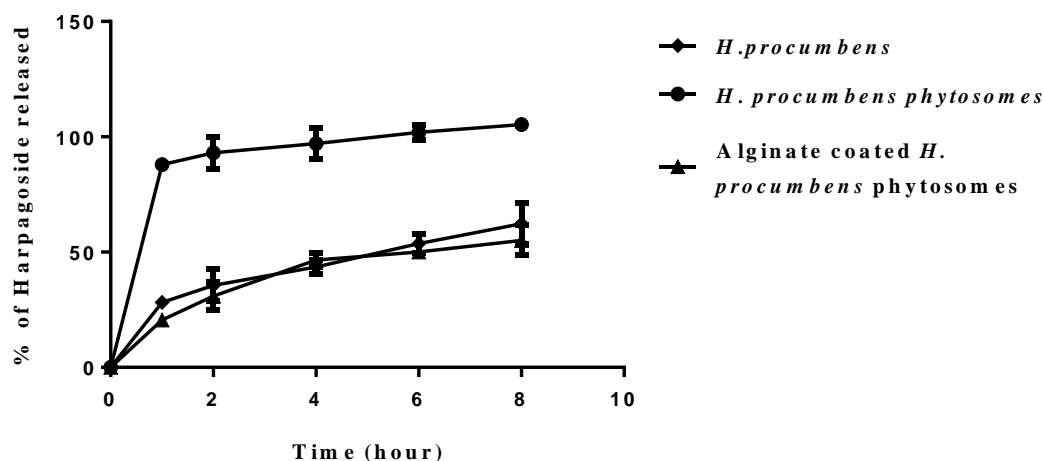


Figure 4-39: In vitro release profile of coated and un coated *H. procumbens* phytosomes and freeze dried plant extract in phosphate buffer solution (pH 7.4, n=3).

During the release process, two distinct release phases were noticed for the phytosomes. The first was characterized by rapid release (pulsatile release) during the first 1 hour, which could be related to release of drug adsorbed on the surface of the phytosomes; in the second phase, the release rate slowed down, demonstrating controlled drug-release behaviour as shown in the figure. From graph shape it is noted that prepared alginate coated and uncoated *H. procumbens* phytosomes exhibited a steady drug release pattern over a period of 8 hours. The harpagoside release from the two formulations was delayed compared to the conventional freeze dried plant extract. Previous studies reported high percentage release over time from phytosomes ranging between 68 % to 96 % (Singh *et al.*, 2013; Singh *et al.*, 2012; Hou *et al.*, 2012; Santra *et al.*, 2010). This variation in percentage drug release is attributed to many factors including the composition of vesicles.

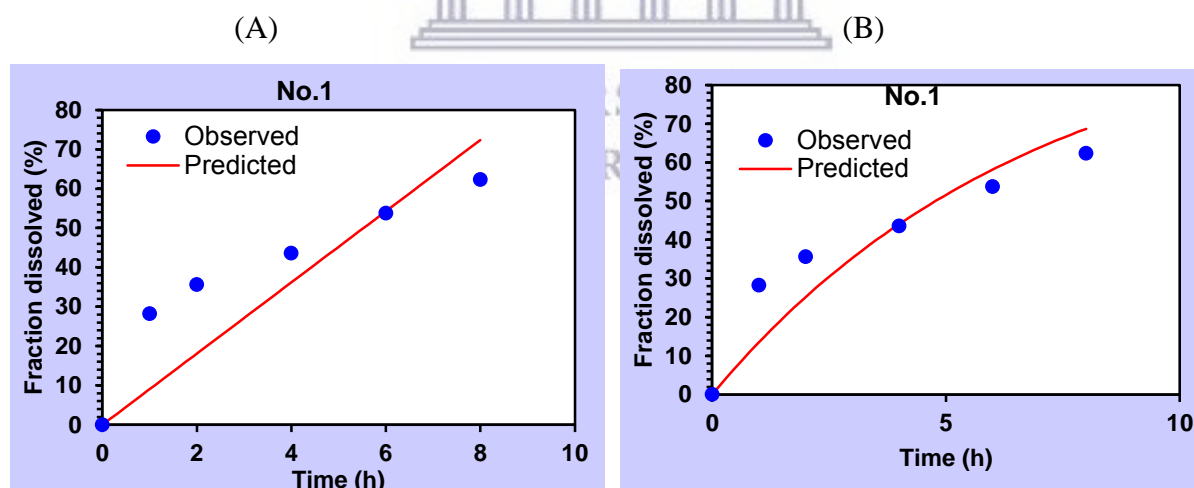
4.9.9 Mechanism of release

To determine the mechanism of drug release from the alginate beads, the data was treated with various models namely, zero-order, first-order, Higuchi, and Korsmeyer-Peppas by using the DDSolver software. The models which best fit; the drug releases from different formulations are shown in (Table 4.16).

Table 4.16: Regression coefficient (R^2) and release exponent (n) values of different *H.procumbens* formulations

F Model	R ² Values				Release exponent, n Values
	Zero Order	First Order	Higuchi	Korsmeyer- Peppas	
<i>H. procumbens</i> Plant extract					
	-0.277	0.991	0.590	0.997	0.105
<i>H. procumbens</i> phytosomes	0.655	0.925	0.978	0.997	0.400
Alginate coated <i>H.</i> <i>procumbens</i> phytosomes					
	0.942	0.985	0.924	0.968	0.752

The best fit model was selected as the one with the highest values of regression coefficient (R^2). The best fit can be observed when looking at the actual versus predicted plots of the various models in figure 4.40.1. From the linear regression model, the Korsmeyer-Peppas model (R^2 0.9971) was the best fit model for the *H. procumbens* phytosomes.



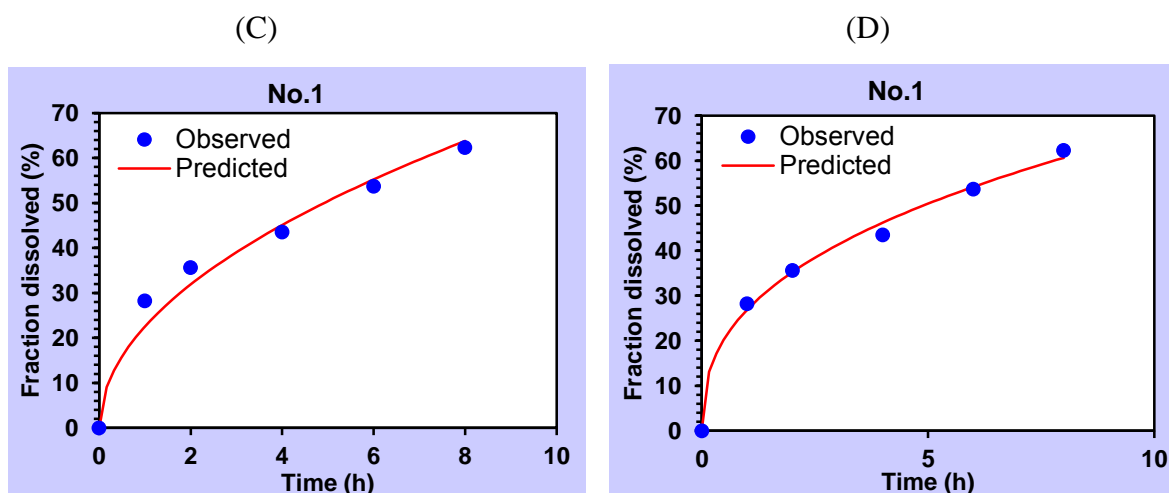


Figure 4-40-1: Release kinetics of phytosomes: (A) zero order plot, (B) first order plot, (C) Higuchi matrix plot, and (D) Korsmeyer Peppas plot.

Drug release mechanism can be determined according to n value. Table 4.17 shows release exponent and the equivalent release mechanism from spherical featured delivery systems (Zuo *et al.*, 2014).

Table 4-17: Exponent n of the power law and drug release mechanism from phytosome delivery systems.

Sphere	Drug release mechanism
0.43	Fickian diffusion
$0.43 < n < 0.85$	Anomalous transport
0.85	Case II transport

The n value obtained for phytosomes indicate that the harpagoside transport out of the phytosomes was driven mainly by a Fickian diffusion release mechanism.

The release kinetics plots for alginate coated *H. procumbens* phytosomes are illustrated in figure 4.40.2. The linear regression analysis, indicates a first order model for alginate beads with R^2 higher than 0.9857. The obtained n value of the alginate beads was 0.75 which is within the specified range of 0.43 and 0.85. This indicates the release from the alginate beads was predominantly by both diffusion controlled drug release and anomalous transport (swelling controlled drug release).

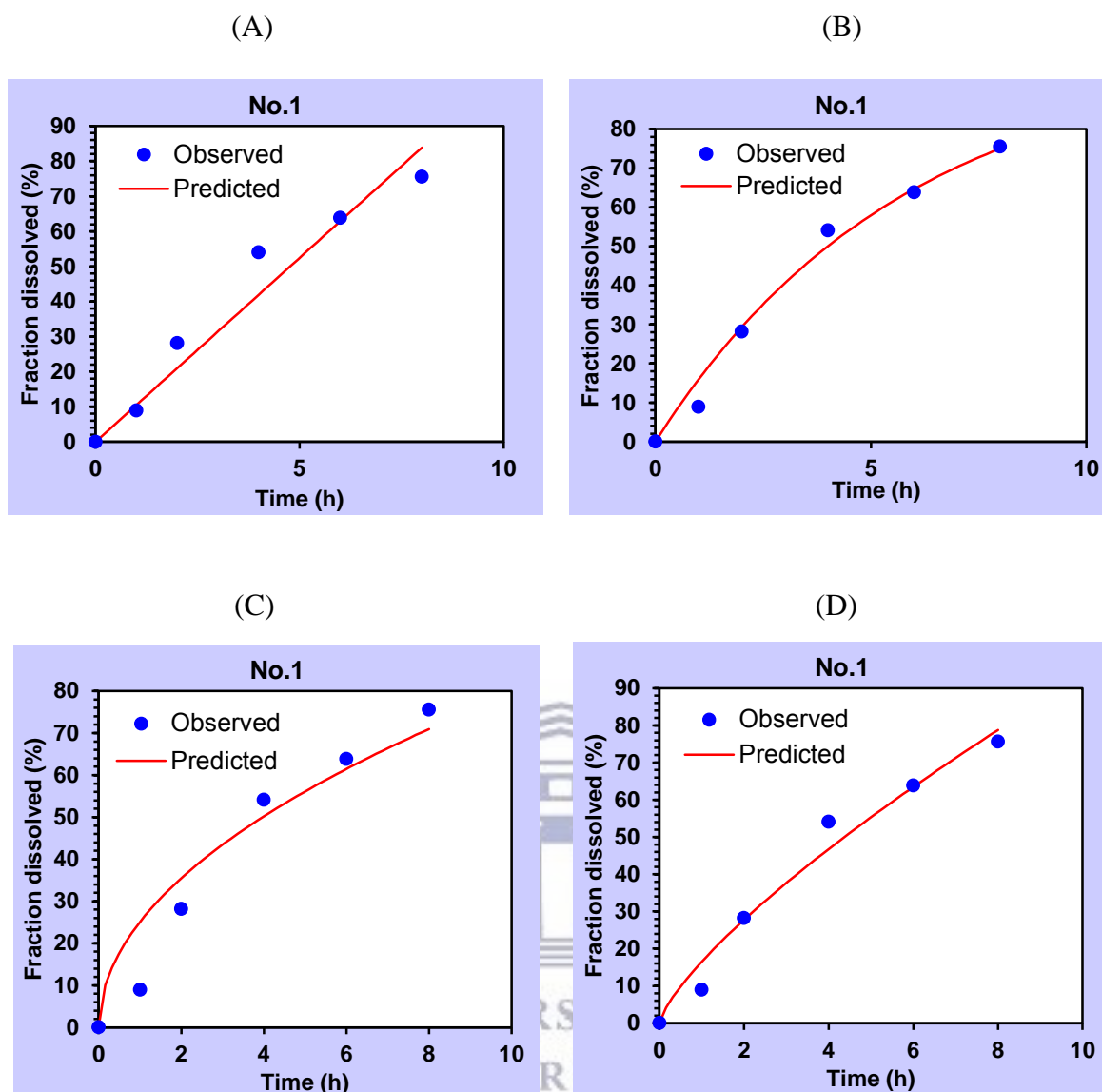


Figure 4-40-2: Release kinetics of alginate beads: (A) zero order plot, (B) first order plot, (C) Higuchi matrix plot and (D) Korsmeyer Peppas plot.

4.9.10 Storage stability study

1) Physical characteristics

The storage stability of the *H. procumbens* phytosomes results are presented in figure 4.41

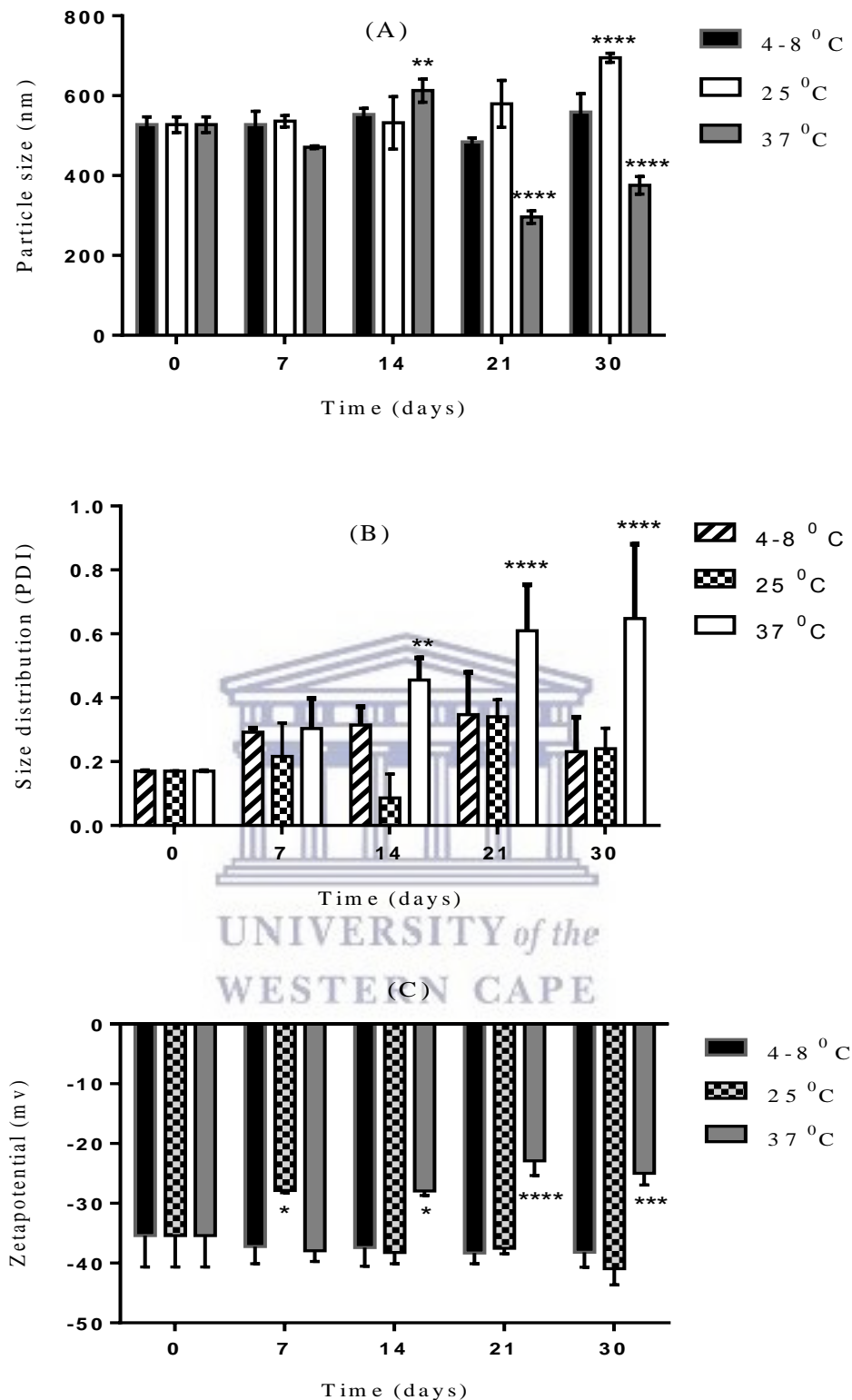


Figure 4-41: Physical stability of optimized *H. procumbens* phytosomes formulation at 3 different temperatures, (A, B, C) are measurements for particle size, polydispersity index and zeta potential respectively of optimized phytosomes formulation. Data shows as mean \pm sd, n=3, (****= P< 0.0001).

At 4-8 °C small variation in size was observed for the *H. procumbens* phytosomes over the tested period with a smallest size at 0 day and the largest size at 30 days ($p > 0.05$) with sizes of $527.3 \pm 19.7 - 558.7 \pm 46.5$ nm respectively. The zeta potential values (-35.4 ± 5.26 to -38.16 ± 2.51 mV) of the phytosome remained relatively stable when exposed at a temperature 4-8 °C, This implies that the prepared phytosomal formulation retained their initial charge and thus tendency for aggregation and flocculation was reduced, indicating that the prepared phytosomal formulation was more stable under refrigeration.

At 25 °C, there was a statistically significant ($p < 0.05$) increase in particle size at the end of 30 days, it changed from 527.3 ± 19.7 to 695.06 ± 11.32 nm. No significant change was observed for PDI ($0.17 \pm 0.001 - 0.24 \pm 0.065$) and zeta potential ($-35.4 \pm 5.26 - -40.9 \pm 2.70$ mV).

At 37 °C all batches displayed a statistically significant ($p < 0.05$) decrease in particle size ($527.3 \pm 19.7 - 375.5 \pm 22.12$), zeta potential ($-35.4 \pm 5.26 - -25 \pm 1.93$) and increase in PDI ($0.17 \pm 0.001 - 0.64 \pm 0.23$). The size reduction and PDI increase is most likely an indication of phytosomal breakdown.

The preferred storage conditions would be 4-8 °C as an increase in storage temperature contributed to instability of the *H. procumbens* phytosomal suspension.

Alginate coated *H. procumbens* phytosomes were also subjected to storage stability for 30 days at different temperatures and were tested for particle size changes. Results demonstrated that alginate coated *H. procumbens* phytosomes exhibited consistent size at all three temperatures for the 30 days period; this indicates that the alginate coated phytosomes are not stable to some extent and are not affected by temperature. The formulation only exhibited not appreciated significant increase in particle size at the end of 30 days at 37 °C.

2) Leakage

Leakage is a crucial characteristic for the evaluation of drug delivery systems. *H. procumbens* phytosomes and alginate coated *H. procumbens* loaded phytosomes formulations were tested for harpagoside leakage over a 30 day period at 4 – 8 °C, 25 °C and 37 °C. Results are shown in figure 4.41.

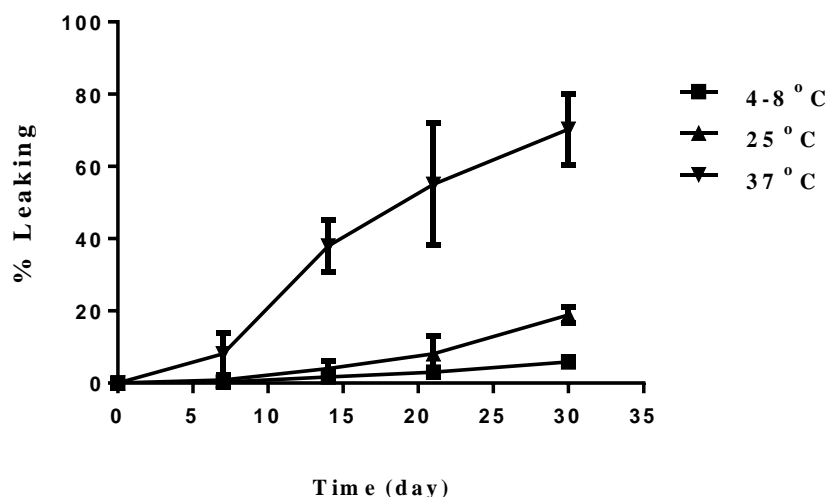


Figure 4-42: Leakage from *H. procumbens* phytosomes at various temperatures over time.

At lower temperature conditions, i.e. 4-8 °C, the phytosomes show fairly high retention of harpagoside inside the phytosomes over 30 days with only 5.85 % leakage. When cholesterol is incorporated into phospholipid bilayers, hydroxyl polar group of cholesterol is placed next to the PC carbonyl groups by formation of hydrogen bonds. Bonding between cholesterol and PC can enhance electrostatic repulsion between the phospholipid bilayer and increase its stability by limiting the movement of acyl chains of PC (Rasaie *et al.*, 2014; Briuglia *et al.*, 2015).

On the other hand, more leakage occurred with increasing storage period and temperature. Leaking of 18.85 % and 70.25 % were measured for samples stored at 25 °C and 37 °C respectively, at 30 days. The leakage of harpagoside from the phytosomes during storage at elevated temperature may be due to the effect of high temperature resulting in transition to a liquid of the lipid bilayers together with possible chemical degradation (oxidation and hydrolysis) of the phospholipid in the bilayers, leading to defects in membrane packing causing vesicle leakage during storage (Shazly, 2012; Agarwal *et al.*, 2002).

According to the ICH guidelines, a maximum limit of the loss of the active or marker constituents at 5–10 % is acceptable (Karioti *et al.*, 2011). Our study suggests the storage between 4 - 8 °C of the phytosomal formulation to prevent leakage from the phytosomes, as similarly reported by (Bhatia *et al.*, 2004; Trivedi *et al.*, 2017; Sudhakar, 2014).

As for alginate coated *H. procumbens* phytosomes, the alginate beads exhibited stability under all conditions as represented in figure 4.42; however, a low quantity of leaking (less than 6 %) was noted at the end of 30 days at high temperature (37 °C).

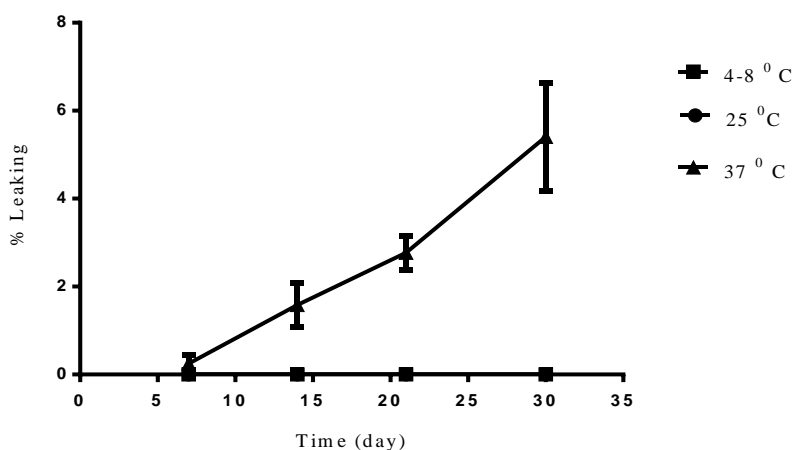


Figure 4-43: Alginate coated *H. procumbens* phytosomes percentage leaking versus storage period.

Overall, the coating of *H. procumbens* phytosomes with alginate polymer could reinforce the phytosomes stability at room and higher temperatures and decrease or limit the loss of the active constituents from the carrier (phytosomes). Moreover, maintain its integrity and show maximum protection against the harmful acidic environment that causes phytosomes deformation and active constituents decomposition.

Chapter 5

Conclusion and Recommendations

To recap:

The aim of the study was to develop an optimized liposomal/phytosomal carrier system consisting of *Harpagophytum procumbens* coated with alginate for protection from gastric medium digestion.

To achieve the aim, the following objectives were set:

- Development and validation of a rapid, simple and reliable UHPLC method for identification and quantification of harpagoside in *Harpagophytum procumbens* crude plant extract.
- Preparation of liposomes and phytosomes formulations containing *Harpagophytum procumbens* plant extract.
- Optimization studies of liposomes and phytosomes formulation parameters using response surface methodology (RSM).
- Physio-chemical characterization of prepared liposomes and phytosomes.
- Formulation and development of an alginate coating method for phytosomal formulation encapsulation.
- To perform *in vitro* stability of the optimized nano lipid vesicles and alginate coated beads in simulated gastric and intestinal medium.
- Determine the mechanism of release of harpagoside from phytosomes and alginate coated phytosomes.
- Determine the stability of harpagoside in phytosomes and alginate coated phytosomes at various temperatures over time.

A simple, accurate, linear, precise and robust UHPLC method for the determination of harpagoside in aqueous plant extract was successfully applied. *Harpagophytum procumbens* extract was complexed with phosphatidylcholine (PC) to form liposomes and phytosomes.

RSM was successfully used as a mathematical tool to provide a prediction model for the response to various inputs factors. The predicted RSM values and experimental values were

closely matched. The optimum preparation conditions were PC 80 %, cholesterol 5 % and the lipid vesicle being a phytosomes. It was observed that PC and cholesterol affect the entrapment efficiency and lipid vesicles size. PC and cholesterol increased the entrapment efficiency, although, PC had a more positive effect on encapsulation efficacy than cholesterol. High cholesterol content generally decreased percentage encapsulation. The particle size of lipid vesicles enhanced as phosphatidylcholine and cholesterol content increases.

The addition of stearic acid to the optimized phytosomal formulation increased the stability by improving zeta potential to a suitable value of 30.6 ± 0.80 mV.

The ionotropic gelation technique was successfully used for preparation of *Harpagophytum procumbens* phytosomes beads using sodium alginate and calcium chloride as a cross linking solution. Parameters such as polymer concentration and calcium chloride concentration played a noticeable role in achieving high entrapment efficiency, particle size and swelling behaviour. In addition, the particle size, zeta potential and leakage rate were the important indicators to evaluate phytosomes stability. The phytosomes showed instability in simulated gastric SGF (pH 1.2), demonstrated by the increase in the particle size, PDI and a reduction in zeta potential after 4 hours of incubation.

The present study has shown that alginate coated *Harpagophytum procumbens* phytosomes could be used to protect phytosomes from the gastric environment. They are suitable as a possible gastro retentive dosage form, as they have a rigid structure that resist biodegradation in gastric pH (simulated gastric fluid) but exhibit complete biodegradation in phosphate buffer pH 7.4 (simulated intestinal fluid) which could lead to increased availability of intact phytosomes for small intestine absorption.

It is recommended that intestinal absorption studies employing phospholipid vesicle-based permeation assays (PVPA) be used to determine uptake of *Harpagophytum procumbens* loaded phytosomes and *in vivo* bio-distribution of these loaded phytosomes. It would thus be of interest to continue developing selected formulations as well as introduce new elements into the formulations to achieve more desirable incorporation and retention of plant extract in phytosomes and *Harpagophytum procumbens* in alginate beads. It is also recommended that stearic acid be included as an input factor in the RSM software to further optimize the

formulation. In addition, this model including the RSM component could be used as a precursor to test other medicinal plants for increased intestinal phytosomal delivery.



References

- Abbas, G., Hanif, M., & Khan, M. A. (2017). pH responsive alginate polymeric rafts for controlled drug release by using box behnken response surface design. *Designed Monomers and Polymers*, 20(1), 1-9.
- Abdalla, K. F., Kamoun, E. A., & El Maghraby, G. M. (2015). Optimization of the entrapment efficiency and release of ambroxol hydrochloride alginate beads. *Journal of Applied Pharmaceutical Science*. 5 (04), 013-019.
- Abdelkader, H., Longman, M. R., Alany, R. G., & Pierscioneck, B. (2016). Phytosome-hyaluronic acid systems for ocular delivery of L-carnosine. *International Journal of Nanomedicine*, 2016(11), 2815-2827.
- Abhinav, M., Neha, J., Anne, G., & Bharti, V. (2016). Role of novel drug delivery systems in bioavailability enhancement: At a glance. *International Journal of Drug Delivery Technology*, 6(1), 7-26.
- Achim, M., Precup, C., Gonganaunitu, D., Barbu-Tudoran, L., Porfire, A. S., Scurtu, R., Ciuce, C. (2009). Thermosensitive liposomes containing doxorubicin. Preparation and in vitro evaluation. *Farmacia*, 57(6), 703-710.
- Afolayan, A., & Adebola, P. (2004). In vitro propagation: A biotechnological tool capable of solving the problem of medicinal plants decimation in South Africa. *African Journal of Biotechnology*, 3(12), 683-687.
- Agarwal, R., & Katare, O. (2002). Miconazole nitrate-loaded topical liposomes. *Pharmaceutical Technology*, 26(11), 48-60.
- Agarwal, R., Katare, O. P., & Vyas, S. P. (2001). Preparation and in vitro evaluation of liposomal/niosomal delivery systems for antipsoriatic drug dithranol. *International Journal of Pharmaceutics*, 228(1), 43-52.

- Ahmed, M. M., El-Rasoul, S. A., Auda, S. H., & Ibrahim, M. A. (2013). Emulsification/internal gelation as a method for preparation of diclofenac sodium–sodium alginate microparticles. *Saudi Pharmaceutical Journal*, 21(1), 61-69.
- Aikawa, T., Ito, S., Shinohara, M., Kaneko, M., Kondo, T., & Yuasa, M. (2015). A drug formulation using an alginate hydrogel matrix for efficient oral delivery of the manganese porphyrin-based superoxide dismutase mimic. *Biomaterials Science*, 3(6), 861-869.
- Aizpurua-Olaizola, O., Navarro, P., Vallejo, A., Olivares, M., Etxebarria, N., & Usobiaga, A. (2016). Microencapsulation and storage stability of polyphenols from vitis vinifera grape wastes. *Food Chemistry*, 190, 614–621.
- Akbarzadeh, A., Rezaei-Sadabady, R., Davaran, S., Joo, S. W., Zarghami, N., Hanifepour, Y., Samiei, M., Kouhi, M & Nejati-Koshki, K. (2013). Liposome: classification, preparation, and applications. *Nanoscale Research Letters*, 1(8), 1-9.
- Akerele, O. (1988). Medicinal plants and primary health care: An agenda for action. *Fitoterapia*, 59(5), 355-363.
- Akhtar, N. (2014). Vesicles: A recently developed novel carrier for enhanced topical drug delivery. *Current Drug Delivery*, 11(1), 87-97.
- Akhtar, N., & Haqqi, T. M. (2012). Current nutraceuticals in the management of osteoarthritis: A review. *Therapeutic Advances in Musculoskeletal Disease*, 4(3), 181-207.
- Al-Kassas, R. S., Al-Gohary, O. M., & Al-Faadhel, M. M. (2007). Controlling of systemic absorption of gliclazide through incorporation into alginate beads. *International Journal of Pharmaceutics*, 341(1), 230-237.
- Allam, A. N., Komeil, I. A., & Abdallah, O. Y. (2015). Curcumin phytosomal softgel formulation: Development, optimization and physicochemical characterization. *Acta Pharmaceutica*, 65(3), 285-297.

- Al-Rimawi, F. (2014). Development and validation of HPLC-UV method for determination of bovine serum albumin and myoglobin proteins. *International Research Journal of Pure & Applied Chemistry*, 4(6), 585-593.
- Alshamrani, O. S. (2017). Construction cost prediction model for conventional and sustainable college buildings in North America. *Journal of Taibah University for Science*, 11(2), 315-323.
- Al-Shdefat, R., Yassin, A. E. B., Anwer, K., & Alsarra, I. (2012). Preparation and characterization of biodegradable paclitaxel loaded chitosan microparticles. *Digest Journal of Nanomaterials and Biostructures*, 7(3), 1139-1147.
- Amit, P., Tanwar, Y., Rakesh, S., & Poojan, P. (2013). Phytosome: Phytolipid drug delivery system for improving bioavailability of herbal drug. *Journal of Pharmaceutical Science and Bioscientific*, 3(2), 51-57.
- Andersen, M. L., Santos, E. H., Maria de Lourdes, V Seabra, da Silva, A. A., & Tufik, S. (2004). Evaluation of acute and chronic treatments with *Harpagophytum procumbens* on Freund's adjuvant-induced arthritis in rats. *Journal of Ethnopharmacology*, 91(2), 325-330.
- Andhale, V. A., Patil, P. R., Dhas, A. U., Chauhan, P. D., & Desai, S. V. (2016). Liposome: an emerging tool in drug carrier system. *International Journal of Pharmacy & Technology*. 8(1), 10982-11011.
- Anwekar, H., Patel, S., & Singhai, A. K. (2011). Liposomes as drug carriers. *International Journal of Pharmacy and Life Sciences*. 2(7), 945-951.
- Ashengroph, M., Nahvi, I., & Amini, J. (2013). Application of taguchi design and response surface methodology for improving conversion of isoeugenol into vanillin by resting cells of psychrobacter sp. CSW4. *Iranian Journal of Pharmaceutical Research*, 12(3), 411-421.
- Babili, F. E., Fouraste, I., Rougaignon, C., Moulis, C., & Chatelain, C. (2012). Anatomical study of secondary tuberized roots of *Harpagophytum procumbens* DC and

- quantification of harpagoside by high-performance liquid chromatography method. *Pharmacognosy Magazine*, 8(30), 175-180.
- Babu, V. R., Sairam, M., Hosamani, K. M., & Aminabhavi, T. M. (2007). Preparation of sodium alginate–methylcellulose blend microspheres for controlled release of nifedipine. *Carbohydrate Polymers*, 69(2), 241-250.
- Balanč, B., Trifković, K., Đorđević, V., Marković, S., Pjanović, R., Nedović, V., Bugarski, B. (2016). Novel resveratrol delivery systems based on alginate-sucrose and alginate-chitosan microbeads containing liposomes. *Food Hydrocolloids*, 61, 832-842.
- Baniasadi, M., & Minary-Jolandan, M. (2015). Alginate-collagen fibril composite hydrogel. *Materials*, 8(2), 799-814.
- Bansal, D., Gulbake, A., Tiwari, J., & Jain, S. K. (2016). Development of liposomes entrapped in alginate beads for the treatment of colorectal cancer. *International Journal of Biological Macromolecules*, 82, 687-695.
- Bassi, P., & Kaur, G. (2015). Polymeric films as a promising carrier for bioadhesive drug delivery: Development, characterization and optimization. *Saudi Pharmaceutical Journal*, 25(1), 32-43.
- Begum, M., Sudhakar, M., & Abbulu, K. (2012). Flurbiprofen-loaded stealth liposomes: Studies on the development, characterization, pharmacokinetics, and biodistribution. *Journal of Young Pharmacists*, 4(4), 209-219.
- Bezerra, M. A., Santelli, R. E., Oliveira, E. P., Villar, L. S., & Escaleira, L. A. (2008). Response surface methodology (RSM) as a tool for optimization in analytical chemistry. *Talanta*, 76(5), 965-977.
- Bhan, M. (2017). Response surface methodology: An important tool in optimization. *International Journal of Advanced Research and Development*, 2(1), 38-40.
- Bhatia, A., Kumar, R., & Katare, O. P. (2004). Tamoxifen in topical liposomes: Development, characterization and in-vitro evaluation. *Journal of Pharmacy & Pharmaceutical Sciences*, 7(2), 252-259.

- Bhattacharya, S., & Ghosh, A. (2009). Phytosomes: The emerging technology for enhancement of bioavailability of botanicals and nutraceuticals. *The Internet Journal of Aesthetic and Antiaging Medicine*, 2(1), 141-153.
- Bhimavarapu, R., Chitra, K. P., Meda, H., Kanikanti, D., Anne, M., & Gowthami, N. (2011). Forced degradation study of paracetamol in tablet formulation using RP-HPLC. *Bulletin of Pharmaceutical Research*, 1(3), 13-17.
- Bhushan, B., Pal, A., & Jain, V. (2015). Improved enzyme catalytic characteristics upon glutaraldehyde cross-linking of alginate entrapped xylanase isolated from *aspergillus flavus* MTCC 9390. *Enzyme Research*, 2015, 1-9.
- Bibi, S., Kaur, R., Henriksen-Lacey, M., McNeil, S. E., Wilkhu, J., Lattmann, E., Christensenb, D., Mohammed, A. R., Perrie, Y. (2011). Microscopy imaging of liposomes: From coverslips to environmental SEM. *International Journal of Pharmaceutics*, 417(1), 138-150.
- Boje, K., Lechtenberg, M., & Nahrstedt, A. (2003). New and known iridoid-and phenylethanoid glycosides from *Harpagophytum procumbens* and their in vitro inhibition of human leukocyte elastase. *Planta Medica*, 69(09), 820-825.
- Bone, K., & Mills, S. Y. (2013). Principles and practice of phytotherapy: Modern herbal medicine. London, U.K. Elsevier Health Sciences.
- Boundless "Biological Macromolecules". *Boundless Biology*. [Accessed June, 2017]. <https://www.boundless.com/biology/textbooks/boundless-biology-textbook/biological-macromolecules-3/lipids-55/phospholipids-300-11433/>.
- Bozzuto, G., & Molinari, A. (2015). Liposomes as nanomedical devices. *International Journal of Nanomedicine*, 10, 975-999.
- Briuglia, M., Rotella, C., McFarlane, A., & Lamprou, D. A. (2015). Influence of cholesterol on liposome stability and on in vitro drug release. *Drug Delivery and Translational Research*, 5(3), 231-242.

- Buwalda, S. J., Vermonden, T., & Hennink, W. E. (2017). Hydrogels for therapeutic delivery: Current developments and future directions. *Biomacromolecules*, 18(2), 316-330.
- Caban, S., Aytekin, E., Sahin, A., & Capan, Y. (2014). Nanosystems for drug delivery. *OA Drug Design and Delivery*, 18(2), 1-7.
- Carafa, M., Marianecchi, C., Marzio, L. D., Caro, V. D., Giandalia, G., Giannola, L. I., Santucci, E. (2010). Potential dopamine prodrug-loaded liposomes: Preparation, characterization, and in vitro stability studies. *Journal of Liposome Research*, 20(3), 250-257.
- Catelan, S.C., Belentani, R.M., Marques, L.C., Silva, E.R., Silva, M.A., Caparroz-Assef, S.M., Cuman, R.K.N., Bersani-Amado, C.A. (2006). The role of adrenal corticosteroids in the anti-inflammatory effect of the whole extract of *Harpagophytum procumbens* in rats, *Phytomedicine*, 13(6), 446-451.
- Cerciello, A., Auriemma, G., Morello, S., Aquino, R. P., Del Gaudio, P., & Russo, P. (2016). Prednisolone delivery platforms: Capsules and beads combination for a right timing therapy. *PloS One*, 11(7), 1-14.
- Chan, L. W., Ching, A. L., Liew, C. V., & Heng, P. W. S. (2007). Mechanistic study on hydration and drug release behaviour of sodium alginate compacts. *Drug Development and Industrial Pharmacy*, 33(6), 667-676.
- Channarong, S., Chaicumpa, W., Sinchaipanid, N., & Mitrevej, A. (2011). Development and evaluation of chitosan-coated liposomes for oral DNA vaccine: The improvement of Peyer's patch targeting using a polyplex-loaded liposomes. *American Association of Pharmaceutical Scientists, Pharmscitech*, 12(1), 192-200.
- Chime, S. A., & Onyishi, I. V. (2013). Lipid-based drug delivery systems (LDDS): Recent advances and applications of lipids in drug delivery. *African Journal of Pharmacy and Pharmacology*, 7(48), 3034-3059.
- Choubey, A. (2011). Phytosome-A novel approach for herbal drug delivery. *International Journal of Pharmaceutical Sciences and Research*, 2(4), 807-815.

- Chowdhury, J. A., Jahan, S. T., Morshed, M. M., Mallick, J., Nath, A. K., Uddin, M. Z., Dutta, M., Islam, M. K., Kawsar, M. H. (2011). Development and evaluation of diclofenac sodium loaded alginate cross-linking beads. *Bangladesh Pharmaceutical Journal*, 14(1), 41-48.
- Chrubasik, J. E., Roufogalis, B. D., & Chrubasik, S. (2007). Evidence of effectiveness of herbal antiinflammatory drugs in the treatment of painful osteoarthritis and chronic low back pain. *Phytotherapy Research*, 21(7), 675-683.
- Chrubasik, S., Sporer, F., Dillmann-Marschner, R., Friedmann, A., & Wink, M. (2000). Physicochemical properties of harpagoside and its in vitro release from *Harpagophytum procumbens* extract tablets. *Phytomedicine*, 6(6), 469-473.
- Clarkson, C., Maharaj, V. J., Crouch, N. R., Grace, O. M., Pillay, P., Matsabisa, M. G., Bhagwandin, N., Smith, P. J., Folb, I. P. (2004). In vitro antiplasmodial activity of medicinal plants native to or naturalised in South Africa. *Journal of Ethnopharmacology*, 92(2), 177-191.
- Cold Spring Harbor Protocols by Cold Spring Harbor Laboratory Press: http://cshprotocols.cshlp.org/site/recipes/nav_p.dtl [accessed Jun, 2015].
- d'Ayala, G. G., Malinconico, M., & Laurienzo, P. (2008). Marine derived polysaccharides for biomedical applications: Chemical modification approaches. *Molecules*, 13(9), 2069-2106.
- Daemi, H., & Barikani, M. (2012). Synthesis and characterization of calcium alginate nanoparticles, sodium homopolymannuronate salt and its calcium nanoparticles. *Scientia Iranica*, 19(6), 2023-2028.
- Das, M. K., & Senapati, P. C. (2007). Evaluation of furosemide-loaded alginate microspheres prepared by ionotropic external gelation technique. *Acta Poloniae Pharmaceutica -Drug Research*, 64(3), 253-262.
- Das, S., & Chaudhury, A. (2011). Recent advances in lipid nanoparticle formulations with solid matrix for oral drug delivery. *American Association of Pharmaceutical Scientists, PharmSciTech*, 12(1), 62-76.

- Davidov-Pardo, G., & McClements, D. J. (2014). Resveratrol encapsulation: Designing delivery systems to overcome solubility, stability and bioavailability issues. *Trends in Food Science & Technology*, 38(2), 88-103.
- De Sousa Lobato, K. B., Paese, K., Forgearini, J. C., Guterres, S. S., Jablonski, A., & de Oliveira Rios, A. (2013). Characterisation and stability evaluation of bixin nanocapsules. *Food Chemistry*, 141(4), 3906-3912.
- De, A., & Venkatesh, D. N. (2012). Design and evaluation of liposomal delivery system for L-asparaginase. *Journal of Applied Pharmaceutical Science*, 2 (8), 112-117.
- Demir, B., Barlas, F. B., Guler, E., Gumus, P. Z., Can, M., Yavuz, M., Coskunol, H., Timur, S. (2014). Gold nanoparticle loaded phytosomal systems: Synthesis, characterization and in vitro investigations. *RSC Advances*, 4(65), 34687-34695.
- Devi, N. K. D., Chandana, M., Sindhura, A., Ratnavali, G., & Kavitha, R. (2010). Comparative evaluation of alginate beads prepared by ionotropic gelation technique. *Pharmacophore*, 1(3), 196-213.
- Dewan, N., Dasgupta, D., Pandit, S., & Ahmed, P. (2016). Review on-herbosomes, a new arena for drug delivery. *Journal of Pharmacognosy and Phytochemistry*, 5(4), 104- 108.
- Dhase, A. S., Saboo, S. S. (2015). Preparation and evaluation of phytosomes containing methanolic extract of leaves of aegle marmelos (bael). *International Journal of PharmTech Research*, 8(6), 231-240.
- Dhoot, N. O., & Wheatley, M. A. (2003). Microencapsulated liposomes in controlled drug delivery: Strategies to modulate drug release and eliminate the burst effect. *Journal of Pharmaceutical Sciences*, 92(3), 679-689.
- Dimitrova, P., Georgiev, M., Khan, M., & Ivanovska, N. (2013). Evaluation of verbascum species and harpagoside in models of acute and chronic inflammation. *Open Life Sciences*, 8(2), 186-194.

- Ding, B. S., Dziubla, T., Shuvaev, V. V., Muro, S., & Muzykantov, V. R. (2006). Advanced drug delivery systems that target the vascular endothelium. *Molecular Interventions*, 6(2), 98-112.
- Ding, B., Xia, S., Hayat, K., & Zhang, X. (2009). Preparation and pH stability of ferrous glycinate liposomes. *Journal of Agricultural and Food Chemistry*, 57(7), 2938-2944.
- Dressman, J. B., & Reppas, C. (2000). In vitro–in vivo correlations for lipophilic, poorly water-soluble drugs. *European journal of pharmaceutical sciences*, 11, 73-80.
- Ebrahim, N., & Uebel, R. (2011). Direct inhibition of cyclooxygenase-2 enzyme by an extract of harpagophytum procumbens, harpagoside and harpagide. *African Journal of Pharmacy and Pharmacology*. 5(20), 2209-2212.
- El-Gazayerly, O., Makhoul, A., Soelm, A., & Mohmoud, M. (2014). Antioxidant and hepatoprotective effects of silymarin phytosomes compared to milk thistle extract in CCl₄ induced hepatotoxicity in rats. *Journal of Microencapsulation*, 31(1), 23-30.
- El-Kamel, A., Al-Gohary, O., & Hosny, E. (2003). Alginate-diltiazem hydrochloride beads: Optimization of formulation factors, in vitro and in vivo availability. *Journal of Microencapsulation*, 20(2), 211-225.
- El-Sherbiny, I. M., Abdel-Mogib, M., Dawidar, A. M., Elsayed, A., & Smyth, H. D. (2011). Biodegradable pH-responsive alginate-poly (lactic-co-glycolic acid) nano/micro hydrogel matrices for oral delivery of silymarin. *Carbohydrate Polymers*, 83(3), 1345-1354.
- Fadda, H. M., Sousa, T., Carlsson, A. S., Abrahamsson, B., Williams, J. G., Kumar, D., & Basit, A. W. (2010). Drug solubility in luminal fluids from different regions of the small and large intestine of humans. *Molecular Pharmaceutics*, 7(5), 1527-1532.
- Fang, J. B., Robertson, V. K., Rawat, A., Flick, T., Tang, Z. J., Cauchon, N. S., & McElvain, J. S. (2010). Development and application of a biorelevant dissolution method using USP apparatus 4 in early phase formulation development. *Molecular Pharmaceutics*, 7(5), 1466-1477.

- Francis, F., Sabu, A., Nampoothiri, K. M., Ramachandran, S., Ghosh, S., Szakacs, G., Pandey, A. (2003). Use of response surface methodology for optimizing process parameters for the production of α -amylase by *aspergillus oryzae*. *Biochemical Engineering Journal*, 15(2), 107-115.
- Freag, M. S., Elnaggar, Y. S., & Abdallah, O. Y. (2013). Lyophilized phytosomal nanocarriers as platforms for enhanced diosmin delivery: Optimization and ex vivo permeation. *International Journal of Nanomedicine*, 8, 2385-2397.
- Fricker, G., Kromp, T., Wendel, A., Blume, A., Zirkel, J., Rebmann, H., Setzer, C., Quinkert, R., Martin, F., Müller-Goymann, C. (2010). Phospholipids and lipid-based formulations in oral drug delivery. *Pharmaceutical Research*, 27(8), 1469-1486.
- Gavhane, Y. N., & Yadav, A. V. (2012). Loss of orally administered drugs in GI tract. *Saudi Pharmaceutical Journal*, 20(4), 331-344.
- Georgiev, M. I., Ivanovska, N., Alipieva, K., Dimitrova, P., & Verpoorte, R. (2013). Harpagoside: From Kalahari Desert to pharmacy shelf. *Phytochemistry*, 92, 8-15.
- Georgiev, M., Alipieva, K., & Denev, P. (2010). Antioxidant activity and bioactive constituents of the aerial parts of *Harpagophytum procumbens* plants. *Biotechnology & Biotechnological Equipment*, 24(1), 438-443.
- Ghanbarzadeh, S., & Arami, S. (2013). Enhanced transdermal delivery of diclofenac sodium via conventional liposomes, ethosomes, and transfersomes. *BioMed Research International*, 2013, 1-7.
- Ghanbarzadeh, S., Khorrami, A., & Arami, S. (2014). Preparation of optimized naproxen nano liposomes using response surface methodology. *Journal of Pharmaceutical Investigation*, 44(1), 33-39.
- Ghanbarzadeh, S., Valizadeh, H., & Zakeri-Milani, P. (2013). Application of response surface methodology in development of sirolimus liposomes prepared by thin film hydration technique. *BioImpacts*, 3(2), 75-81.

- Gombotz, W. R., & Wee, S. F. (2012). Protein release from alginate matrices. *Advanced Drug Delivery Reviews*, 64, 194-205.
- Grant, L., McBean, D., Fyfe, L., & Warnock, A. (2007). A review of the biological and potential therapeutic actions of *Harpagophytum procumbens*. *Phytotherapy Research*, 21(3), 199-209.
- Grijalvo, S., Mayr, J., Eritja, R., & Díaz, D. D. (2016). Biodegradable liposome-encapsulated hydrogels for biomedical applications: A marriage of convenience. *Biomaterials Science*, 4(4), 555-574.
- Gruberova, L., & Kratochvil, B. (2017). Biorelevant dissolution of candesartan cilexetil. *ADMET and DMPK*, 5(1), 39-46.
- Gyurkovska, V., Alipieva, K., Maciuk, A., Dimitrova, P., Ivanovska, N., Haas, C., Bley, T., Georgiev, M. (2011). Anti-inflammatory activity of Devil's claw in vitro systems and their active constituents. *Food Chemistry*, 125(1), 171-178.
- Haidar, Z. S., Hamdy, R. C., & Tabrizian, M. (2008). Protein release kinetics for core-shell hybrid nanoparticles based on the layer-by-layer assembly of alginate and chitosan on liposomes. *Biomaterials*, 29(9), 1207-1215.
- Hostanska, K., Melzer, J., Rostock, M., Suter, A., & Saller, R. (2014). Alteration of anti-inflammatory activity of *Harpagophytum procumbens* (devil's claw) extract after external metabolic activation with S9 mix. *Journal of Pharmacy and Pharmacology*, 66(11), 1606-1614.
- Hou, Z., Li, Y., Huang, Y., Zhou, C., Lin, J., Wang, Y., Cui, F., Zhou, S., Jia, M., Ye, S., Zhang, Q. (2012). Phytosomes loaded with mitomycin C-soybean phosphatidylcholine complex developed for drug delivery. *Molecular Pharmaceutics*, 10(1), 90-101.
- <https://avantilipids.com/>. [Accessed October, 2016].
- Hua, S., & Wu, S. Y. (2013). The use of lipid-based nanocarriers for targeted pain therapies. *Frontiers in Pharmacology*, 4, (143), 1-7.

- Hung, W., Lee, M., Chen, F., & Huang, H. W. (2007). The condensing effect of cholesterol in lipid bilayers. *Biophysical Journal*, 92(11), 3960-3967.
- ICH Harmonised Tripartite Guideline Q2 (R1). (2005): Validation of analytical procedures: Text and methodology.
- Imura, T., Otake, K., Hashimoto, S., Gotoh, T., Yuasa, M., Yokoyama, S., Sakai, H., Rathman, J. F., Abe, M. (2003). Preparation and physicochemical properties of various soybean lecithin liposomes using supercritical reverse phase evaporation method. *Colloids and Surfaces B: Biointerfaces*, 27(2), 133-140.
- Indira, M. Y., & Ch, R. (2012). Design and evaluation of multi-unit floating alginate beads of famotidine. *International Journal of Pharmacy and Industrial Research*, 2 (3), 344-353.
- Jaafarzadeh, N., Omidinasab, M., & Ghanbari, F. (2016). Combined electrocoagulation and UV-based sulfate radical oxidation processes for treatment of pulp and paper wastewater. *Process Safety and Environmental Protection*, 102, 462-472.
- Jahan, S. T., Sadat, S. M. A., Islam, M. S., Jalil, R., & Chowdhury, J. A. (2010). Effect of various excipients on theophylline-loaded alginate beads prepared by ionic cross linking technique. *Dhaka University Journal of Pharmaceutical Sciences*, 9(1), 15-22.
- Jain, N., Gupta, B. P., Thakur, N., Jain, R., Banweer, J., Jain, D. K Jain, S. (2010). Phytosome: A novel drug delivery system for herbal medicine. *International Journal of Pharmaceutical Sciences and Drug Research*, 2(4), 224-228.
- Jaiswal, D., Bhattacharya, A., Yadav, I. K., Singh, H. P., Chandra, D., & Jain, D. (2009). Formulation and evaluation of oil entrapped floating alginate beads of ranitidine hydrochloride. *International Journal of Pharmacy and Pharmaceutical Sciences*, 1(3), 128-140.
- Juárez, G. A. P., Spasojevic, M., Faas, M. M., & de Vos, P. (2014). Immunological and technical considerations in application of alginate-based microencapsulation systems. *Frontiers in Bioengineering and Biotechnology*, 2(26), 1-15.

- Junyaprasert, V. B., Teeranachaideekul, V., & Supaperm, T. (2008). Effect of charged and non-ionic membrane additives on physicochemical properties and stability of niosomes. *Aaps Pharmscitech*, 9(3), 851- 859.
- Kalepu, S., Manthina, M., & Padavala, V. (2013). Oral lipid-based drug delivery systems—an overview. *Acta Pharmaceutica Sinica B*, 3(6), 361-372.
- Kalepu, S., Sunilkumar, K., Betha, S., & Mohanvarma, M. (2013). Liposomal drug delivery system—a comprehensive review. *International Journal of Drug Delivery Research*, 5(4), 62-75.
- Kan, P., Tsao, C. W., Wang, A. J., Su, W. C., & Liang, H. F. (2010). A liposomal formulation able to incorporate a high content of Paclitaxel and exert promising anticancer effect. *Journal of Drug Delivery*, 2011. 1-9.
- Karimi, N., Ghanbarzadeh, B., Hamishehkar, H., Keivani, F., Pezeshki, A., & Gholian, M. M. (2015). Phytosome and liposome: The beneficial encapsulation systems in drug delivery and food application. *Applied Food Biotechnology*, 2(3), 17-27.
- Karioti, A., Fani, E., Vincieri, F. F., & Bilia, A. R. (2011). Analysis and stability of the constituents of curcuma longa and *Harpagophytum procumbens* tinctures by HPLC-DAD and HPLC-ESI-MS. *Journal of Pharmaceutical and Biomedical Analysis*, 55(3), 479-486.
- Kashid, P., Doijad, R., Shete, A., Sajane, S., & Bhagat, A. (2016). Studies on rebamipide loaded gastroretentive alginate based mucoadhesive beads: Formulation & in-vitro, in-vivo evaluation. *Pharmaceutical Methods*, 7(2), 132-138.
- Kassem, M. A., El Assal, M., & Al-Badrawy, A. (2012). Preparation and evaluation of certain hydrophilic drug-loaded microspheres. *International Research Journal of Pharmaceuticals*, 2(4), 82-90.
- Kaza, R., Pravallika, P., Reddy, T. V., & Naga Priya, K. R. (2011). Formulation and evaluation of controlled release microspheres of acyclovir sodium. *International Journal of Innovative Pharmaceutical Research*, 2(1), 98-101.

- Khajeh, M. (2012). Multivariate optimization of microwave-assisted digestion of copper and zinc from powder milk. *Journal of the Brazilian Chemical Society*, 23(9), 1704-1711.
- Khan R. and Irchhaiya. R. (2017). An overview on niosomes as efficient drug carriers. *International Journal of Pharma and Bio Sciences*, 8(2), 106 -116.
- Kiaee, G., Javar, H. A., Kiaee, B., & Kiaei, S. (2016). Preparation and characterization of liposome containing minoxidil and rosemary essential oil. *Journal of in Silico & in Vitro Pharmacology*, 2(3), 1-4.
- Kim, J. (2016). Liposomal drug delivery system. *Journal of Pharmaceutical Investigation*, 46(4), 387-392.
- Kim, T. K., & Park, K. S. (2015). Inhibitory effects of harpagoside on TNF- α -induced pro-inflammatory adipokine expression through PPAR- γ activation in 3T3-L1 adipocytes. *Cytokine*, 76(2), 368-374.
- Kimura, T., & Higaki, K. (2002). Gastrointestinal transit and drug absorption. *Biological and Pharmaceutical Bulletin*, 25(2), 149-164.
- Klein, S. (2010). The use of biorelevant dissolution media to forecast the in vivo performance of a drug. *The AAPS journal*, 12(3), 397-406.
- Koziolek, M., Grimm, M., Becker, D., Iordanov, V., Zou, H., Shimizu, J., Wanke, C., Garbacz, G., & Weitschies, W. (2015). Investigation of pH and temperature profiles in the GI tract of fasted human subjects using the Intellicap® system. *Journal of Pharmaceutical Sciences*, 104(9), 2855-2863.
- Kuete, V. (2013). Medicinal plant research in Africa: Pharmacology and chemistry. *Newnes*.
- Kumar, A., Badde, S., Kamble, R., & Pokharkar, V. B. (2010). Development and characterization of liposomal drug delivery system for nimesulide. *International Journal of Pharmacy and Pharmaceutical Sciences*, 2(4), 87-89.
- Kumari, A., Kumar, V., & Yadav, S. (2012). Nanotechnology: A tool to enhance therapeutic values of natural plant products. *Trends in Medical Research*, 7(2), 34-42.

- Kundu, A., & Datta, S. (2012). Formulation and characterization of alginate microbeads of norfloxacin by ionotropic gelation. *International Journal of Advances in Pharmacy, Biology and Chemistry* 1(3), 266-270.
- Laouini, A., Jaafar-Maalej, C., Limayem-Blouza, I., Sfar, S., Charcosset, C., & Fessi, H. (2012). Preparation, characterization and applications of liposomes: State of the art. *Journal of Colloid Science and Biotechnology*, 1(2), 147-168.
- Lee, K. Y., & Mooney, D. J. (2012). Alginate: Properties and biomedical applications. *Progress in Polymer Science*, 37(1), 106-126.
- Lei, Z., Huhman, D. V., & Sumner, L. W. (2011). Mass spectrometry strategies in metabolomics. *The Journal of Biological Chemistry*, 286(29), 25435-25442.
- Li, J., Wang, X., Zhang, T., Wang, C., Huang, Z., Luo, X., Deng, Y. (2015). A review on phospholipids and their main applications in drug delivery systems. *Asian Journal of Pharmaceutical Sciences*, 10(2), 81-98.
- Li, Y., Zou, C., & Liu, H. (1999). Determination of harpagide and harpagoside in *Scrophularia ningpoensis* by capillary electrophoresis. *Chromatographia*, 50(5), 358-362.
- Lim, D. W., Kim, J. G., Han, D., & Kim, Y. T. (2014). Analgesic effect of *Harpagophytum procumbens* on postoperative and neuropathic pain in rats. *Molecules*, 19(1), 1060-1068.
- Lin, S., Chen, Y., Chen, R., Chen, L., Ho, H., Tsung, Y., Sheu, M., Liu, D. (2016). Improving the stability of astaxanthin by microencapsulation in calcium alginate beads. *PloS One*, 11(4), 1-10.
- Liu, L., Yao, W., Rao, Y., Lu, X., & Gao, J. (2017). PH-responsive carriers for oral drug delivery: Challenges and opportunities of current platforms. *Drug Delivery*, 24(1), 569-581.
- Ludwig-Müller, J., Georgiev, M., & Bley, T. (2008). Metabolite and hormonal status of hairy root cultures of devil's claw (*Harpagophytum procumbens*) in flasks and in a bubble column bioreactor. *Process Biochemistry*, 43(1), 15-23.

- Ma, J., Guan, R., Ri, C., Liu, M., Ye, X., & Jiang, J. (2012). Response surface methodology for the optimization of lactoferrin nano-liposomes. *Advance Journal of Food Science and Technology*, 4(5), 249-256.
- Mahomed, I. M., & Ojewole, J. A. (2006). Anticonvulsant activity of *Harpagophytum procumbens* DC [pedaliaceae] secondary root aqueous extract in mice. *Brain Research Bulletin*, 69(1), 57-62.
- Mahomoodally, M. F. (2013). Traditional medicines in Africa: An appraisal of ten potent African medicinal plants. *Evidence-Based Complementary and Alternative Medicine: ECAM*, 2013, 1-14.
- Malakar, J., Nayak, A. K., & Goswami, S. (2012). Use of response surface methodology in the formulation and optimization of bisoprolol fumarate matrix tablets for sustained drug release. *International Scholarly Research Network, Pharmaceutics*, 2012, 1-10.
- Mandal, B., Alexander, K., & Riga, A. (2010). Evaluation of the drug-polymer interaction in calcium alginate beads containing diflunisal. *Die Pharmazie-an International Journal of Pharmaceutical Sciences*, 65(2), 106-109.
- Mandal, S., Kumar, S. S., Krishnamoorthy, B., & Basu, S. K. (2010). Development and evaluation of calcium alginate beads prepared by sequential and simultaneous methods. *Brazilian Journal of Pharmaceutical Sciences*, 46(4), 785-793.
- Manjanna, K., Kumar, P., & Shivakumar, B. (2009). Effect of manufacturing conditions on physico-chemical characteristics and drug release profiles of aceclofenac sodium microbeads. *Drug Invention Today*, 1(2), 98-107.
- Manjanna, K., Rajesh, K., & Shivakumar, B. (2013). Formulation and optimization of natural polysaccharide hydrogel microbeads of aceclofenac sodium for oral controlled drug delivery. *American Journal of Medical Sciences and Medicine*, 1(1), 5-17.
- Marsanasco, M., Márquez, A. L., Wagner, J. R., Alonso, S. d. V., & Chiaramoni, N. S. (2011). Liposomes as vehicles for vitamins E and C: An alternative to fortify orange juice and offer vitamin C protection after heat treatment. *Food Research International*, 44(9), 3039-3046.

- Mathur, M. (2013). Approaches for improving the pharmacological and pharmacokinetics properties of herbal drugs. *International Research Journal of Pharmaceutical and Applied Sciences*, 3(4), 40-50.
- Mayuri, K., Chinnala, K., M. (2016) .Preparation, Optimization and evaluation of liposomes encapsulating diclofenac sodium and charge inducers to enhance stability using lipid hydration method. *International Journal of Pharmacy and Pharmaceutical Research*, 6(3), 180-191.
- Medina, J.R., Hernandez, J., Hurtado, M. (2017). *In vitro* release studies of carbamazepine tablets and benzoyl metronidazole suspensions using the flow-through cell apparatus and simulated gastrointestinal fluids. *International Journal of Applied Pharmaceutics*, 9(4), 54-60.
- Mello, V. A. d., & Ricci-Júnior, E. (2011). Encapsulation of naproxen in nanostructured system: Structural characterization and in vitro release studies. *Química Nova*, 34(6), 933-939.
- Mishra, B., Reddy, K.H., Manikanta, A., Anand, A., Raju, M.S.K. (2016) Formulation and Optimization of Clarithromycin Loaded with Pullulan Acetate Microsphere for Sustained Release by Response Surface Methodology. *International Journal of Drug Development and Research*, 8(3); 011-015.
- Mittal, H., Ray, S. S., & Okamoto, M. (2016). Recent progress on the design and applications of Polysaccharide-Based graft copolymer hydrogels as adsorbents for wastewater purification. *Macromolecular Materials and Engineering*, 301(5), 496-522.
- Mncwangi, N. P., Viljoen, A. M., Zhao, J., Vermaak, I., Chen, W., & Khan, I. (2014). What the devil is in your phytomedicine? Exploring species substitution in *Harpagophytum* through chemometric modeling of ¹ H-NMR and UHPLC-MS datasets. *Phytochemistry*, 106, 104-115.
- Mncwangi, N., Chen, W., Vermaak, I., Viljoen, A. M., & Gericke, N. (2012). Devil's Claw—A review of the ethnobotany, phytochemistry and biological activity of *Harpagophytum procumbens*. *Journal of Ethnopharmacology*, 143(3), 755-771.

- Mncwangi, N., Vermaak, I., & Viljoen, A. M. (2014). Mid-infrared spectroscopy and short wave infrared hyperspectral imaging—A novel approach in the qualitative assessment of *Harpagophytum procumbens* and *H. zeyheri* (devil's claw). *Phytochemistry Letters*, 7, 143-149.
- Mohammed, A., Weston, N., Coombes, A., Fitzgerald, M., & Perrie, Y. (2004). Liposome formulation of poorly water soluble drugs: Optimisation of drug loading and ESEM analysis of stability. *International Journal of Pharmaceutics*, 285(1), 23-34.
- Mohandas, A., Sudheesh, P. T., Raja, B., Lakshmanan, V. K., & Jayakumar, R. (2015). Exploration of alginate hydrogel/nano zinc oxide composite bandages for infected wounds. *International Journal of Nanomedicine*, 10(1), 53-66.
- Mokale, V., Jitendra, N., Yogesh, S., & Gokul, K. (2014). Chitosan reinforced alginate controlled release beads of losartan potassium: Design, formulation and in vitro evaluation. *Journal of Pharmaceutical Investigation*, 44(4), 243-252.
- Mondal, S., & Sarkar, M. (2011). Membrane fusion induced by small molecules and ions. *Journal of Lipids*, 2011, 1-14.
- Mourabet, M., El Rhilassi, A., El Boujaady, H., Bennani-Ziatni, M., & Taitai, A. (2014). Use of response surface methodology for optimization of fluoride adsorption in an aqueous solution by brushite. *Arabian Journal of Chemistry*, 10, 3292–3302.
- Muppidi, K., Pumerantz, A. S., Wang, J., & Betageri, G. (2012). Development and stability studies of novel liposomal vancomycin formulations. *International Scholarly Research Network Pharmaceutics*, 2012, 1-8.
- Muzila, M. (2016). Genetic, Morphological and Chemical Variation in the Genus *Harpagophytum*, (Doctoral dissertation), Swedish University of Agricultural Sciences.
- Nagpal, M., Maheshwari, D., Rakha, P., Dureja, H., Goyal, S., & Dhingra, G. (2012). Formulation development and evaluation of alginate microspheres of ibuprofen. *Journal of Young Pharmacists*, 4(1), 13-16.

- Naidoo, Y., Heneidak, S., Bhatt, A., Kasim, N., & Naidoo, G. (2014). Morphology, histochemistry, and ultrastructure of foliar mucilage-producing trichomes of *harpagophytum procumbens* (pedaliaceae). *Turkish Journal of Botany*, 38(1), 60-67.
- Nayak, A., Khatua, S., Hasnain, M., & Sen, K. (2011). Development of diclofenac sodium-loaded alginate-PVP K 30 microbeads using central composite design. *DARU Journal of Faculty of Pharmacy, Tehran University of Medical Sciences*, 19(5), 356-366.
- Nimase, P. K., & Vidyasagar, G. (2010). Preparation and evaluation of floating calcium alginate beads of clarithromycin. *Der Pharmacia Sinica*, 1(1), 29-35.
- Nimmathota, M. (2016). Colloidal dispersions (liposomes and ethosomes) for skin drug delivery and their role on rheumatoid arthritis. *Asian Journal of Pharmaceutics*, 10(3), 208-221.
- Ong, S. G. M., Chitneni, M., Lee, K. S., Ming, L. C., & Yuen, K. H. (2016). Evaluation of extrusion technique for nanosizing liposomes. *Pharmaceutics*, 8(4), 1-12.
- Pandey, R., Ahmad, Z., Sharma, S., & Khuller, G. (2005). Nano-encapsulation of azole antifungals: Potential applications to improve oral drug delivery. *International Journal of Pharmaceutics*, 301(1), 268-276.
- Paques, J. P., van der Linden, E., van Rijn, C. J., & Sagis, L. M. (2014). Preparation methods of alginate nanoparticles. *Advances in Colloid and Interface Science*, 209, 163-171.
- Patel, N., Lalwani, D., Gollmer, S., Injeti, E., Sari, Y., & Nesamony, J. (2016). Development and evaluation of a calcium alginate based oral ceftriaxone sodium formulation. *Progress in Biomaterials*, 5(2), 117-133.
- Patel, Y. L., Sher, P., & Pawar, A. P. (2006). The effect of drug concentration and curing time on processing and properties of calcium alginate beads containing metronidazole by response surface methodology. *AAPS Pharmscitech*, 7(4), 24-30.
- Patidar, A., Birla, D., PurviJaveri, M. C., & Sharma, V. (2015). Liposome: New strategy in drug delivery. *International journal of pharmacy & life sciences*. 6(7), 4615-4619.

- Patil, J., Mandave, S., & Jadhav, S. (2014). Ionotropically crosslinked and chitosan reinforced losartan potassium loaded complex alginate beads: Design, characterization and evaluation. *Malaya Journal of Biosciences*, 1(3), 126-133.
- Pattni, B. S., Chupin, V. V., & Torchilin, V. P. (2015). New developments in liposomal drug delivery. *Chemical Reviews*, 115(19), 10938-10966.
- Pawar, H. A., & Bhangale, B. D. (2015). Phytosome as a novel biomedicine: A microencapsulated drug delivery system. *Journal of Bioanalysis & Biomedicine*, 7(1), 6-12.
- Perkins, W., Minchey, S., Ahl, P., & Janoff, A. (1993). The determination of liposome captured volume. *Chemistry and Physics of Lipids*, 64(1-3), 197-217.
- Pincet, F., Cribier, S., & Perez, E. (1999). Bilayers of neutral lipids bear a small but significant charge. *The European Physical Journal B-Condensed Matter and Complex Systems*, 11(1), 127-130.
- Poukens-Renwart, P., Tits, M., & Angenot, L. (1996). Quantitative densitometric evaluation of harpagoside in the secondary roots of *Harpagophytum procumbens* DC. *Journal of Planar Chromatography-Modern TLC*, 9(3), 199-202.
- Pouton, C. W. (2006). Formulation of poorly water-soluble drugs for oral administration: Physicochemical and physiological issues and the lipid formulation classification system. *European Journal of Pharmaceutical Sciences*, 29(3), 278-287.
- Prasad, B.S., Bhatia, S., & Singh, S. (2016). Phytosome: Phytoconstituent based lipid delivered drug delivery system. *Journal of Chemical and Pharmaceutical Research*, 8(5), 664-670.
- Raissi, S., & Farsani, R. (2009). Statistical process optimization through multi-response surface methodology. *World Academy of Science, Engineering and Technology*, 51(46), 267-271.

- Ramana, L. N., Sethuraman, S., Ranga, U., & Krishnan, U. M. (2010). Development of a liposomal nanodelivery system for nevirapine. *Journal of Biomedical Science*, 17(57), 1-9.
- Rani, B., Vandana, N. M., & Arora, S. (2007). Phytosomes: Potential carriers for herbal drugs. *International Journal of Research and Reviews in Pharmacy and Applied science*, 2(3), 566-577.
- Rasaie, S., Ghanbarzadeh, S., Mohammadi, M., & Hamishehkar, H. (2014). Nano phytosomes of quercetin: A promising formulation for fortification of food products with antioxidants. *Pharmaceutical Sciences*, 20(3), 96-101.
- Ravi, G. S., Chandur, V., Shabaraya, A.R., Sanjay, K. (2015). Phytosomes: An advanced herbal drug delivery system. *International Journal of Pharmaceutical Research and Bioscience*, 4(3), 415-432.
- Rawat, S., & Motwani, S. (2012). Phytosomal drug delivery systems. *International Journal of Research and Development in Pharmacy and Life Sciences*, 1(3), 143-150.
- Reis, C. P., Neufeld, R. J., Vilela, S., Ribeiro, A. J., & Veiga, F. (2006). Review and current status of emulsion/dispersion technology using an internal gelation process for the design of alginate particles. *Journal of Microencapsulation*, 23(3), 245-257.
- Saha, S., Sarma, A., Saikia, P., & Chakrabarty, T. (2013). Phytosome: A brief overview. *Scholars Academic Journal of Pharmacy*, 2(1), 12-20.
- Saleem, M., Kotadia, D. R., & Kulkarni, R. V. (2012). Effect of formulation variables on dissolution of water-soluble drug from polyelectrolyte complex beads. *Dissolution Technologies*, 19, 21-28.
- Sanders, M., & Grundmann, O. (2011). The use of glucosamine, devil's claw (*harpagophytum procumbens*), and acupuncture as complementary and alternative treatments for osteoarthritis. *Alternative Medicine Review*, 16(3), 228.
- Sankalia, M. G., Mashru, R. C., Sankalia, J. M., & Sutariya, V. B. (2005). Papain entrapment in alginate beads for stability improvement and site-specific delivery: Physicochemical

characterization and factorial optimization using neural network modeling. *AAPS Pharmscitech*, 6(2), 209-222.

Santra K, Rudra A, Mukherjee B. (2010). Development and physicochemical, and in vitro evaluation of dexamethasone containing liposomes. *International Journal of Biomedical and Pharmaceutical Sciences*, 4(1), 43-47.

Saoji, S. D., Raut, N. A., Dhore, P. W., Borkar, C. D., Popielarczyk, M., & Dave, V. S. (2016). Preparation and evaluation of phospholipid-based complex of standardized centella extract (SCE) for the enhanced delivery of phytoconstituents. *The Journal of the American Association of Pharmaceutical Scientists*, 18(1), 102-114.

Saraf, S. (2010). Applications of novel drug delivery system for herbal formulations. *Fitoterapia*, 81(7), 680-689.

Sathali, A., & Varun, J. (2012). Formulation, development and in vitro evaluation of candesartan cilexetil mucoadhesive microbeads. *International Journal of Current Pharmaceutical Research*, 4(3), 109-118.

Sha, X., Guo, J., Chen, Y., & Fang, X. (2012). Effect of phospholipid composition on pharmacokinetics and biodistribution of epirubicin liposomes. *Journal of Liposome Research*, 22(1), 80-88.

Shabir, G. A. (2003). Validation of high-performance liquid chromatography methods for pharmaceutical analysis: Understanding the differences and similarities between validation requirements of the US Food and Drug Administration, the US Pharmacopeia and the International Conference on Harmonization. *Journal of chromatography A*, 987(1), 57-66.

Shailesh, S., Neelam, S., & Sandeep, K. (2009). Liposomes: A review. *Journal of Pharmacy Research*. 2(7), 1163-1167.

Shaji, J., & Shah, A. (2016). Optimization of tenoxicam loaded niosomes using quadratic design. *International Journal of Current Pharmaceutical Research*. 8(1), 62-67.

- Sharma, A. K., Keservani, R. K., & Kesharwani, R. K. (2016). Biosimilars: Concept and regulation. In Keservani, R., K., Sharma, A., K., Kesharwani, R., K. Novel Approaches for Drug Delivery, 171-188. DOI: 10.4018/978-1-5225-0751-2.ch007.
- Sharma, M. (2014). Applications of nanotechnology based dosage forms for delivery of herbal drugs. *Research and Reviews: Journal of Pharmaceutics and Nanotechnology*, 2(1), 23-30.
- Sharma, P., Verma, S., & Misri, P. (2016). Global need for novel herbal drug formulations. *International Journal of Pharmacognosy and Phytochemical Research*, 8(9), 1535-1544.
- Shashi, K., Satinder, K., & Bharat, P. (2012). A complete review on: Liposomes. *International Research Journal of Pharmacy*, 3(7), 10-16.
- Shazly, G. A. G. (2012). Design and evaluation of sustained released liposomal preparations containing adenosine monophosphate. *Digest Journal of Nanomaterials and Biostructures*, 7(4), 1679-1687.
- Shazly, G., Nawroth, T., & Langguth, P. (2008). Comparison of dialysis and dispersion methods for in vitro release determination of drugs from multilamellar liposomes. *Dissolution Technologies*, 15(2), 7-10.
- Shelke, S. S. (2012). Phytosomes-A new herbal drug delivery system. *International Journal of Research in Pharmaceutical and Biomedical Sciences*, 3(4), 1710-1715.
- Sheu, S., Hong, Y., Sun, J., Liu, M., Chen, C., & Ke, C. (2015). Radix scrophulariae extracts (harpagoside) suppresses hypoxia-induced microglial activation and neurotoxicity. *BMC Complementary and Alternative Medicine*, 15(1), 1-9.
- Shi, J., Alves, N. M., & Mano, J. F. (2006). Drug release of pH/Temperature-Responsive calcium Alginate/Poly (N-isopropylacrylamide) Semi-IPN beads. *Macromolecular Bioscience*, 6(5), 358-363.

- Shivakumar, H., Patel, P., Desai, B., Ashok, P., & Arulmozhi, S. (2007). Design and statistical optimization of glipizide loaded lipospheres using response surface methodology. *Acta Pharmaceutica*, 57(3), 269-285.
- Shrestha, H., Bala, R., & Arora, S. (2014). Lipid-based drug delivery systems. *Journal of Pharmaceutics*, 2014, 1-10.
- Singh, D. (2015). Application of novel drug delivery system in enhancing the therapeutic potential of phytoconstituents. *Asian Journal of Pharmaceutics*, 9(4), 1-12.
- Singh, D., Rawat, M., Semalty, A., & Semalty, M. (2012). Emodin–phospholipid complex. *Journal of Thermal Analysis and Calorimetry*, 108(1), 289-298.
- Singh, D., Rawat, M., Semalty, A., & Semalty, M. (2013). Chrysophanol–phospholipid complex. *Journal of Thermal Analysis and Calorimetry*, 111(3), 2069-2077.
- Singh, G., Pai, R. S., & Devi, V. K. (2012). Response surface methodology and process optimization of sustained release pellets using taguchi orthogonal array design and central composite design. *Journal of Advanced Pharmaceutical Technology & Research*, 3(1), 30-40.
- Singh, R. P., & Narke, R. (2015). Preparation and evaluation of phytosome of lawsone. *International Journal of Pharmaceutical Sciences and Research*, 6(12), 5217-5226.
- Singh, S., Gogoi, B. K., & Bezbaruah, R. L. (2012). Calcium alginate as a support material for immobilization of L-amino acid oxidase isolated from aspergillus fumigatus. *IIOAB Journal*, 3(5), 7-11.
- Singhal, P., Tomar, A., Goel, K., Pandey, M., & Saraf, S. A. (2010). Preparation and evaluation of stomach-specific ion tropically emulsion gelled alginate beads of tinidazole. *Der Pharmacia Lettre*, 2(6), 272-282.
- Smith, A. M., Jaime-Fonseca, M. R., Grover, L. M., & Bakalis, S. (2010). Alginate-loaded liposomes can protect encapsulated alkaline phosphatase functionality when exposed to gastric pH. *Journal of Agricultural and Food Chemistry*, 58(8), 4719-4724.

- Smrdel, P., Bogataj, M., & Mrhar, A. (2008). The influence of selected parameters on the size and shape of alginate beads prepared by ionotropic gelation. *Scientia Pharmaceutica*, 76(1), 77-90.
- Soema, P. C., Willems, G., Jiskoot, W., Amorij, J., & Kersten, G. F. (2015). Predicting the influence of liposomal lipid composition on liposome size, zeta potential and liposome-induced dendritic cell maturation using a design of experiments approach. *European Journal of Pharmaceutics and Biopharmaceutics*, 94, 427-435.
- Solano-Umaña, V., Vega-Baudrit, J. R., & González-Paz, R. (2015). The new field of the nanomedicine. *International Journal of Applied Science and Technology*, 5(1), 79- 88.
- Song, Y., Zhuang, J., Guo, J., Xiao, Y., & Ping, Q. (2008). Preparation and properties of a silybin-phospholipid complex. *Die Pharmazie- an International Journal of Pharmaceutical Sciences*, 63(1), 35-42.
- Soulimani, R., Younos, C., Mortier, F., & Derrieu, C. (1994). The role of stomachal digestion on the pharmacological activity of plant extracts, using as an example extracts of *Harpagophytum procumbens*. *Canadian Journal of Physiology and Pharmacology*, 72(12), 1532-1536.
- Pravathi, M., & Krishna, J. S. (2013). Phytosomes: A novel drug delivery for herbal extracts. *International Journal of Pharmaceutical Sciences and Research*, 4(3), 949-959.
- Stewart, K. M., & Cole, D. (2005). The commercial harvest of devil's claw (*Harpagophytum* spp.) in southern Africa: The devil's in the details. *Journal of Ethnopharmacology*, 100(3), 225-236.
- Street, R., & Prinsloo, G. (2012). Commercially important medicinal plants of South Africa: A review. *Journal of Chemistry*, 2013, 1-16.
- Street, R., Stirk, W., & Van Staden, J. (2008). South African traditional medicinal plant trade-challenges in regulating quality, safety and efficacy. *Journal of Ethnopharmacology*, 119(3), 705-710.

- Sudhakar, B., Ravi Varma, J., & Ramana Murthy, K. (2014). Formulation, characterization and ex vivo studies of terbinafine HCl liposomes for cutaneous delivery. *Current Drug Delivery*, 11(4), 521-530.
- Süleymanoglu, E. (2009). The use of IR spectroscopy after rehydration to follow ternary lipoplex formation and design as a metal-based DNA nanopharmaceuticals. *Prilozi*, 1, 61-80.
- Sun, J., & Tan, H. (2013). Alginate-based biomaterials for regenerative medicine applications. *Materials*, 6(4), 1285-1309.
- Suriyakala, P.C., Satheesh, B.N., Senthil, R.D., Prabakaran, L. (2014). Phospholipids as versatile polymer in drug delivery systems. *International Journal of Pharmacy and Pharmaceutical Sciences*, 6(1), 8-11.
- Suruse, P. (2014). Development of microcapsules of glimepiride using fenugreek seed extract. *International Journal of Pharmaceutical and Phytopharmacological Research*, 3(3), 212-215.
- Suzery, M., Setyawan, D., Majid, D., & Sutanto, H. (2017). Encapsulation of phycocyanin-alginate for high stability and antioxidant activity. *IOP Conference Series: Earth and Environmental Science*, 55(1), 1-8.
- Takka S, A. F. (1999). Calcium alginate microparticles for oral administration: II effect of formulation factors on drug release and drug entrapment efficiency. *Journal of Microencapsulation*, 16(3), 291-301.
- Takka, S., Ocak, Ö. H., & Acartürk, F. (1998). Formulation and investigation of nicardipine HCl-alginate gel beads with factorial design-based studies. *European Journal of Pharmaceutical Sciences*, 6(3), 241-246.
- Tan, B. H., & Ong, C. E. (2016). The use of natural remedies to treat osteoarthritis. *Tang*, 6(1), 1-9.

- Tan, Q., Liu, S., Chen, X., Wu, M., Wang, H., Yin, H., He, D., Xiong, H., Zhang, J. (2012). Design and evaluation of a novel evodiamine-phospholipid complex for improved oral bioavailability. *AAPS Pharmscitech*, 13(2), 534-547.
- Thapa, R. K., Khan, G. M., Parajuli-Baral, K., & Thapa, P. (2013). Herbal medicine incorporated nanoparticles: Advancements in herbal treatment. *Asian Journal of Biomedical and Pharmaceutical Sciences*, 3(24), 7- 14.
- Thassu, D., & Chader, G. J. (2012). Ocular drug delivery systems: Barriers and application of nanoparticulate systems. *CRC Press*. DOI: 10.1201/B12950.
- Thomas, L. M., & Khalil, Y. I. (2011). Preparation and evaluation of atenolol floating beads as a controlled delivery system. *Iraqi Journal of Pharmaceutical Sciences*, 20(1), 70-80.
- Thulasirammaraju, T., Babu, A., Arunachalam, A., Prathap, M., Srikanth, S., & Sivaiah, P. (2012). Liposome: A novel drug delivery system. *International Journal of Biopharmacuties*, 3(1): 5-16.
- Tiwari, G. (2013). Preparation and Characterization of ketoconazole encapsulated liposome and ethosome: A Comparative study, (Doctoral dissertation). National institute of technology, Rourkela. India.
- Tønnesen, H. H., & Karlsen, J. (2002). Alginate in drug delivery systems. *Drug Development and Industrial Pharmacy*, 28(6), 621-630.
- Tous, S., Fathy, M., Fetih, G., & Gad, S. F. (2014). Preparation and evaluation of ketoprofen-loaded calcium alginate beads. *International Journal of PharmTech Research*, 6(3), 1100-1112.
- Trivedi R.V., Taksande J. B., Awandekar N. B., Umekar M. J. (2017). Effect of lipid composition on liposomal formulation of pramipexole. *World Journal of Pharmaceutical Research*, 6(1), 1073-1089.
- Udapurkar, P., Bhusnure, O., Kamble, S., & Biyani, K. (2016). Phyto-phospholipid complex vesicles for phytoconstituents and herbal extracts: A promising drug delivery system. *International Journal of Herbalmedicine*; 4(5) 14-20.

- Van Nieuwenhuyzen, W., & Tomás, M. C. (2008). Update on vegetable lecithin and phospholipid technologies. *European Journal of Lipid Science and Technology*, 110(5), 472-486.
- Van Wyk, B. E. (2011). The potential of South African plants in the development of new medicinal products. *South African Journal of Botany*, 77(4), 812-829.
- Vankudri, R., Habbu, P., Hiremath, M., Patil, B., & Savant, C. (2016). Preparation and therapeutic evaluation of rutin-phospholipid complex for antidiabetic activity. *Journal of Applied Pharmaceutical Science*, 6(1), 90-101.
- Venkatesh, S., Kumar, M. B., Ramachandran, S., & Sameer, G. N. (2010). HPLC method development, validation and its application to stability studies of chlorpromazine hydrochloride tablets. *International Research Journal of Pharmacy*, 1(1) 225-232.
- Viljoen, A., Mncwangi, N., & Vermaak, I. (2012). Anti-inflammatory iridoids of botanical origin. *Current Medicinal Chemistry*, 19(14), 2104-2127.
- Vinod, M., Jitendra, N., Gayatri, K., & Gokul, K. (2013). Formulation and development of diltiazem hydrochloride sustained release alginate beads by ionotropic external gelation technique. *Advances in Pharmacology and Pharmacy*, 1(3), 139-143.
- Voo, W., Lee, B., Idris, A., Islam, A., Tey, B., & Chan, E. (2015). Production of ultra-high concentration calcium alginate beads with prolonged dissolution profile. *RSC Advances*, 5(46), 36687-36695.
- Wagner, H., Bauer, R., Melchart, D., Xiao, P. G., & Staudinger, A. (2011). Chromatographic fingerprint analysis of herbal medicines: Thin-layer and high performance liquid chromatography of Chinese drugs. Berlin, Germany: Springer Science & Business Media. DOI: 10.1007/978-3-7091-0763-8.
- Wang, H., Liu, M., & Du, S. (2014). Optimization of madecassoside liposomes using response surface methodology and evaluation of its stability. *International Journal of Pharmaceutics*, 473(1), 280-285.

- Wang, W., Waterhouse, G. I., & Sun-Waterhouse, D. (2013). Co-extrusion encapsulation of canola oil with alginate: Effect of quercetin addition to oil core and pectin addition to alginate shell on oil stability. *Food Research International*, 54(1), 837-851.
- World Health Organization. (1998). Regulatory situation of herbal medicines: A worldwide review.
- World health organization. (2012). The international pharmacopoeia. Geneva; world health organization, Dept. of essential medicines and pharmaceutical policies.
- Xego, S., Kambizi, L., & Nchu, F. (2016). Threatened medicinal plants of South Africa: Case of the family hyacinthaceae. *African Journal of Traditional, Complementary and Alternative Medicines*, 13(3), 169-180.
- Xu, F., Dong, F., Wang, P., Cao, H. Y., Li, C. Y., Li, P. Y., Pang, X. H., Zhang, Y.Z., Chen, X .L. (2017). Novel molecular insights into the catalytic mechanism of marine bacterial alginate lyase AlyGC from polysaccharide lyase family 6. *The Journal of Biological Chemistry*, 292(11), 4457-4468.
- Yas, A. (2014). Development and optimization of liposomal ketotifen fumarate dry powder using response surface methodology. *International Journal of Pharmaceutical Sciences and Research*, 5(6), 2264-2278.
- Yingchoncharoen, P., Kalinowski, D. S., & Richardson, D. R. (2016). Lipid-based drug delivery systems in cancer therapy: What is available and what is yet to come. *Pharmacological Reviews*, 68(3), 701-787.
- Yu, F., Li, Y., Chen, Q., He, Y., Wang, H., Yang, L., Guo, S., Meng, Z., Cui, J., Xue, M., Chen, X. (2016). Monodisperse microparticles loaded with the self-assembled berberine-phospholipid complex-based phytosomes for improving oral bioavailability and enhancing hypoglycemic efficiency. *European Journal of Pharmaceutics and Biopharmaceutics*, 103, 136-148.
- Zhang, X., Qi, J., Lu, Y., He, W., Li, X., & Wu, W. (2014). Biotinylated liposomes as potential carriers for the oral delivery of insulin. *Nanomedicine: Nanotechnology, Biology and Medicine*, 10(1), 167-176.

- Zhang, Z., Zhang, R., Zou, L., & McClements, D. J. (2016). Protein encapsulation in alginate hydrogel beads: Effect of pH on microgel stability, protein retention and protein release. *Food Hydrocolloids*, 58, 308-315.
- Zhao, L., Su, C., Zhu, B., & Jia, Y. (2014). Development and optimization of insulin-chitosan nanoparticles. *Tropical Journal of Pharmaceutical Research*, 13(1), 3-8.
- Zuo, J., Gao, Y., Bou-Chacra, N., & Lobenberg, R. (2014). Evaluation of the DDSolver software applications. *BioMed Research International*, 2014, 1-9.

